



Title	Development of Catalytic Asymmetric Reactions Involving Transition Metal Alkoxides
Author(s)	村山, 大明
Citation	北海道大学. 博士(理学) 甲第13681号
Issue Date	2019-03-25
DOI	10.14943/doctoral.k13681
Doc URL	http://hdl.handle.net/2115/91463
Type	theses (doctoral)
File Information	Hiroaki_Murayama.pdf



[Instructions for use](#)

**Development of Catalytic Asymmetric Reactions
Involving Transition Metal Alkoxides**

遷移金属アルコキシドが関与する触媒的不斉反応の開発

Hiroaki MURAYAMA

2019

Contents

General Introduction -----	1
Chapter 1 -----	19
Copper(I)-Catalyzed Intramolecular Hydroalkoxylation of Unactivated Alkenes	
Chapter 2 -----	39
Iridium-Catalyzed Asymmetric Transfer Hydrogenation of Ketones with a Prolinol-Phosphine Chiral Ligand	
Publication List -----	81
Acknowledgement -----	82

General Introduction

Transition metal alkoxides are chemical species in which chemical bonds exist between positively charged transition metal atoms and negatively charged oxygen atoms. There are mainly two methods to generate the transition metal alkoxide: 1) a reaction of transition metal halides and main group metal-alkoxides, 2) a reaction of metal halides and alcohols in the presence of a strong base.¹

A metal-oxygen bond of an early transition metal-alkoxide is strong, stable, and thus exhibits low reactivity. This conclusion follows particularly because oxygen atoms carry two lone pairs while generally at most one lone pair is involved in ‘filling’ an empty metal d orbital (Figure 1a).² On the other hand, a metal-oxygen bond of a late transition metal-alkoxide is weaker, less stable, and higher reactivity than those of an early transition metal-alkoxides. Because a late transition metal has more valence electrons than an early transition metal, the alkoxide lone pair is involved in destabilizing interaction with an occupied d_{π} orbital (Figure 1b).

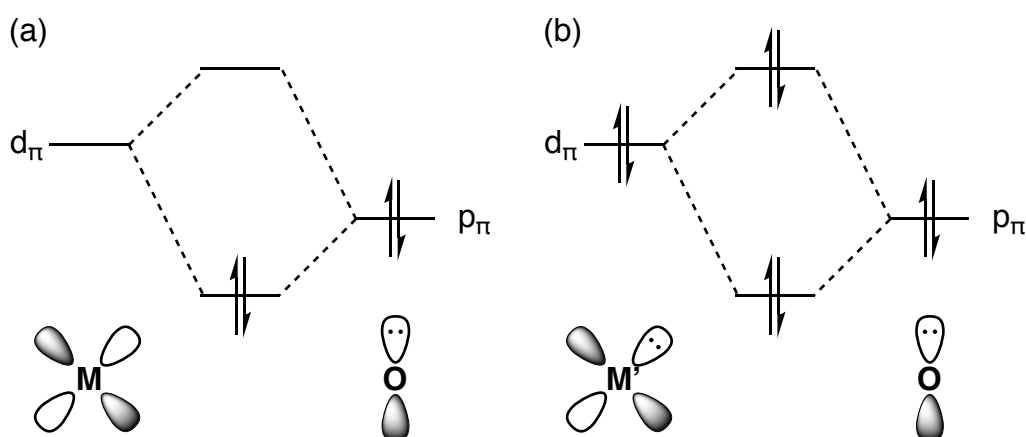


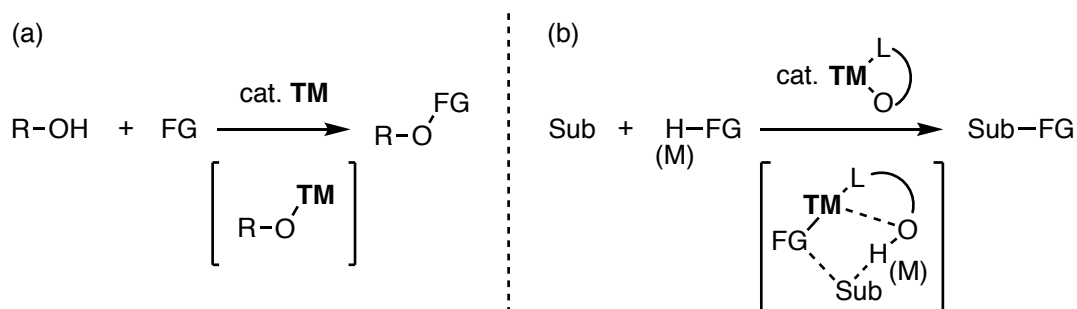
Figure 1 Interaction between π -Symmetry Lone Pair Orbital on O and the Empty and Filled d -Orbitals of a Transition Metal

A coordination of a chiral ligand to the late transition metal alkoxides enables an enantioselective reaction. These properties of late transition metal alkoxides have been utilized for the development of organic synthesis reactions.

Catalytic reactions involving transition metal alkoxides are classified into two-type reactions; the alkoxide unit is derived from a substrate moiety, or from a ligand moiety. The former type reaction is related to incorporation of an alcohol group to a product via the in situ generated reactive late transition metal alkoxide as an active intermediate (Scheme 1a). Formation of the metal alkoxide realizes reactions, which are difficult to achieve with the

neutral alcohol. The latter is smooth activation of substrates by deprotonation, transmetalation and so on. The high reactivity of metal–oxygen bond of late transition metal alkoxides is a key for activation of various substrates (Scheme 1b). Moreover, the OH or OM (M: main group metal), which is formed during substrate activation, is expected to work as a beneficial secondary interaction site: activation of another substrates, construction of a proper chiral space through the interaction with the metal catalyst or/and the substrates.

Scheme 1 Late Transition Metal Alkoxides-Mediated Reactions



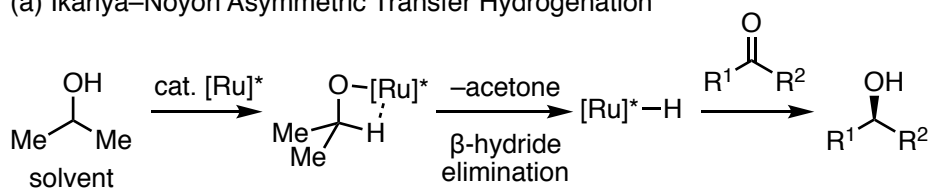
On the other hand, due to the high reactivity of the late transition metal alkoxides, various reaction pathways are possible: β -hydride elimination, reductive elimination, migratory insertion, and so on. It is necessary to control the reactivity to develop a desired reaction via late transition metal alkoxides. This research aims to control the reactivity of late transition metal alkoxides and to develop catalytic asymmetric reactions.

1. Catalytic Reactions through Late Transition Metal Alkoxides

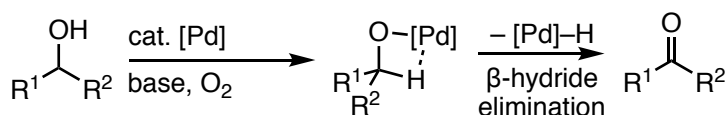
A transformation of substrates via late transition metal alkoxide intermediates often proceeds through one of three type pathways as a metal–oxygen bond cleavage step; β -hydride elimination pathway, reductive elimination pathway, and migratory insertion pathway. Ikariya–Noyori asymmetric transfer hydrogenation and Uemura oxidation are typical reactions via β -hydride elimination pathway (Scheme 2a, b).^{3,4} Cross coupling reaction is a representative example of reductive elimination pathway; Buchwald–Hartwig etherification and Chan–Lam–Evans coupling and so on (Scheme 3a, b).^{5,6} The migratory insertion of alkenes into metal alkoxides is particularly useful for multifunctionalization because formation of a carbon(sp³)–oxygen bond is accompanied by formation of carbon(sp³)–metal bond which can further react with an electrophile (Scheme 4). However, number of reports on migratory insertion of alkenes into metal alkoxides is smaller than other pathways of late transition metal alkoxide related conversions.⁷ Thus, there is much room to investigate in this field for development of novel reactions.

Scheme 2 Metal Alkoxide-Mediated Reactions via β -Hydride Elimination

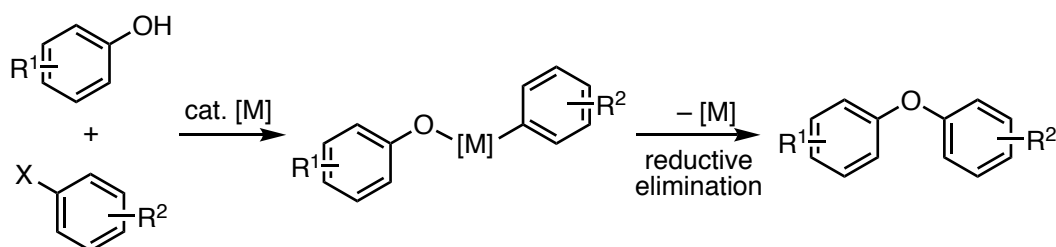
(a) Ikariya–Noyori Asymmetric Transfer Hydrogenation



(b) Uemura Oxidation



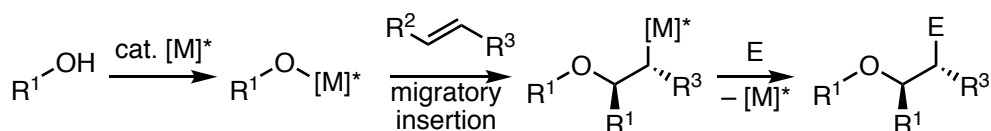
Scheme 3 Metal Alkoxide-Mediated Reactions via Reductive Elimination



(a) Buchwald–Hartwig Etherification
M = Pd, X = halide

(b) Chan–Lam–Evans Coupling
M = Cu, X = B(OH)₂

Scheme 4 Metal Alkoxide-Mediated Reactions via Migratory Insertion (few reports)

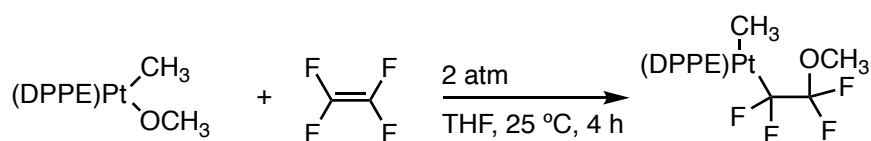


1.1. Catalytic Reactions Using Alcohol-Substrates via Migratory Insertion

1.1.1. Stoichiometric Reactions via Migratory Insertion of Alkenes into Metal Alkoxides

In 1984, Bryndza reported that a late transition metal alkoxide reacted with an olefin to give the product expected of migratory insertion (Scheme 5).^{8a} DPPE-Pt(OMe)Me complex reacts with tetrafluoroethylene (TFE) in THF solution to form an oxyplatination product.

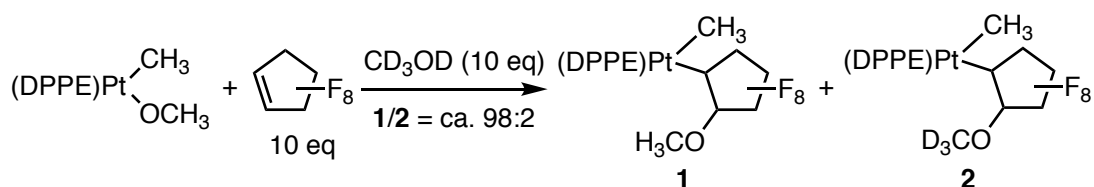
Scheme 5 A First Report about Migratory Insertion of Alkene into Metal Alkoxide



In following year, he reported mechanistic studies for above oxyplatination of alkenes.^{8b} The reaction of the platinum complex and perfluorocyclopentene (10 equiv.) in the presence

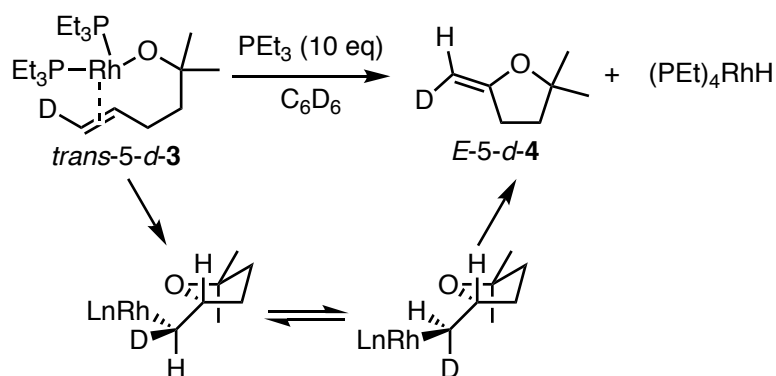
of d_4 -methanol afforded oxyplatination of alkene, and little deuterated product was obtained even though the d_4 -methanol existed in large excess (Scheme 6). This result showed that perfluoroalkene reacts with platinum complex faster than methanol exchange on platinum and that methoxide never dissociated from platinum center during oxyplatination. Thus, this reaction seems to proceed via migratory insertion of alkene into metal alkoxide.

Scheme 6 Mechanistic Studies of Migratory Insertion of Alkene into Metal Alkoxide



Migratory insertion of unactivated alkenes was also reported. Hartwig and co-workers revealed that the intramolecular migratory insertion of deuterated unactivated alkenes into rhodium alkoxides proceeds in the presence of excess amount of triethylphosphine (Scheme 7).⁹ Excess amount of triethylphosphine was added to produce coordinatively saturated rhodium hydride, produced by β -hydride elimination, and inhibiting re-insertion of alkenes. From the configuration of an obtained alkene, *syn*-selective oxyrhodation occurs, which suggest migratory insertion of alkene into alkoxyrhodium.

Scheme 7 Insertion of Alkene into Rhodium Alkoxide

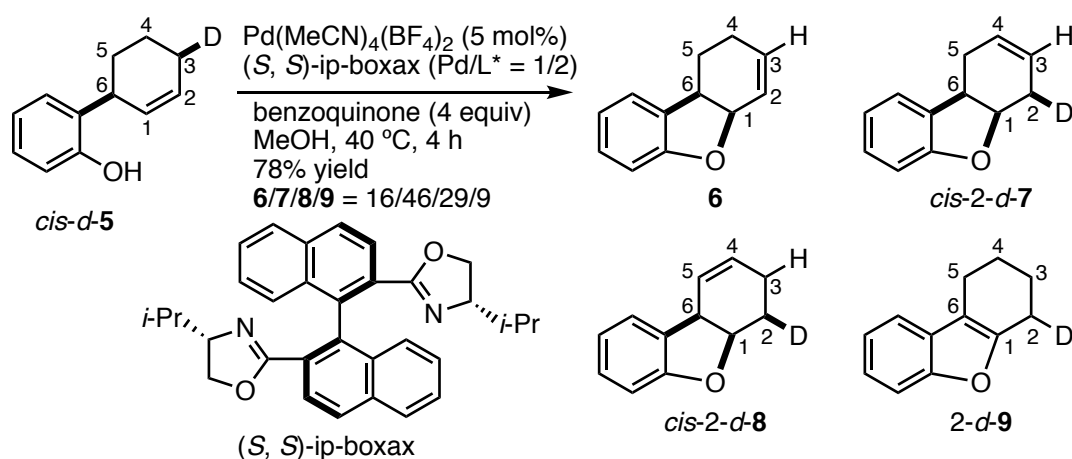


1.1.2. Catalytic Oxidative Cyclization via *syn*-Oxymetalation of Alkenes

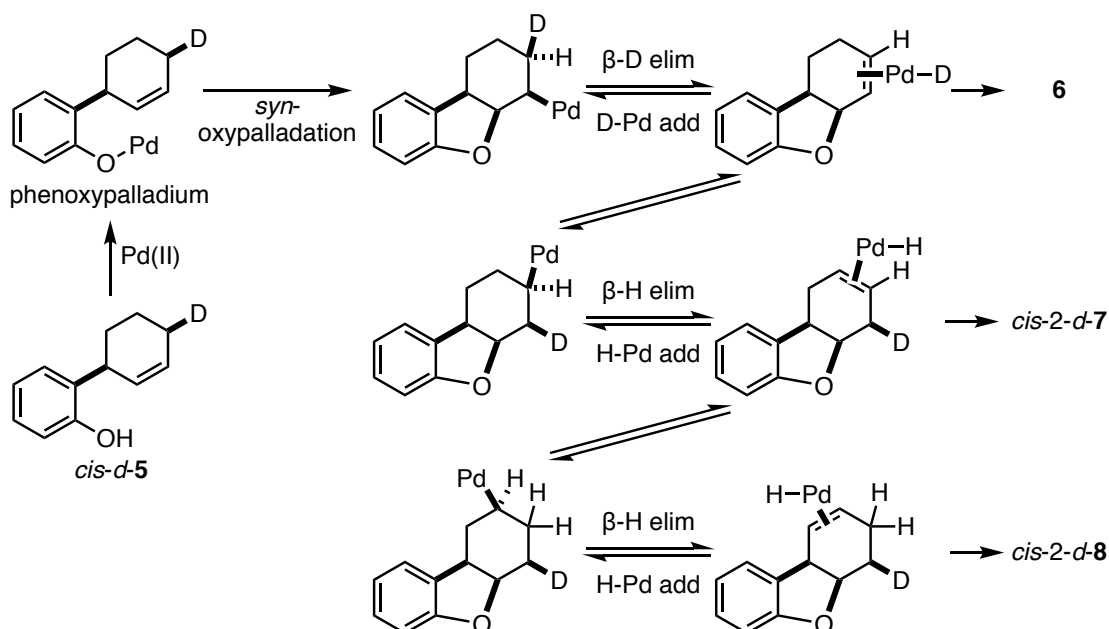
Catalytic oxidative cyclization of alkenes is a simple reaction which proceeds via the migratory insertion of alkenes into metal alkoxides. Mechanistic studies have been performed by utilizing deuterium labeled-starting materials. As the pioneering work, Hayashi *et al.* reported a following experiment.¹⁰ Palladium-catalyzed oxidative cyclization of racemic 6-(2-hydroxy-phenyl)-3-deuteriocyclohexene proceeded to afford a mixture of **6**, *cis*-2- d -7,

cis-2-d-8, and *2-d-9* (Scheme 8). All the products can be explained by exclusive β -deuteride elimination and following re-insertion and β -hydride eliminations (Scheme 9). Because β -deuteride elimination should proceed with *syn*-selectivity, the observation means that β -deuteride elimination occurs after *syn*-selective addition of phenoxypalladium to alkenes. It is also important evidence that 3-position-deuterated product is obtained when *trans*-substrate is used (Scheme 10). Based on these results, it is concluded that migratory insertion of alkene into phenoxypalladium proceeds under the reaction conditions.

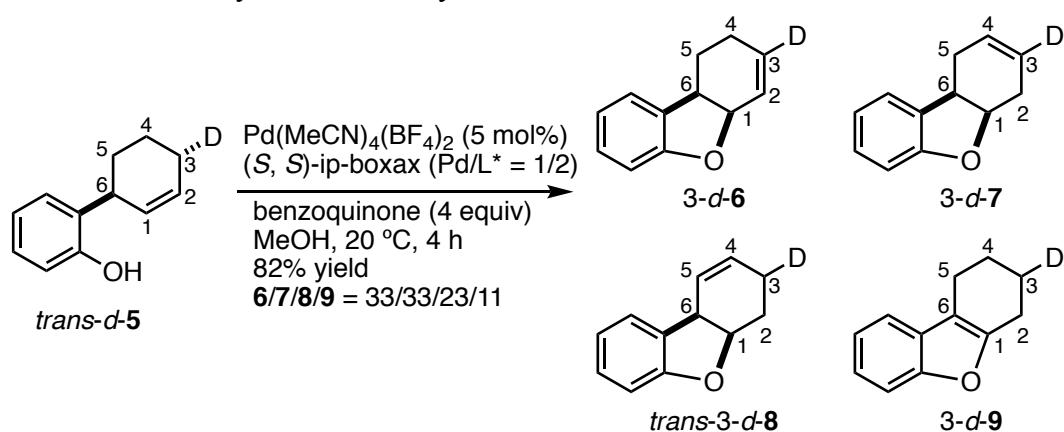
Scheme 8 Pd-Catalyzed Oxidative Cyclization with *cis*-substrate



Scheme 9 Mechanism when *cis*-substrate is used

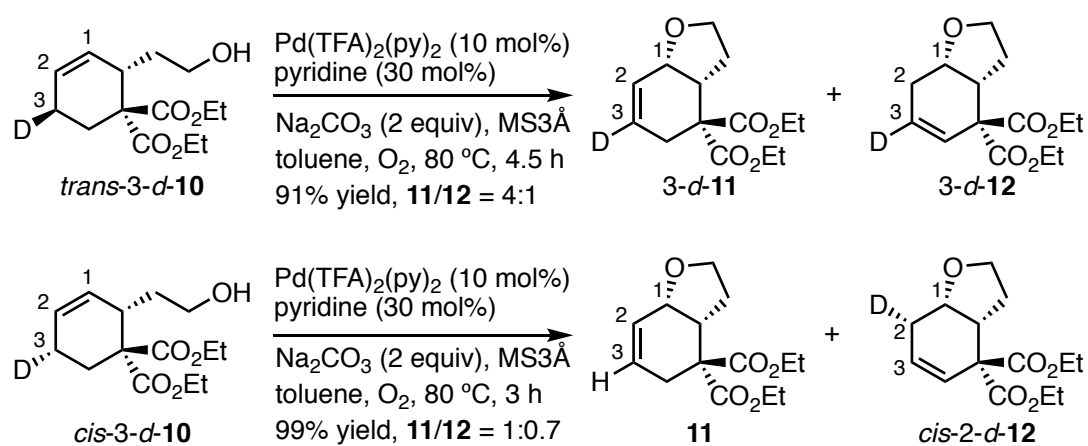


Scheme 10 Pd-Catalyzed Oxidative Cyclization with *trans*-substrate



Stoltz and co-workers reported *syn*-selective oxypalladation proceeds even when primary alcohols are used (Scheme 11).¹¹

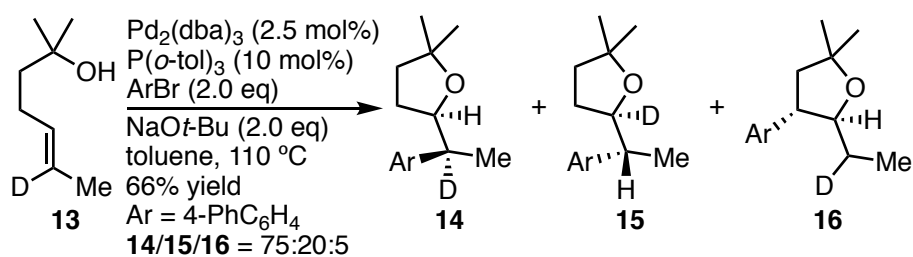
Scheme 11 Oxidative Cyclization of Hydroxylalkenes



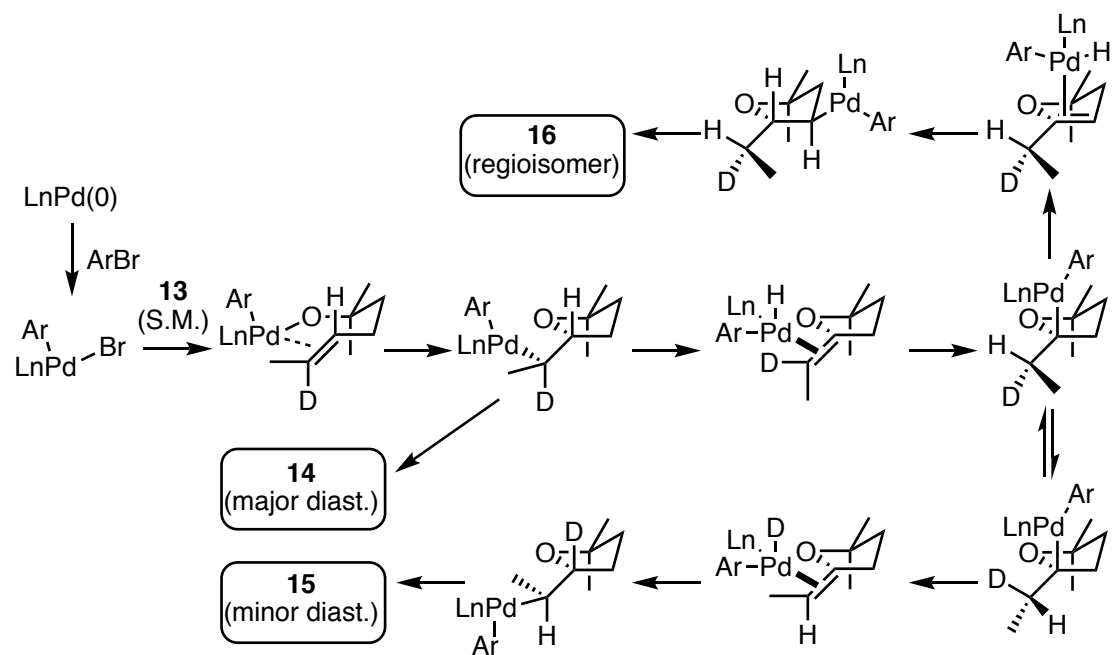
1.1.3. Multifunctionalization via *syn*-Oxymetallation of Alkenes

Not only oxidative cyclization, but also multifunctionalization of alkenes has been known as a metal alkoxide-mediated reaction. A well-recognized example is Wolfe's palladium-catalyzed oxyarylation of alkenes.¹² In this reaction, oxidative addition of ArBr to palladium(0) proceeded first and migratory insertion of alkenes into a palladium alkoxide, and following reductive elimination occurs immediately or after β -hydride elimination/re-insertion process. This pathway was revealed by deuterium-labeling experiment (Scheme 12,13).

Scheme 12 Palladium-Catalyzed Oxyarylation of Unactivated Alkenes



Scheme 13 Mechanism of Oxyarylation



1.2. Catalytic Reactions Using Alkoxide-contained-Ligands

Alkoxide ligands behave as σ -donating ligands to electronically enrich metal centers and improve the activity of metal catalysts. A lot of chiral ligands with alkoxide moieties have been developed: BINOL-, TADDOL-, and salen-type ligands are representatives (Figure 2).¹³⁻¹⁵

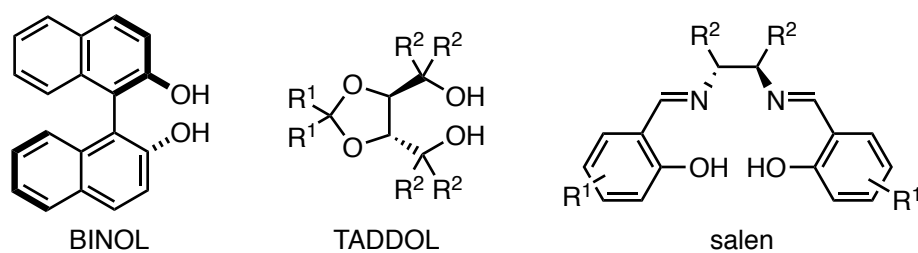


Figure 2 Chiral Alkoxide Ligands

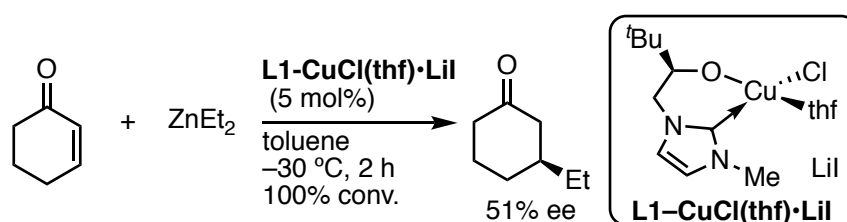
These days, alcohol containing bifunctional ligands have been developed. The alcohol

moiety forms metal alkoxide bond intramolecularly and the high reactivity of the bond is applied for activation of pronucleophiles. Resulting O–H group or O–M group (M: main group metal) involved in either the activation of the electrophiles and/or the construction of the chiral space, thereby development of highly active and stereoselective reactions has been achieved.

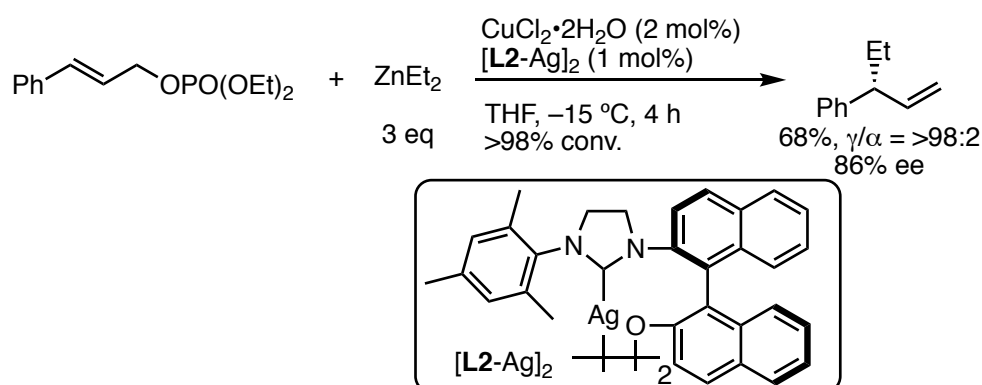
1.2.1. Catalytic Reactions Using *N*-Heterocyclic Carbene Ligands with Alkoxide Moieties

For multidentate ligands with alkoxide moieties, *N*-heterocyclic carbene (NHC) with alkoxide moieties have been extensively studied.¹⁶ In 2004, Arnold and co-workers synthesized alkoxy-NHC ligand to stabilize high oxidation state and Lewis acidic metal catalysts.¹⁷ They isolated alkoxy-NHC–copper(II) complex as lithium iodide adducts. Using this complex, they achieved copper-catalyzed conjugate addition, which undergoes through copper(III)-enolate, with moderate enantioselectivity (Scheme 14). In the same year, Hoveyda isolated a naphthoxy-NHC **L2**-silver complex as a dimer. The ligand **L2** was effective for copper catalysis and they achieved catalytic asymmetric allylic alkylations with the **L2**/copper catalyst (Scheme 15).¹⁸ After this report, they also achieved asymmetric conjugate addition of dialkylzinc reagents to enones and constructed all-carbon quaternary stereogenic centers using phenoxy-carbene ligand **L3** (Scheme 16).¹⁹

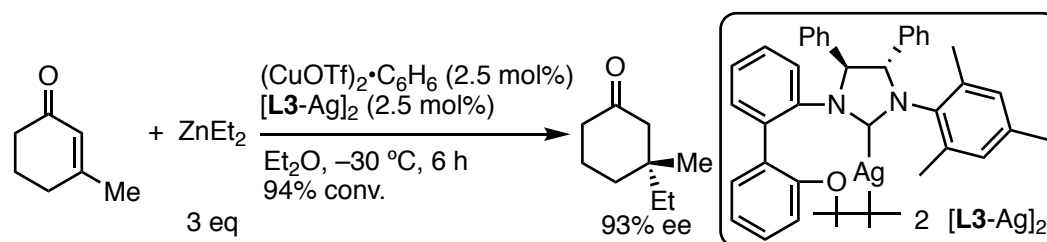
Scheme 14 Alkoxy-NHC-Copper-Catalyzed Asymmetric Conjugate Addition of Diethylzinc



Scheme 15 Enantioselective Allylic Alkylation

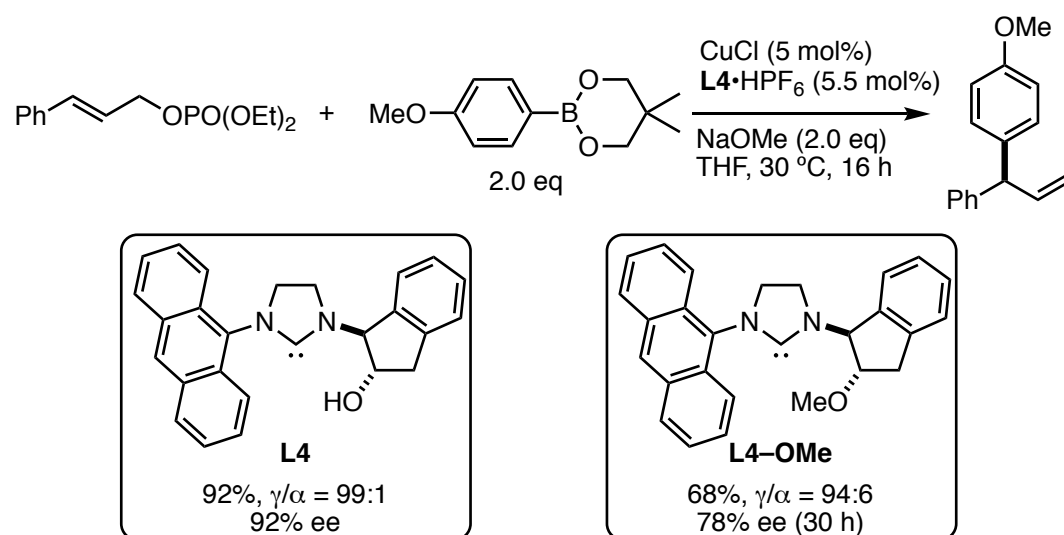


Scheme 16 Enantioselective Synthesis of All-Carbon Quaternary Stereogenic Centers

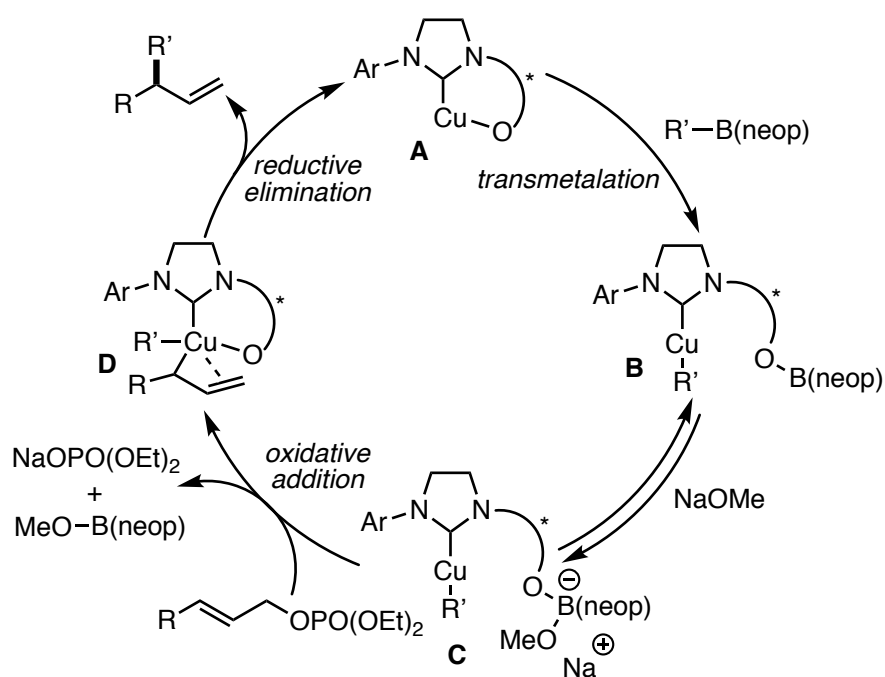


Not only organozinc reagents, but also milder pronucleophiles have been used. Shintani and Hayashi achieved copper-catalyzed asymmetric allylic substitution using organoboronates as pronucleophiles (Scheme 17).^{20a} The ligand **L4-OMe**, which has a methoxy group instead of a hydroxy group in **L4**, slightly diminished the regioselectivity (94:6), the yield and enantioselectivity (68% yield, 78% ee). From these knowledge, they proposed the catalytic cycle shown as Scheme 18. An alkoxy-NHC ligand is considered to play an important role in oxidative addition of allyl phosphates to the in situ generated arylcopper **B**. The sodium cation contained in copper complex **C**, which is generated through transmetalation of the organoboronate to copper catalyst, interacts with the allyl phosphate, thereby the oxidative addition step proceeds with regio- and enantioselectivities (Scheme 18). The catalyst can be applied to both asymmetric conjugate addition to alkylidene cyanoacetates and allylic substitution of allyl phosphates.^{20b}

Scheme 17 Asymmetric Allylic Substitution with Organoboronates

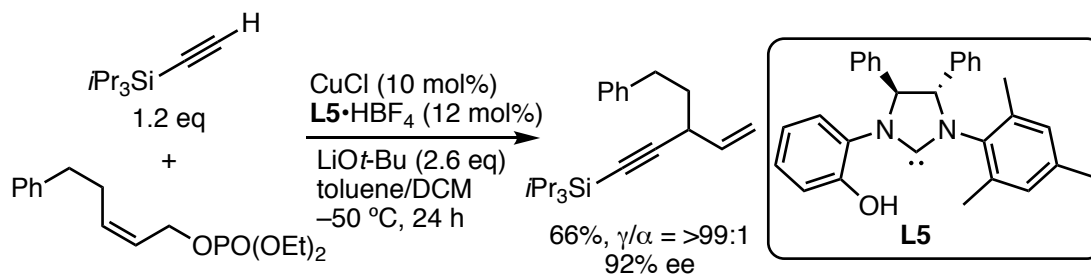


Scheme 18 Possible Catalytic Cycle for the Allylic Substitution

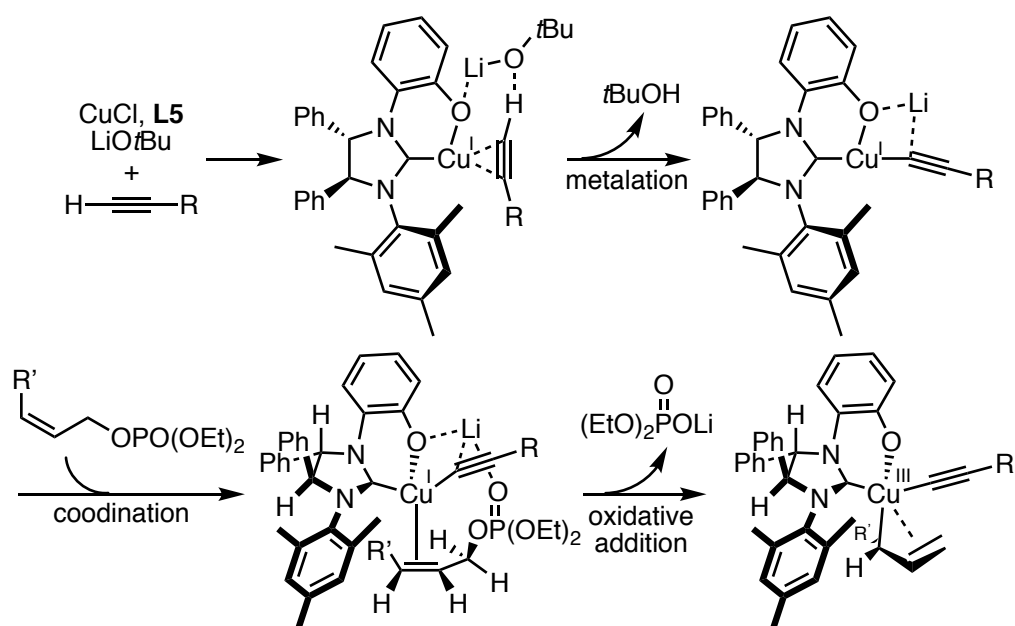


Recently, Ohmiya and Sawamura achieved a several number of copper-catalyzed enantioselective allylic substitutions.²¹ In 2014, they reported enantioselective alkylation of terminal alkyne pronucleophiles using phenoxy-carbene ligands **L5** (Scheme 19).^{21a} Phenoxy moiety seems to promote a generation of cuprate complex, which should exhibit higher nucleophilicity. Lithium cation, which is counter cation of the phenoxy moiety, plays an important role in this reaction. The lithium cation assists the oxidative addition step as Lewis acid to activate the phosphate leaving group (Scheme 20). After achieving this alkylation, they introduced azole, allyl, and formimidoyl groups to the allylic positions with high enantioselectivity using phenoxy- or naphthoxy-NHC-copper systems.^{21b-d}

Scheme 19 Enantioselective Allylic Alkylation of Terminal Alkyne Pronucleophiles

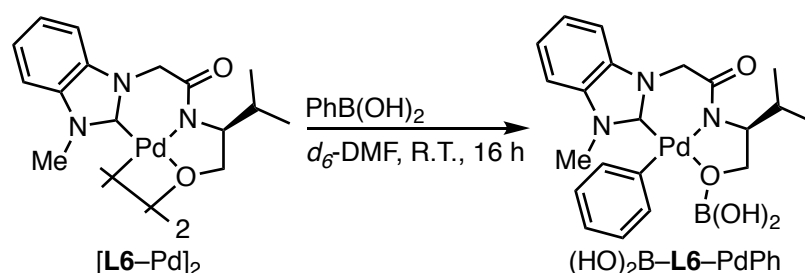


Scheme 20 Proposed Reaction Pathway

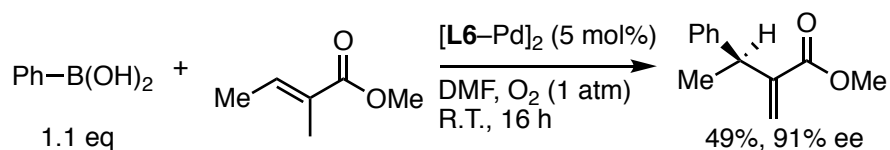


Not only copper-catalysis, but also alkoxy-NHC-palladium-catalysis was reported. Jung and co-workers synthesized NHC-amido-alkoxide ligand **L6**, and isolated palladium complex as a dimer $[\mathbf{L6-Pd}]_2$.²² This complex reacts with phenylboronic acid to produce $(\text{HO})_2\text{B-L6-PdPh}$ complex bearing the pendant boric acid moiety (Scheme 21). The observed intermediate structure can provide evidence of a transmetalation of ary boronic acid to palladium. Based on this result, they achieved catalytic oxidative Heck-type reaction of aryl boronic acid with acyclic alkenes catalyzed by $[\mathbf{L6-Pd}]_2$ (Scheme 22).

Scheme 21 Transmetalation of Phenylboronic Acid to $[\mathbf{L6-Pd}]_2$ Complex



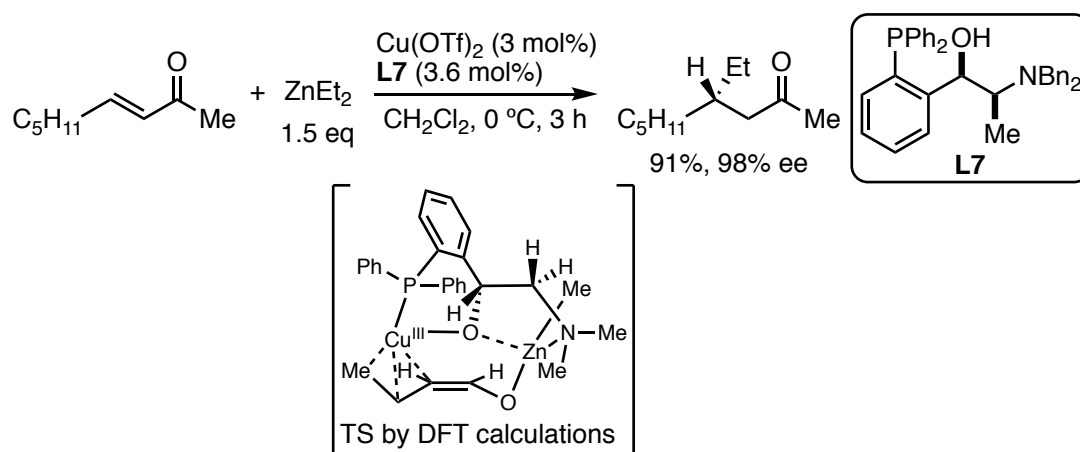
Scheme 22 Oxidative Heck-type reaction catalyzed by $[\mathbf{L6-Pd}]_2$ complex



1.2.2. Catalytic Reactions Using Other-type Ligands with Alkoxide Moieties

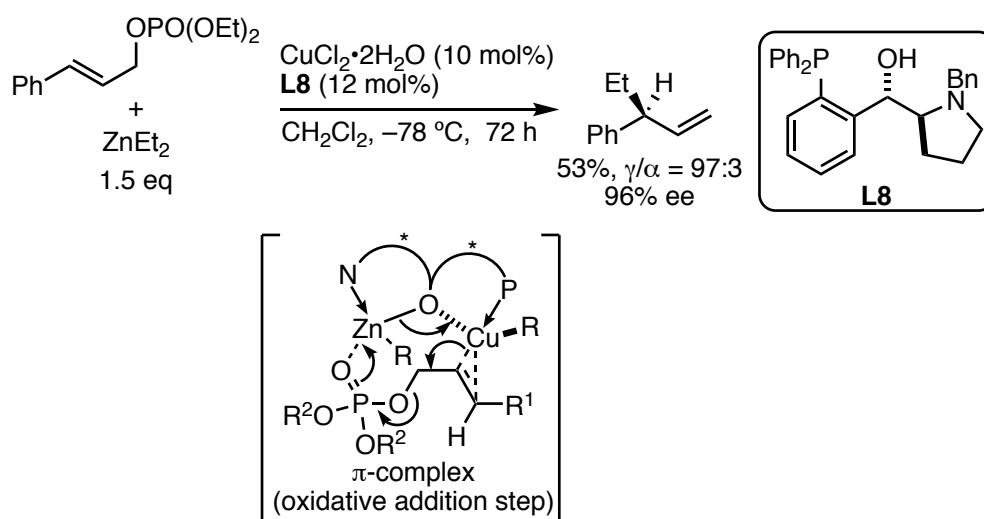
Not only *N*-heterocyclic carbene ligands, but also other-type ligand with alkoxides have been developed. However, these ligands have not been systematically studied compared to NHC ligands, and they have been mostly used in copper catalysis. In 2006, Nakamura and co-workers developed the alanine-derived aminohydroxyphosphine ligand, and achieved copper-catalyzed asymmetric conjugate addition of organozinc reagents to α , β -unsaturated carbonyl compounds (Scheme 23).²³ Using a simple model, they calculated the transition state of the oxidative addition of enone to copper center (Scheme 23 below). The calculation revealed that Lewis acidic zinc atom, which is close to the alkoxy moiety of the ligand, and the nucleophilic copper atom are properly located to effect ligand acceleration of the conjugate addition.

Scheme 23 Asymmetric Conjugate Addition with the Aminohydroxyphosphine



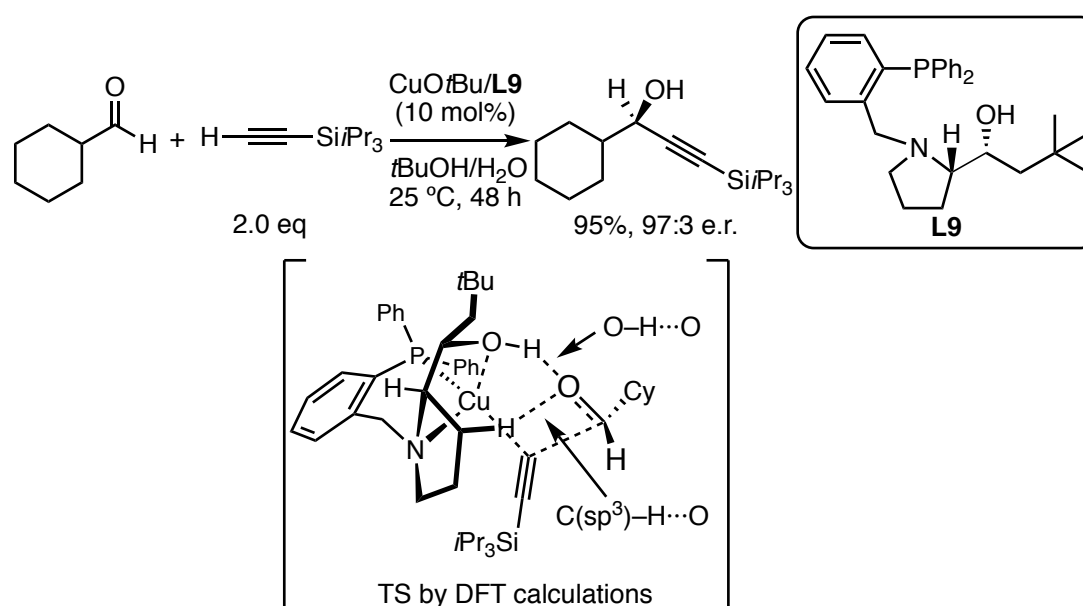
They also reported that a proline-derived ligand induced excellent regio- and enantioselectivities in the copper-catalyzed allylic alkylation with diethylzinc (Scheme 24).²⁴ A mixture of the aminohydroxyphosphine and copper(II) and diethylzinc generates copper/zinc bimetallic complex, the oxygen atom bridges the two metals. By copper–olefin and zinc–oxygen interactions with the allylic phosphate, the bimetallic complex produces a π -complex.

Scheme 24 Asymmetric Allylic Alkylation with the Aminohydroxyphosphine



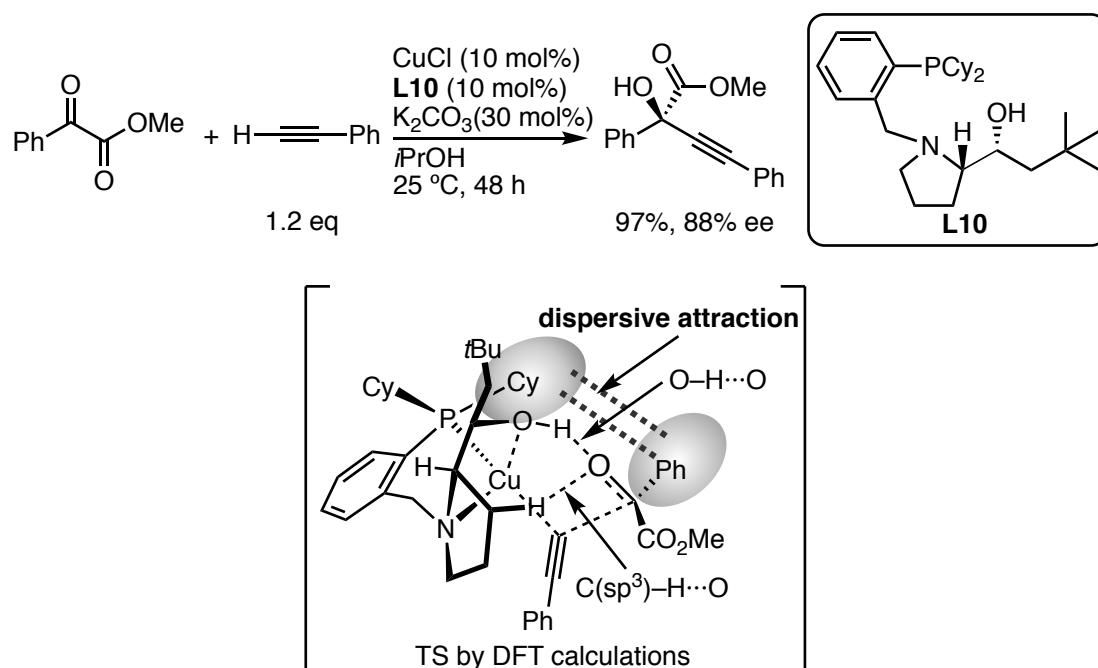
Recently, the catalytic systems, which involve hydrogen bond derived from OH group of ligand, have been developed. Sawamura and Mori reported a P/N/OH ligands, which is derivatized from proline, enables a copper-catalyzed asymmetric direct alkynylation of aldehydes (Scheme 25).^{25a} Copper alkoxide, in which Cu-O covalent bond is formed between copper atom and hydroxy group of the ligand, reacts with a terminal alkyne to produce copper acetylide species. Then, this copper acetylide complex reacts with an aldehyde to give chiral propargyl alcohols. DFT calculations revealed the involvement of $\text{O}-\text{H}\cdots\text{O}$, as well as non-classical $\text{C}(\text{sp}^3)-\text{H}\cdots\text{O}$ hydrogen bonds, in the transition state and interactions properly orient the substrates.

Scheme 25 Copper-Catalyzed Asymmetric Direct Alkynylation of Aldehydes



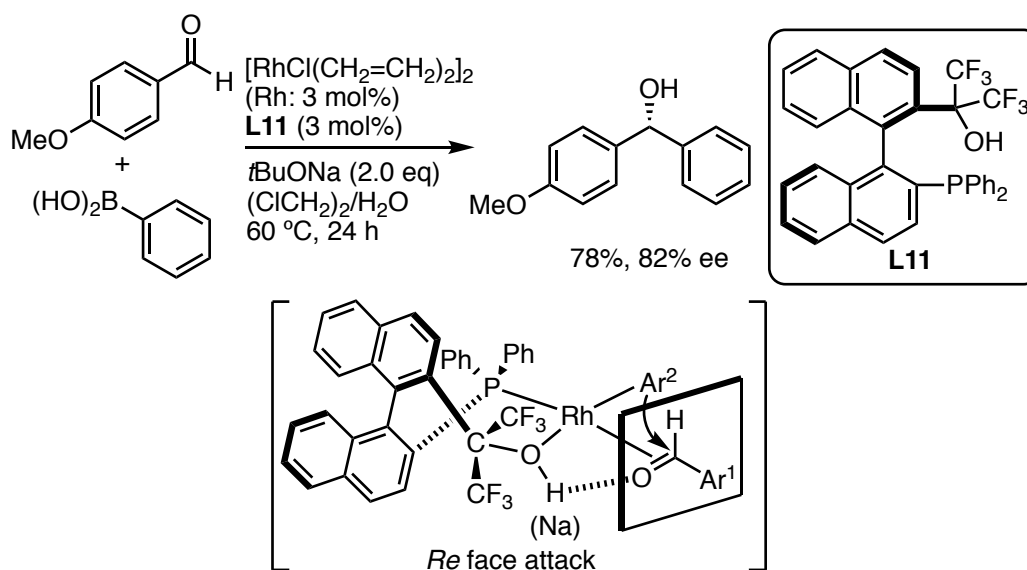
The prolinol-phosphine-copper system also allows asymmetric alkylation of α -ketoesters to proceed efficiently (Scheme 26).^{25b} They calculated enantio-determining transition state to reveal that O–H \cdots O/C(sp³)–H \cdots O two-point hydrogen bonding between the chiral ligand and the carbonyl group of the ketoester fixes orientation of the ketoester. Moreover, enantiotopic π -face is discriminated by dispersive attractions between the *P*-cyclohexyl of a ligand and the aryl substituent of ketoester (Scheme 27 below). These weak but important attractive interactions between a chiral ligand and a substrate also play a significant role in Chapter 2.

Scheme 26 Copper-Catalyzed Asymmetric Direct Alkylation of α -Ketoesters



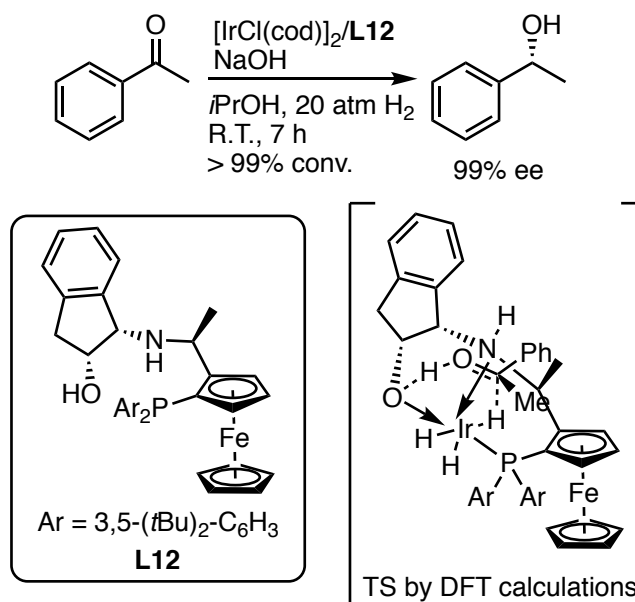
Alkoxy-contained ligands are effective not only for copper catalysts, but also for other metals. In 2010, Amii and co-workers reported hydroxylphosphine-rhodium-catalyzed 1, 2-addition of organoboronic acids to aldehydes (Scheme 27).²⁶ Migratory insertion of the C–O double bond of aldehyde into arylrhodium with the assist of OH–O or ONa–O interaction is proposed.

Scheme 27 Rhodium-Catalyzed Asymmetric 1,2-addition of aryl boronic acids to aldehydes



Recently, Zhang and co-workers reported iridium-catalyzed asymmetric hydrogenation of ketones using P/NH/OH ligands (Scheme 28).²⁷ They calculated the transition state in this reaction, and the result suggests that this reaction seems to proceed via alcohol-alkoxide interconversion at the ligand.²⁸

Scheme 28 Ir-Catalyzed Asymmetric Hydrogenation of Ketones using a P/NH/OH ligand



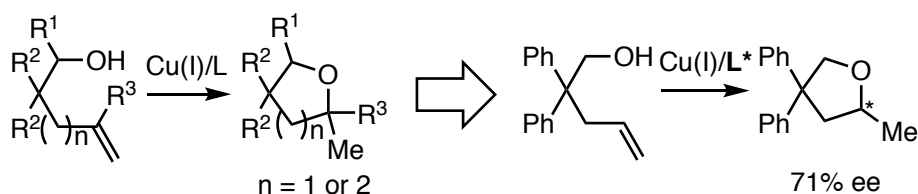
2. Overview of this Thesis

The author developed catalytic asymmetric reactions involving metal alkoxides. In Chapter 1, copper(I)-catalyzed intramolecular hydroalkoxylation of unactivated alkenes is described: the catalytic asymmetric incorporation of alcohol group to products taking advantage of high reactivity of copper-alkoxide bond. In Chapter 2, iridium-catalyzed asymmetric transfer hydrogenation of ketones with a chiral prolinol-phosphine ligand is described: the iridium-alkoxide bond efficiently activates a substrate and resulting hydroxy group of the ligand generates chiral environment.

2.1. Copper-Catalyzed Intramolecular Hydroalkoxylation of Unactivated Alkenes (Chapter 1)

Chapter 1 describes intramolecular hydroalkoxylation of unactivated alkenes by copper-bisphosphine system (Scheme 29). A reaction pathway involving the migratory insertion of the C–C double bond into the Cu–O bond is proposed. A chiral copper catalyst system promoted enantioselective reaction with moderate enantioselectivity.

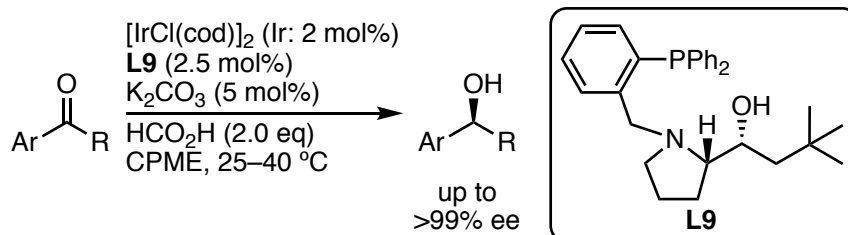
Scheme 29 Copper-Catalyzed Intramolecular Hydroalkoxylation of Unactivated Alkenes



2.2. Iridium-Catalyzed Asymmetric Transfer Hydrogenation of Ketones with a Prolinol-Phosphine Chiral Ligand (Chapter 2)

Chapter 2 describes asymmetric transfer hydrogenation of ketones by a chiral prolinol-phosphine-iridium complex using formic acid as a hydrogen source (Scheme 30). This reaction likely proceeds through alcohol-alkoxide interconversion. Moreover, DFT calculation suggests the existence of weak attractive interaction between non-polar C(sp³)-H bond and the substrates in the stereodiscriminating step.

Scheme 30 Iridium-Catalyzed Asymmetric Transfer Hydrogenation of Ketones



References

- (1) (a) Meherotra, R. C. *J. Non-Cryst. Solids* **1988**, *100*, 1. (b) Fulton, J. R.; Holland, A. W.; Fox, D. J.; Bergman, R. G. *Acc. Chem. Res.* **2002**, *35*, 44.
- (2) Caulton, K. G. *New J. Chem.* **1994**, *18*, 25.
- (3) (a) Hashiguchi, S.; Fujii, A.; Takehara, J.; Ikariya, T.; Noyori, R. *J. Am. Chem. Soc.* **1995**, *117*, 7562. (b) Dub, P. A.; Gordon, J. C. *Dalton. Trans.* **2016**, *45*, 6756.
- (4) Nishimura, T.; Onoue, T.; Ohe, K.; Uemura, S. *Tetrahedron Lett.* **1998**, *39*, 6011.
- (5) (a) Palucki, M.; Wolfe, J. P.; Buchwald, S. L. *J. Am. Chem. Soc.* **1996**, *118*, 10333. (b) Mann, G.; Hartwig, J. F. *J. Am. Chem. Soc.* **1996**, *118*, 13109. (c) Mann, G.; Shelby, Q.; Roy, A. H.; Hartwig, J. F. *Organometallics* **2003**, *22*, 2275.
- (6) (a) Chan, D. M. T.; Monaco, K. L.; Wang, R.-P.; Winters, M. P. *Tetrahedron Lett.* **1998**, *39*, 2933. (b) Evans, D. A.; Katz, J. L.; West, T. R. *Tetrahedron Lett.* **1998**, *39*, 2937. (c) King, A. E.; Ryland, B. L.; Brunold, T. C.; Stahl, S. S. *Organometallics* **2012**, *31*, 7948.
- (7) Hanley, P. S.; Hartwig, J. F. *Angew. Chem. Int., Ed.* **2013**, *52*, 8510.
- (8) (a) Bryndza, H. E.; Calabrese, J. C.; Wreford, S. S. *Organometallics* **1984**, *3*, 1603. (b) Bryndza, H. E. *Organometallics* **1985**, *4*, 406.
- (9) Zhao, P.; Incarvito, C. D.; Hartwig, J. F. *J. Am. Chem. Soc.* **2006**, *128*, 9643.
- (10) Hayashi, T.; Yamasaki, K.; Mimura, M.; Uozumi, Y. *J. Am. Chem. Soc.* **2004**, *126*, 3036.
- (11) Trend, R. M.; Ramtohl, Y. K.; Stolts, B. M. *J. Am. Chem. Soc.* **2005**, *127*, 17778.
- (12) Wolfe, J. P.; Rossi, M. A. *J. Am. Chem. Soc.* **2004**, *126*, 1620. (b) Hay, M. B.; Wolfe, J. P. *J. Am. Chem. Soc.* **2005**, *127*, 16468. (c) Nakhla, J. S.; Kampf, J. W.; Wolfe, J. P. *J. Am. Chem. Soc.* **2006**, *128*, 2893. (d) Wolfe, J. P. *Synlett* **2008**, *19*, 2913. (e) Ward, A. F.; Wolfe, J. P. *Org. Lett.* **2010**, *12*, 1268.
- (13) Chen, Y.; Yekta, S.; Yudin, A. K. *Chem. Rev.* **2003**, *103*, 3155.
- (14) Seebach, D.; Back, A. K.; Heckel, A. *Angew. Chem., Int. Ed.* **2001**, *40*, 92.
- (15) Cozzi, P. G. *Chem. Soc. Rev.* **2004**, *33*, 410.
- (16) Pape, F.; Teichert, J. F. *Eur. J. Org. Chem.* **2017**, 4206.
- (17) Arnold, P. L.; Rodden, M.; Davis, K. M.; Scarisbrick, A. C.; Blake, A. J.; Wilson, C. *Chem. Commun.* **2004**, 1612.
- (18) Larsen, A. O.; Leu, W.; Oberhuber, C. N.; Campbell, J. E.; Hoveyda, A. H. *J. Am. Chem. Soc.* **2004**, *126*, 11130.
- (19) Lee, K.-S.; Brown, M. K.; Hird, A. W.; Hoveyda, A. H. *J. Am. Chem. Soc.* **2006**, *128*, 7182.
- (20) (a) Shintani, R.; Takatsu, K.; Takeda, M.; Hayashi, T. *Angew. Chem., Int. Ed.* **2010**, *50*,

8656. (b) Takatsu, K.; Shintani, R.; Hayashi, T. *Angew. Chem., Int. Ed.* **2010**, *50*, 5548.
- (21) (a) Harada, A.; Makida, Y.; Sato, T.; Ohmiya, H.; Sawamura, M. *J. Am. Chem. Soc.* **2014**, *136*, 13932. (b) Ohmiya, H.; Zhang, H.; Shibata, S.; Harada, A.; Sawamura, M. *Angew. Chem., Int. Ed.* **2016**, *55*, 4777. (c) Yasuda, Y.; Ohmiya, H.; Sawamura, M. *Angew. Chem., Int. Ed.* **2016**, *55*, 10816. (d) Hojoh, K.; Ohmiya, H.; Sawamura, M. *J. Am. Chem. Soc.* **2017**, *139*, 2184.
- (22) Sakaguchi, S.; Yoo, K. S.; O'Neill, J.; Lee, J. H.; Stewart, T.; Jung, K. W. *Angew. Chem., Int. Ed.* **2008**, *47*, 9326.
- (23) Hajra, A.; Yoshikai, N.; Nakamura, E. *Org. Lett.* **2006**, *8*, 4153.
- (24) Yoshikai, N.; Miura, K.; Nakamura, E. *Adv. Synth. Catal.* **2009**, *351*, 1014.
- (25) For prolinol-phosphine-promoted asymmetric alkynylation, see; (a) Ishii, T.; Watanabe, R.; Moriya, T.; Ohmiya, H.; Mori, S.; Sawamura, M. *Chem. –Eur. J.* **2013**, *19*, 13547. (b) Schwarzer, M. C.; Fujioka, A.; Ishii, T.; Ohmiya, H.; Mori, S.; Sawamura, M. *Chem. Sci.* **2018**, *9*, 3484. For prolinol-phosphine-promoted another asymmetric reaction, see; (c) Takayama, Y.; Ishii, T.; Ohmiya, H.; Iwai, T.; Schwarzer, M. C.; Mori, S.; Taniguchi, T.; Monde, K.; Sawamura, M. *Chem. –Eur. J.* **2017**, *23*, 8400.
- (26) Morikawa, S.; Michigami, K.; Amii, H. *Org. Lett.* **2010**, *12*, 2520.
- (27) Yu, J.; Duan, M.; Wu, W.; Qi, X.; Xue, P.; Lan, Y.; Dong, X.-Q.; Zhang, X. *Chem. –Eur. J.* **2017**, *23*, 970.
- (28) Because excess amount of NaOH was used in Zhang's catalytic system, it is likely that the alcohol group of the ligand might take alkoxide form during the reaction. Thus suggested alcohol–alkoxide interconversion may not occur in this system.

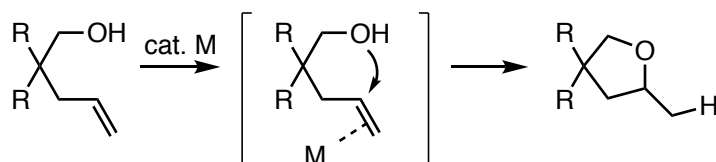
Chapter 1

Copper(I)-Catalyzed Intramolecular Hydroalkoxylation of Unactivated Alkenes

Introduction

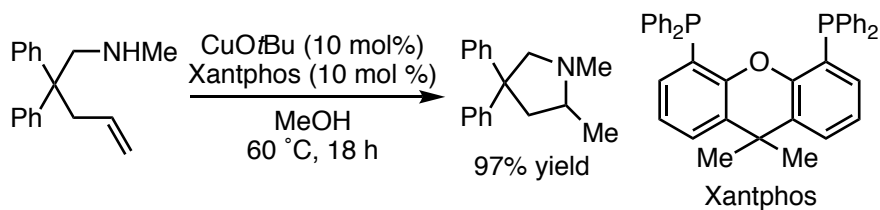
Oxygen-containing heterocyclic compounds are found in many biologically active natural products and pharmaceuticals.¹ Metal-catalyzed intramolecular hydroalkoxylation of unactivated alkenes is a straightforward method for the preparation of *O*-heterocycles.² To date, these types of reactions have been realized by using various catalysts with different metals such as Pt(II), Au(I), Ag(I), Al(III), Fe(III), Ru(II), and Cu(II).^{3,4} Notably, all of these reactions were achieved through electrophilic activation of hydroxylalkenes at the C–C double bond by π Lewis acid metals that promote outer-sphere nucleophilic addition of the hydroxy group to the alkene (Scheme 1).

Scheme 1 Outer-Sphere Nucleophilic Addition of the Hydroxy group



The author's laboratory reported copper(I)-catalyzed intramolecular hydroamination of unactivated alkenes bearing a primary or secondary amino group (Scheme 2).⁵ In sharp contrast to the outer-sphere mechanism shown above, this reaction seems to proceed via the migratory insertion of the C–C double bond into the Cu–N bond. The author considered that this catalytic system is also applicable to hydroalkoxylation of alkenes.

Scheme 2 Copper(I)-Catalyzed Hydroamination of Unactivated Alkenes

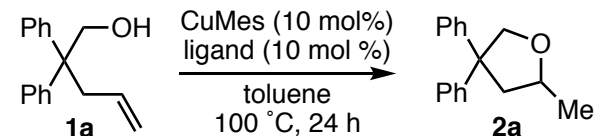


Chapter 1 describes that a Cu(I)-Xantphos catalyst system promotes the intramolecular hydroalkoxylation of unactivated terminal alkenes to give five- or six-membered ring ethers.⁶ This new copper catalysis should be mechanistically different from the previously reported intramolecular hydroalkoxylation of unactivated alkenes. Instead, addition of the Cu–O bond of an alkoxocopper(I) intermediate across the C–C double bond followed by alcoholysis of the Cu–C bond is proposed. A chiral Cu(I) catalyst system based on the (*R*)-DTBM-SEGPHOS ligand promoted enantioselective reaction with moderate enantioselectivity.

Results and Discussion

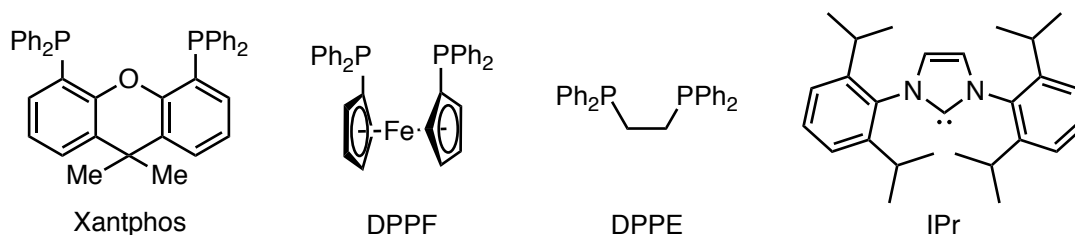
Ligand screening for the reaction of 2,2-diphenyl-4-penten-1-ol (**1a**) revealed that Xantphos, featuring an extraordinary large bite angle, was the most effective ligand. The author's laboratory previously developed the first application of Xantphos ligand to copper catalysis in dehydrogenative alcohol silylation using silane reagents.⁷ The large bite angle of Xantphos ligand is effective to inhibit the formation of dimer of copper hydride complex, which is inactive species, and stabilize the active monomeric species in dehydrogenative alcohol silylation. Accordingly, Xantphos seems to play a role of promoting the generation of active monomeric species in hydroalkoxylation of alkene. The reaction of **1a** in the presence of mesitylcopper(I) (10 mol%) and Xantphos (10 mol%) in toluene at 100 °C over 24 h afforded five-membered ring ether **2a** in 97% yield (Scheme 1, entry 1). DPPF, similarly having a large bite angle, was also effective, but the product yield was slightly decreased (entry 2). DPPE was much less effective, giving only 18% yield (entry 3). Monophosphines such as PPh₃ and PCy₃ gave low product yields (entry 4,5). *N*-heterocyclic carbene such as IPr was not available, and no reaction also occurred in the absence of a ligand (entry 6,7).

Table 1 Copper-Catalyzed Intramolecular Hydroalkoxylation



1a $\xrightarrow[\text{toluene, 100 }^\circ\text{C, 24 h}]{\text{CuMes (10 mol\%), ligand (10 mol\%)}}$ **2a**

entry	ligand	yield (%) ^b
1	Xantphos	97 (97)
2	DPPF	82
3	DPPE	18
4 ^c	PPh ₃	30
5 ^c	PCy ₃	15
6	IPr	0
7	None	0



^aConditions: CuMes (10 mol%), ligand (10 mol%), **1a** (0.15 mmol), toluene (0.3 mL), 100 °C, 24 h. ^bYield was determined by ¹H NMR (Yield of isolated product in parenthesis). ^cligand (20 mol%) was used.

It is well-known that σ -bond metathesis between the Cu–C bond of mesitylcopper(I) and the O–H bond of alcohols produces the corresponding copper(I) alkoxides, which are generally poor Lewis acids.⁸ Accordingly, a π Lewis acid mechanism involving outer-sphere nucleophilic addition of the hydroxy group to the alkene should be ruled out for the present Cu(I)-catalyzed intramolecular hydroalkoxylation. Instead, Figure 1 describes a mechanism involving the insertion of the alkene into the Cu–O bond of the copper(I) alkoxide. The catalytic cycle would be initiated by the reaction between the mesitylcopper–Xantphos complex and the H–O bond of the substrate (**1**) to form copper alkoxide **A**. Subsequently, the terminal alkene forms Cu–alkene π -complex **B**. Next, the intramolecular addition of the Cu–O bond across the C–C double bond affords alkylcopper intermediate **C** with an oxygen heterocycle. Finally, protonolysis of the Cu–C bond of **C** with the H–O bond of **1** gives the product (**2**).

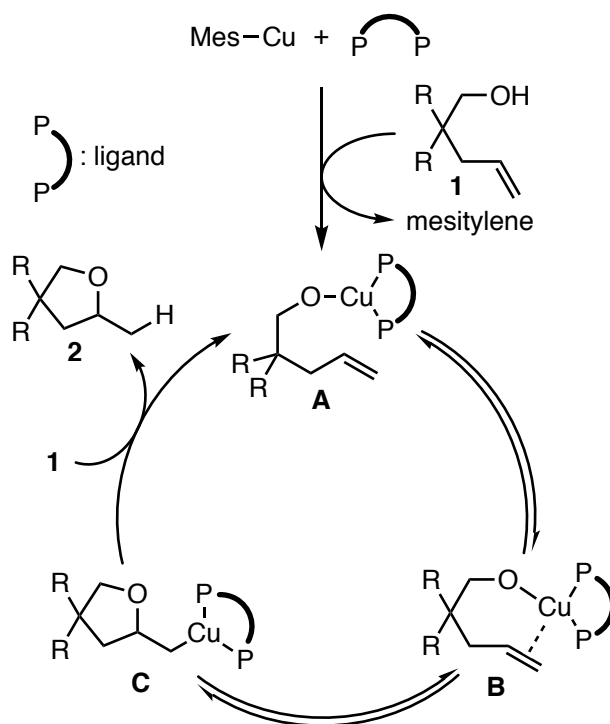


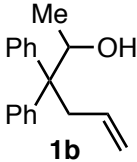
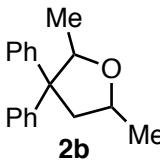
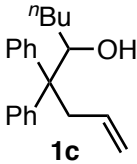
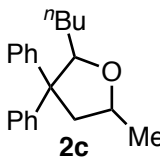
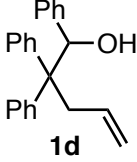
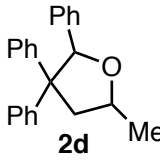
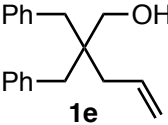
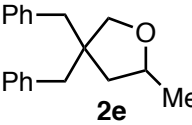
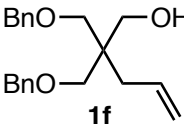
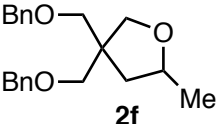
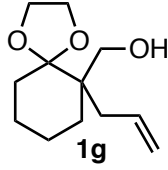
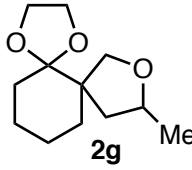
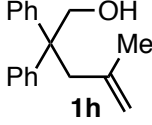
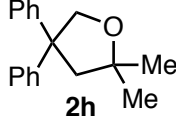
Figure 1 Possible Catalytic Cycle

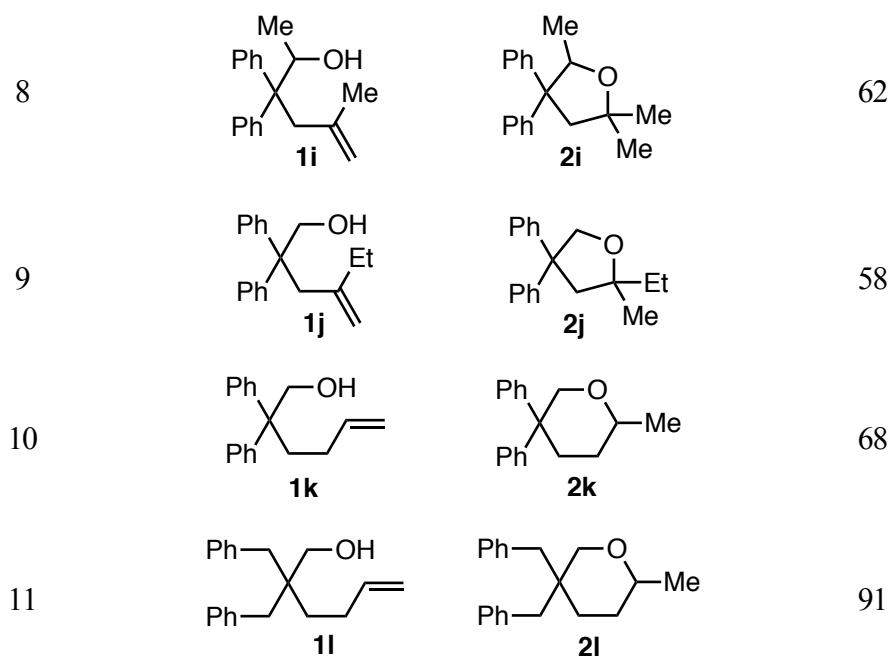
The author examined various hydroxyalkenes as substrates for the Cu-catalyzed hydroalkoxylation for preparing tetrahydrofuran derivatives (Table 2). The Cu(I)–Xantphos catalyst system was also effective for the reaction of secondary alcohols (**1b–d**) (entries 1–3), tolerating various substituents such as Me, *n*-Bu, and Ph groups at the position α to the hydroxy group. The hydroxyalkenes with a dibenzylmethylene (**1e**) or a di-(benzyloxymethyl)methylene (**1f**) inserted in the linker chain underwent the reaction in moderate yields (entries 4 and 5). Spirocyclization of the cyclohexanone acetal derivative **1g**

proceeded efficiently and cleanly with the acetal moiety untouched (entry 6). The geminally disubstituted alkenes **1h–j** also underwent the hydroxylation to construct a quaternary carbon center (entries 7–9). The hydroalkoxylation of 1,2-disubstituted alkene did not proceed at all (data not shown).

The extension of this methodology to six-membered ring formation was feasible (Table 2, entries 10 and 11). Thus, the reaction of 5-hexene-1-ol derivatives **1k** and **1l** occurred to give the corresponding tetrahydrofuran derivatives (**2k**, **2l**) in good yields.

Table 2 Substrate Scope^a

entry	substrate	product	yield (%) ^b
1			77 ^c
2			85 ^c
3			81 ^c
4			40
5			77
6			96 ^d
7			82



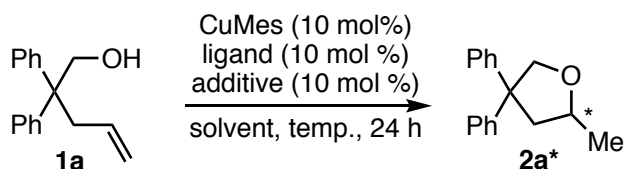
^aConditions: CuMes–Xantphos (10 mol%), **1** (0.15 mmol), toluene (0.3 mL), 100 °C, 24 h. ^bYield of the isolated product. ^cDiastereomeric ratio (3:1). ^dDiastereomeric ratio (1:1)

Next, the author explored the catalytic enantioselective hydroalkoxylation. Copper complexes prepared from mesitylcopper (10 mol%), and various chiral bisphosphine ligands were examined in the reaction of **1a** in toluene at 60 °C for 24 h (Table 3). The catalyst prepared from (*S,S*)-Chiraphos (**L1**) or (*R,S*)-Josiphos (**L2**) did not promote the reaction at all (entries 1 and 2). (*S,S*)-(*R,R*)-Ph-TRAP (**L3**)⁹ and (*R*)-SEGPHOS (**L4**) induced only low catalytic activity and enantioselectivity (entries 3 and 4). Further screening of chiral ligands revealed that introducing 3,5-di-*tert*-butyl-4-methoxyphenyl (DTBM) substituents on the phosphorus atoms of chiral bisphosphines was important not only for enantiocontrol but also catalytic activity (entries 5–7).¹⁰ The bulky substituent such as DTBM group stabilize the monomeric metal complex, and exerts a steric effect around the reaction center. Thus, (*R*)-DTBM-BINAP (**L5**) induced a moderate enantioselectivity, albeit with a poor product yield (entry 5). The use of (*R*)-DTBM-MeO-BIPHEP (**L6**) increased product yield, but this change did not improve the enantioselection (entry 6). The use of (*R*)-DTBM-SEGPHOS (**L7**)¹¹ led to a significant improvement in the product yield with the enantioselectivity unchanged (entry 7). It should be noted that this is the first metal-catalyzed enantioselective intramolecular hydroalkoxylation of unactivated alkenes.

The enantioselection could be improved to 62% ee by carrying out the reaction at 30 °C, but with a serious reduction of the yield (Table 3, entry 8). Interestingly, the enantioselectivity could be increased to 67% ee by adding a catalytic amount of *t*BuOH (10 mol%), also with a

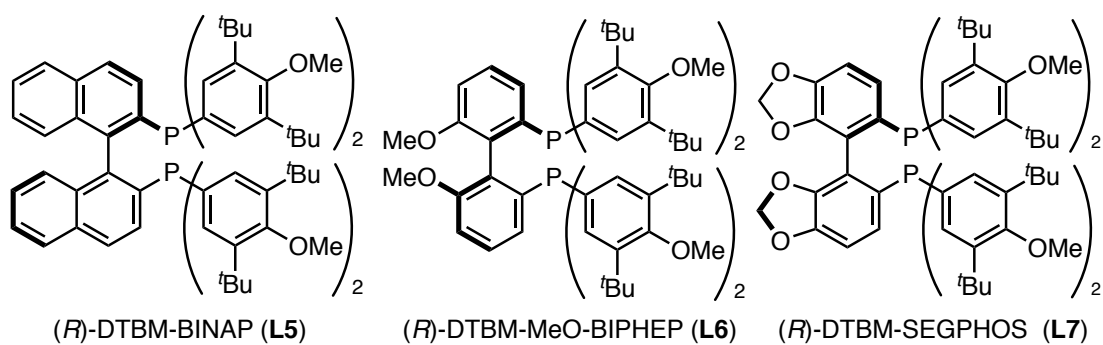
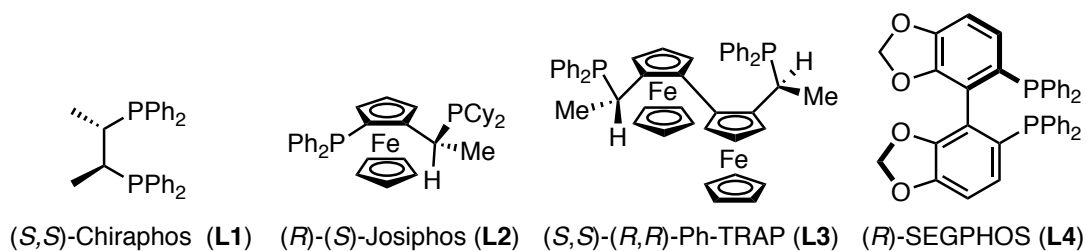
reduction of the yield (30 %) (entry 9). The enantioselectivity was further improved to 71% ee using hexane as a solvent with an increase in the product yield (39%) (entry 10).¹² This result suggested the reversibility of the Cu-alkene π -complex **B** and alkylcopper intermediate **C** (see Figure 1).

Table 3 Enantioselective Reaction^a



entry	ligand	additive	solvent	temp (° C)	yield (%) ^b	ee (%) ^c
1	L1	none	toluene	60	0	
2	L2	none	toluene	60	0	
3	L3	none	toluene	60	22	9
4	L4	none	toluene	60	23	4
5	L5	none	toluene	60	7	51
6	L6	none	toluene	60	60	51
7	L7	none	toluene	60	94	51
8	L7	none	toluene	30	46	62
9	L7	<i>t</i> BuOH	toluene	30	30	67
10	L7	<i>t</i> BuOH	hexane	30	39	71

^aConditions: CuMes (10 mol%), ligand (10 mol%), **1a** (0.15 mmol), solvent (0.3 mL), 24 h. ^bYield of the isolated product. ^cThe enantiomeric excess was determined by HPLC analysis.



Conclusion

The Cu–Xantphos system catalyzed the intramolecular hydroalkoxylation of unactivated terminal alkenes, giving five- and six-membered ring ethers. This system is applicable to both primary and secondary alcohols. A reaction pathway involving the addition of the Cu–O bond across the C–C double bond is proposed. A chiral Cu(I) catalyst system based on the (*R*)-DTBM-SEGPHOS ligand promoted enantioselective reaction with moderate enantioselectivity.

Experimental Section

Instrumentation and Chemicals

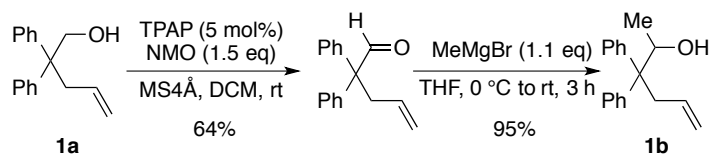
NMR spectra were recorded on a JEOL ECX-400, operating at 400 MHz for ^1H NMR and 100.5 MHz for ^{13}C NMR. Chemical shift values for ^1H and ^{13}C are referenced to Me_4Si . Chemical shifts are reported in δ ppm. Mass spectra were obtained with Thermo Fisher Scientific Exactive, JEOL JMS-T100LP or JEOL JMS-700TZ at the Instrumental Analysis Division, Equipment Management Center, Creative Research Institution, Hokkaido University. Elemental analysis was performed at the Instrumental Analysis Division, Equipment Management Center, Creative Research Institution, Hokkaido University. HPLC analyses were conducted on a HITACHI ELITE LaChrom system with a HITACHI L-2455 diode array detector. TLC analyses were performed on commercial glass plates bearing 0.25-mm layer of Merck Silica gel 60F₂₅₄. Silica gel (Kanto Chemical Co., Silica gel 60 N, spherical, neutral) was used for column chromatography.

All reactions were carried out under nitrogen or argon atmosphere. Materials were obtained from commercial suppliers or prepared according to standard procedures unless otherwise noted. Mesityl copper and (*R*)-DTBM-SEGPHOS[®] were purchased from Strem Chemical Int., and stored under nitrogen, and used as it is. Xantphos was purchased from Tokyo Kasei Kogyo Co., Ltd., stored under nitrogen, and used as it is. Toluene, hexane and *t*-BuOH were purchased from Kanto Chemical Co., stored over 4Å molecular sieves under nitrogen. Hydroxyalkenes **1a**^{3a}, **1e**¹³, **1g**¹⁴, **1h**¹⁵ and **1k**^{3a} are known compounds.

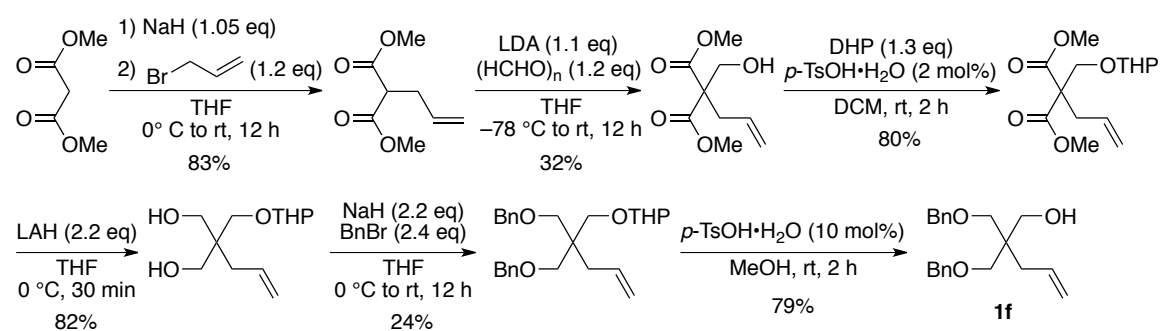
Preparation of Hydroxyalkenes

Hydroxyalkenes **1b–d** and **1i** were prepared from **1a** or **1h**. The preparation of **1b** is representative (Scheme 3). Hydroxyalkene **1f** was synthesized in 6 steps from dimethyl malonate (Scheme 4). **1j** and **1l** were prepared in accordance to the literature procedure^{3a,13}.

Scheme 3

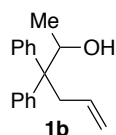


Scheme 4



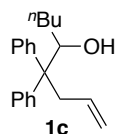
Characterization Data for Hydroxyalkenes

3,3-Diphenyl-5-hexen-2-ol (1b)



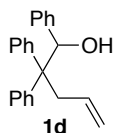
Colorless oil. $^1\text{H NMR}$ (400 MHz, CDCl_3) δ 1.05 (d, $J = 6.0$ Hz, 3H), 1.37 (d, $J = 8.4$ Hz, 1H), 2.87 (dd, $J = 13.6, 6.8$ Hz, 1H), 2.98 (dd, $J = 13.6, 6.8$ Hz, 1H), 4.63 (dq, $J = 8.4, 6.0$ Hz, 1H), 4.93–5.05 (m, 2H), 5.40 (ddt, $J = 17.2, 10.0, 6.8$ Hz, 1H), 7.22–7.32 (m, 10H). $^{13}\text{C NMR}$ (100.5 MHz, CDCl_3) δ 18.89, 42.77, 55.63, 69.38, 117.59, 126.18, 126.29, 127.60, 127.72, 129.48, 129.64, 134.68, 143.46, 144.42. **HRMS-ESI** (m/z): $[\text{M}+\text{Na}]^+$ calcd for $\text{C}_{18}\text{H}_{20}\text{ONa}$, 275.14064; found, 275.14051.

4,4-Diphenyl-1-nonen-5-ol (1c)



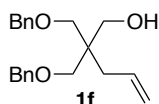
Colorless oil. $^1\text{H NMR}$ (400 MHz, CDCl_3) δ 0.74 (m, 1H), 0.86 (t, $J = 7.2$ Hz, 3H), 1.18–1.40 (m, 4H), 1.51 (m, 1H), 1.69 (m, 1H), 2.88 (dd, $J = 13.6, 7.6$ Hz, 1H), 3.03 (dd, $J = 13.6, 7.6$ Hz, 1H), 4.34 (t, $J = 9.6$ Hz, 1H), 4.94 (d, $J = 10.4$ Hz, 1H), 5.01 (d, $J = 17.2$ Hz, 1H), 5.40 (ddt, $J = 17.2, 10.4, 7.6$ Hz, 1H), 7.17–7.35 (m, 10H). $^{13}\text{C NMR}$ (100.5 MHz, CDCl_3) δ 14.12, 22.64, 29.00, 32.67, 42.82, 55.62, 73.84, 117.63, 126.18 ($\times 2\text{C}$), 127.61, 127.67, 129.43, 129.55, 134.81, 144.07, 144.37. **HRMS-ESI** (m/z): $[\text{M}+\text{Na}]^+$ calcd for $\text{C}_{21}\text{H}_{26}\text{ONa}$, 317.18759; found, 317.18828.

1,2,2-Triphenyl-4-penten-1-ol (1d)



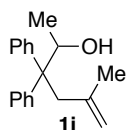
Colorless oil. $^1\text{H NMR}$ (400 MHz, CDCl_3) δ 2.20 (d, $J = 4.8$ Hz, 1H), 2.64 (dd, $J = 14.8$, 7.6, 1H), 2.75 (ddt, $J = 14.8$, 5.6, 2.0 Hz, 1H), 4.95–4.99 (m, 2H), 5.51 (m, 1H), 5.59 (d, $J = 4.8$ Hz, 1H), 6.66–6.69 (m, 2H), 7.11–7.31 (m, 13 H). $^{13}\text{C NMR}$ (100.5 MHz, CDCl_3) δ 42.63, 56.14, 77.21, 117.94, 126.10, 126.57, 127.05, 127.15, 127.66, 127.80, 128.33, 129.29, 130.59, 134.74, 140.41, 142.18, 145.24. **HRMS–ESI** (m/z): $[\text{M}+\text{Na}]^+$ calcd for $\text{C}_{23}\text{H}_{22}\text{ONa}$, 337.15629; found, 337.15701.

2,2-Bis(benzyloxy)methyl-4-penten-1-ol (1f)



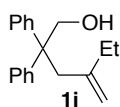
Colorless oil. $^1\text{H NMR}$ (400 MHz, CDCl_3) δ 2.17 (d, $J = 7.6$ Hz, 2H), 2.78 (t, $J = 6.0$ Hz, 1H), 3.46 (d, $J = 8.8$ Hz, 2H), 3.50 (d, $J = 8.8$ Hz, 2H), 3.64 (d, $J = 6.0$ Hz, 2H), 4.47 (d, $J = 12.4$ Hz, 2H), 4.51 (d, $J = 12.4$ Hz, 2H), 5.03 (d, $J = 10.8$ Hz, 1H), 5.04 (d, $J = 16.8$ Hz, 1H), 5.76 (ddt, $J = 16.8$, 10.8, 7.6 Hz, 1H), 7.26–7.38 (m, 10H). $^{13}\text{C NMR}$ (100.5 MHz, CDCl_3) δ 35.13, 43.18, 67.25, 72.66, 73.44, 117.97, 127.42, 127.55, 128.32, 133.78, 138.16. **HRMS–ESI** (m/z): $[\text{M}+\text{Na}]^+$ calcd for $\text{C}_{21}\text{H}_{26}\text{O}_3\text{Na}$, 349.17742; found, 349.17804.

5-Methyl-3,3-diphenyl-5-hexen-2-ol (1i)



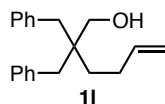
Colorless oil. $^1\text{H NMR}$ (400 MHz, CDCl_3) δ 1.02 (s, 3H), 1.07 (d, $J = 6.0$ Hz, 3H), 1.36 (d, $J = 8.4$ Hz, 1H), 2.75 (d, $J = 13.2$ Hz, 1H), 3.14 (d, $J = 13.2$ Hz, 1H), 4.64 (s, 1H), 4.76–4.83 (m, 2H), 7.20–7.31 (m, 10H). $^{13}\text{C NMR}$ (100.5 MHz, CDCl_3) δ 19.37, 24.43, 45.53, 55.52, 68.38, 115.48, 126.17, 126.20, 127.49, 127.55, 129.66, 129.76, 143.16, 144.38, 144.50. **HRMS–ESI** (m/z): $[\text{M}+\text{Na}]^+$ calcd for $\text{C}_{19}\text{H}_{22}\text{ONa}$, 289.15629; found, 289.15689.

4-Methylene-2,2-diphenyl-1-hexanol (1j)



Colorless oil. $^1\text{H NMR}$ (400 MHz, CDCl_3) δ 0.77 (t, $J = 7.6$ Hz, 3H), 1.07 (t, $J = 6.8$ Hz, 1H), 1.27 (q, $J = 7.6$ Hz, 2H), 2.95 (s, 2H), 4.24 (d, $J = 6.8$ Hz, 2H), 4.67 (m, 1H), 4.85 (m, 1H), 7.17–7.30 (m, 10H). $^{13}\text{C NMR}$ (100.5 MHz, CDCl_3) δ 12.54, 29.85, 41.94, 51.58, 67.07, 113.24, 126.36, 128.10, 128.33, 145.88, 148.09. **HRMS–ESI** (m/z): $[\text{M}+\text{Na}]^+$ calcd for $\text{C}_{19}\text{H}_{22}\text{ONa}$, 289.15629; found, 289.15629.

2,2-Dibenzyl-5-hexen-1-ol (11)



Colorless oil. $^1\text{H NMR}$ (400 MHz, CDCl_3) δ 1.17 (m, 1H), 1.25 (dt, $J = 8.6, 4.8$ Hz, 2H), 2.23–2.29 (m, 2H), 2.66 (d, $J = 13.2$ Hz, 2H), 2.79 (d, $J = 13.2$ Hz, 2H), 3.32 (d, $J = 5.2$ Hz, 2H), 4.96 (d, $J = 10.4$ Hz, 1H), 5.05 (dt, $J = 16.0, 2.0$ Hz, 1H), 5.80 (ddq, $J = 16.0, 10.4, 6.0$ Hz, 1H), 7.21–7.31 (m, 10H). $^{13}\text{C NMR}$ (100.5 MHz, CDCl_3) δ 27.80, 31.64, 40.92, 42.73, 66.11, 114.37, 126.17, 128.12, 130.45, 138.34, 138.64. **HRMS–APCI** (m/z): $[\text{M}+\text{H}]^+$ calcd for $\text{C}_{20}\text{H}_{25}\text{O}$, 281.18999; found, 281.19008.

Procedures for Copper(I)-Catalyzed Intramolecular Hydroalkoxylation of Unactivated Alkenes

Typical Procedure for Copper(I)-Catalyzed Intramolecular Hydroalkoxylation of Unactivated Alkenes.

The reaction in Scheme 1 is representative. In a glove box, mesityl copper (2.7 mg, 0.015 mmol) and Xantphos (8.7 mg, 0.015 mmol) were placed in a screw vial containing a magnetic stirring bar. Toluene (0.3 mL) was added to the vial and the mixture was stirred at room temperature for 5 min to give a pale yellow solution. Next, hydroxyalkene 1a (35.8 mg, 0.15 mmol) was added. The vial was sealed with a screw cap, and was removed from the glove box. After 24 h stirring at 100 °C, the mixture was filtered through a short plug of silica gel. The solvent was removed under reduced pressure. Flash chromatography on silica gel (0–8% EtOAc/hexane) gave 2a (34.7 mg, 0.146 mmol) in 97% yield.

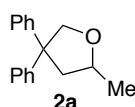
Typical Procedure for Enantioselective Intramolecular Hydroalkoxylation of 1a.

The reaction in Table 2, entry 10 is representative. In a glove box, mesityl copper (2.7 mg, 0.015 mmol) and (R)-DTBM-SEGPHOS® (17.7 mg, 0.015 mmol) were placed in a screw vial containing a magnetic stirring bar. Hexane (0.3 mL) was added to the vial, and the

mixture was stirred at room temperature for 5 min to give a yellow suspension. Next, *t*-BuOH (1.4 μ L, 0.015 mmol) and hydroxyalkene **1a** (35.8 mg, 0.15 mmol) was added to the vial. The vial was sealed with a screw cap, and was removed from the glove box. After 24 h stirring at 30 $^{\circ}$ C, the mixture was filtered through a short plug of silica gel. The solvent was removed under reduced pressure. Flash chromatography on silica gel (0–8% EtOAc/hexane) gave **2a**^{*} (14.0 mg, 0.059 mmol) in 39% yield.

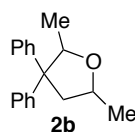
Characterization Data for Cyclic Ethers

2-Methyl-4,4-diphenyltetrahydrofuran (**2a**)



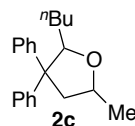
The product **2a** was purified by flash chromatography on silica gel (0–8% EtOAc/hexane) (34.7 mg, 97% isolated yield from **1a**). **2a** was consistent with the the literature data.^{3a}

2,5-Dimethyl-3,3-diphenyltetrahydrofuran (**2b**)



The product **2b** (dr 3:1) was purified by flash chromatography on silica gel (0–8% EtOAc/hexane) (29.1 mg, 77% isolated yield from **1b**). **2b** was consistent with the the literature data.^{3f}

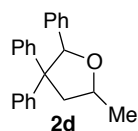
2-Butyl-5-methyl-3,3-diphenyltetrahydrofuran (**2c**)



The product **2c** (dr 3:1) was purified by flash chromatography on silica gel (0–8% EtOAc/hexane) (37.5 mg, 85% isolated yield from **1c**). Colorless oil. ¹H NMR (400 MHz, CDCl₃) δ 0.81–1.60 (m, 0.25 \times 12H, 0.75 \times 12H), 2.09 (dd, *J*=13.2, 6.4 Hz, 0.25 \times 1H), 2.35 (dd, *J*=12.0, 6.0 Hz, 0.75 \times 1H), 2.52 (dd, *J*=12.0, 9.6 Hz, 0.75 \times 1H), 3.10 (dd, *J*=13.2, 8.0 Hz, 0.25 \times 1H), 3.99 (dtq, *J*=9.6, 6.0, 6.0 Hz, 0.75 \times 1H), 4.52–4.62 (m, 0.25 \times 2H, 0.75 \times 1H), 6.98–7.35 (m, 0.25 \times 10H, 0.75 \times 10H). ¹³C NMR (100.5 MHz, CDCl₃) δ 14.10, 14.15, 21.74, 22.62, 22.79, 22.86, 28.83, 29.66, 31.65, 34.05, 46.07, 48.81, 58.61, 59.21, 72.77, 73.24, 82.43,

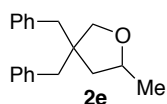
84.39, 125.93 ($\times 2C$), 125.98, 126.07, 127.62, 127.71, 127.85, 127.87, 128.03, 128.14, 128.49, 128.68, 145.33, 145.56, 147.88, 148.30. **HRMS–APCI** (m/z): $[M+H]^+$ calcd for $C_{21}H_{27}O$, 295.20564; found, 295.20557.

5-Methyl-2,3,3-triphenyltetrahydrofuran (**2d**)



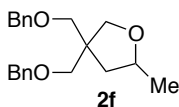
The product **2d** (dr 3:1) was purified by flash chromatography on silica gel (0–8% EtOAc/hexane) (36.3 mg, 77% isolated yield from **1d**). Colorless oil. **1H NMR** (400 MHz, $CDCl_3$) δ 1.34 (d, $J=6.4$ Hz, $0.75 \times 1H$), 1.56 (d, $J=5.6$ Hz, $0.25 \times 3H$, $0.75 \times 2H$), 2.18 (dd, $J=11.2, 5.2$, Hz, $0.75 \times 1H$), 2.26 (dd, $J=13.4, 7.6$ Hz, $0.25 \times 1H$), 2.75 (t, $J=11.2$ Hz, $0.75 \times 1H$), 3.32 (dd, $J=13.4, 7.6$ Hz, $0.25 \times 1H$), 4.17 (dq, $J=11.2, 5.6, 5.2$ Hz, $0.75 \times 1H$), 4.82 (tq, $J=7.6, 6.4, 0.25 \times 1H$), 5.78 (s, $0.25 \times 1H$), 5.81 (s, $0.75 \times 1H$), 6.82–7.59 (m, $0.25 \times 15H$, $0.75 \times 15H$). **^{13}C NMR** (100.5 MHz, $CDCl_3$) δ 20.12, 22.95, 43.90, 49.62, 60.94, 61.66, 73.49, 73.84, 84.97, 87.40, 125.94, 126.07, 126.15, 126.22, 126.59, 127.11, 127.15, 127.31, 127.34, 127.55, 127.88, 127.93, 128.02, 128.13, 128.26 ($\times 2C$), 128.76, 129.60, 138.80, 141.44, 143.10, 143.66, 147.35, 148.29. **HRMS–ESI** (m/z): $[M+Na]^+$ calcd for $C_{23}H_{22}ONa$, 337.15629; found, 337.15701.

4,4-Dibenzyl-2-methyltetrahydrofuran (**2e**)



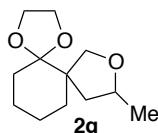
The product **2e** was purified by flash chromatography on silica gel (0–8% EtOAc/hexane) (16.0 mg, 40% isolated yield from **1e**). Colorless oil. **1H NMR** (400 MHz, $CDCl_3$) δ 1.15 (d, $J=6.4$ Hz, 3H), 1.42 (dd, $J=12.8, 8.8$ Hz, 1H), 1.95 (dd, $J=12.8, 6.4$ Hz, 1H), 2.73–2.81 (m, 4H), 3.68 (dd, $J=8.8, 3.6$ Hz, 2H), 3.98 (ddq, $J=8.8, 6.4, 6.4$ Hz, 1H), 7.15–7.30 (m, 10H). **^{13}C NMR** (100.5 MHz, $CDCl_3$) δ 21.64, 42.43, 42.94, 43.09, 48.42, 74.73, 74.86, 126.22 ($\times 2C$), 128.07 ($\times 2C$), 130.59, 130.64, 138.37, 138.56. **HRMS–APCI** (m/z): $[M+H]^+$ calcd for $C_{19}H_{23}O$, 267.17434; found, 267.17439.

4,4-Bis[(benzyloxy)methyl]-2-methyltetrahydrofuran (**2f**)



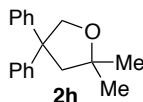
The product **2f** was purified by flash chromatography on silica gel (0–10% EtOAc/hexane) (37.7 mg, 77% isolated yield from **1f**). Colorless oil. $^1\text{H NMR}$ (400 MHz, CDCl_3) δ 1.23 (d, $J = 6.0$ Hz, 3H), 1.28 (dd, $J = 12.4, 8.8$ Hz, 1H), 1.95 (dd, $J = 12.4, 6.0$ Hz, 1H), 3.42–3.51 (m, 4H), 3.55 (d, $J = 9.2$ Hz, 1H), 3.78 (d, $J = 9.2$ Hz, 1H), 3.96 (dq, $J = 15.2, 6.0$ Hz, 1H), 4.48–4.54 (m, 4H), 7.24–7.36 (m, 10H). $^{13}\text{C NMR}$ (100.5 MHz, CDCl_3) δ 20.81, 40.38, 49.35, 72.07, 73.18, 73.22, 73.25, 73.28, 75.23, 127.38, 127.44, 128.28, 138.51. **HRMS–ESI** (m/z): $[\text{M}+\text{Na}]^+$ calcd for $\text{C}_{21}\text{H}_{26}\text{O}_3\text{Na}$, 349.17742; found, 349.17801.

9-Methyl-1,4,8-trioxadispiro[4,0,4,4]tetradecane (**2g**)



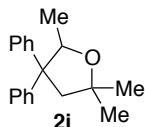
The product **2g** (dr 1:1) was purified by flash chromatography on silica gel (0–10% EtOAc/hexane) (30.6 mg, 96% isolated yield from **1g**). Colorless oil. $^1\text{H NMR}$ (400 MHz, CDCl_3) δ 1.15 (dd, $J = 12.4, 9.2$ Hz, $0.5 \times 1\text{H}$), 1.25 (t, $J = 6.4$ Hz, $0.5 \times 3\text{H}$, $0.5 \times 3\text{H}$), 1.36–1.77 (m, $0.5 \times 9\text{H}$, $0.5 \times 9\text{H}$), 2.18 (dd, $J = 12.4, 6.0$ Hz, $0.5 \times 1\text{H}$), 3.42 (d, $J = 8.8$ Hz, $0.5 \times 1\text{H}$), 3.60 (d, $J = 8.8$ Hz, $0.5 \times 1\text{H}$), 3.79 (d, $J = 8.4$ Hz, $0.5 \times 1\text{H}$), 3.94–4.04 (m, $0.5 \times 6\text{H}$, $0.5 \times 5\text{H}$). $^{13}\text{C NMR}$ (100.5 MHz, CDCl_3) δ 20.42, 21.08, 22.04, 22.21, 23.05, 23.16, 32.31 ($\times 2\text{C}$), 34.82, 37.17, 40.98, 42.94 ($\times 2\text{C}$), 52.22, 64.65 ($\times 2\text{C}$), 64.75, 64.87, 74.32, 74.37, 74.94, 76.18, 111.12, 111.54. **HRMS–EI** (m/z): $[\text{M}]^+$ calcd for $\text{C}_{12}\text{H}_{20}\text{O}_3$, 212.14124; found, 212.14068.

2,2-Dimethyl-4,4-diphenyltetrahydrofuran (**2h**)



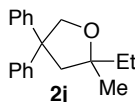
The product **2h** was purified by flash chromatography on silica gel (0–10% EtOAc/hexane) (31.0 mg, 82% isolated yield from **1h**). **2h** was consistent with the literature data.¹⁵

2,2,5-Trimethyl-4,4-diphenyltetrahydrofuran (**2i**)



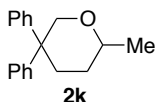
The product **2i** was purified by flash chromatography on silica gel (0–8% EtOAc/hexane) (24.8 mg, 62% isolated yield from **1i**). Colorless oil. $^1\text{H NMR}$ (400 MHz, CDCl_3) δ 0.97 (d, $J = 6.4$ Hz, 3H), 1.06 (s, 3H), 1.50 (s, 3H), 2.52 (d, $J = 13.2$, 1H), 2.93 (d, $J = 13.2$ Hz, 1H), 4.99 (q, $J = 6.4$ Hz, 1H), 7.03–7.06 (m, 2H), 7.13–7.33 (m, 8H). $^{13}\text{C NMR}$ (100.5 MHz, CDCl_3) δ 19.00, 28.72, 30.45, 52.71, 59.44, 78.96, 79.31, 125.85, 125.91, 127.72, 127.99, 128.12, 128.43, 146.63, 148.26. **HRMS–APCI** (m/z): $[\text{M}+\text{H}]^+$ calcd for $\text{C}_{19}\text{H}_{23}\text{O}$, 267.17434; found, 267.17440.

2-Ethyl-2-methyl-4,4-diphenyltetrahydrofuran (**2j**)



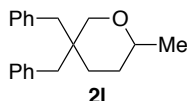
The product **2j** was purified by flash chromatography on silica gel (0–8% EtOAc/hexane) (23.2 mg, 58% isolated yield from **1j**). **2j** was consistent with the the literature data.¹⁶

2-Methyl-5,5-diphenyltetrahydro-2H-pyran (**2k**)



The product **2k** was purified by flash chromatography on silica gel (0–8% EtOAc/hexane) (25.7 mg, 68% isolated yield from **1k**). **2k** was consistent with the the literature data.^{3a}

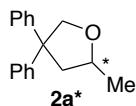
5,5-Dibenzyl-2-methyltetrahydro-2H-pyran (**2l**)



The product **2l** was purified by flash chromatography on silica gel (0–8% EtOAc/hexane) (38.3 mg, 91% isolated yield from **1l**). Colorless oil. $^1\text{H NMR}$ (400 MHz, CDCl_3) δ 1.19 (d, $J = 6.0$ Hz, 3H), 1.45–1.50 (m, 3H), 1.68 (m, 1H), 2.43 (d, $J = 13.6$ Hz, 1H), 2.48 (d, $J = 13.6$ Hz, 1H), 2.79 (d, $J = 13.2$ Hz, 1H), 2.99 (d, $J = 13.2$ Hz, 1H), 3.16–3.22 (m, 2H), 3.62 (d, $J = 11.6$ Hz, 1H), 7.00–7.02 (m, 2H), 7.19–7.32 (m, 8H). $^{13}\text{C NMR}$ (100.5 MHz, CDCl_3) δ 21.79, 29.75, 30.65, 36.81, 40.76, 42.97, 73.41, 73.83, 126.00, 126.04, 127.74, 127.94, 130.87,

130.99, 137.55, 138.57. **HRMS–EI** (m/z): $[M]^+$ calcd for $C_{20}H_{24}O$, 280.18271; found, 280.18251.

(+)-2-Methyl-4,4-diphenyltetrahydrofuran ($2a^*$)



The product $2a^*$ was purified by flash chromatography on silica gel (0–8% EtOAc/hexane) (14.0 mg, 39% isolated yield from **1a**). $[\alpha]_D^{24} +53.7$ (c 1.00, $CHCl_3$). The ee value (71% ee) was determined by chiral HPLC analysis of $2a^*$, [CHIRALCEL[®] AD-H column, 4.6 mm × 250 mm, Daicel Chemical Industries, *i*-PrOH/hexane = 1/99, 0.5 mL/min, 40 °C, 220 nm UV detector, retention time = 12.9 min for (+) isomer and 15.6 min for (–) isomer].

References and Notes

- (1) (a) Elliott, M. C.; *J. Chem. Soc., Perkins Trans.* **2000**, 1291. (b) Elliott, M. C.; Williams, E. *J. Chem. Soc., Perkins. Trans.* **2001**, 2303. (c) Alali, F. Q.; Liu, X.-X.; McLaughlin, J. L. *J. Nat. Prod.* **1999**, *62*, 504.
- (2) For a review, see: Patil, N. T.; Kavthe, R. D.; Shinde, V. S. *Tetrahedron* **2012**, *68*, 8079.
- (3) (a) Qian, H.; Han X.; Widenhoefer, R. A. *J. Am. Chem. Soc.* **2004**, *126*, 9536. (b) Yang, C.-G.; Reich, N. W.; Shi, Z.; He, C. *Org. Lett.* **2005**, *7*, 4553. (c) Yang, C.-G.; He, C. *J. Am. Chem. Soc.* **2005**, *127*, 6966. (d) Yang, C.-G.; Reich, N. W.; Shi, Z.; He, C. *Org. Lett.* **2005**, *7*, 4553. (e) Coulombel, L.; Rajzmann, M; Pons, J.-M.; Olivero, S.; Duñach, E. *Chem. –Eur. J.* **2006**, *12*, 6356. (f) Kamiya, I.; Tsunoyama, H.; Tsukuda, T.; Sakurai, H. *Chem. Lett.* **2007**, *36*, 646. (g) Komeyama, K.; Morimoto, T.; Nakayama, Y.; Takaki, K. *Tetrahedron Lett.* **2007**, *48*, 3259. (h) Ohta, T.; Kataoka, Y.; Miyoshi, A.; Oe, Y.; Furukawa, I.; Ito, Y. *J. Organomet. Chem.* **2007**, *692*, 691. (j) Adrio, L. A.; Quek, L. S.; Taylor, J. G.; Hii, K. K. *Tetrahedron* **2009**, *65*, 10334.
- (4) For lanthanide-catalyzed intramolecular hydroalkoxylation of alkenes, see: Dzudza, A.; Markes, T. J. *Org. Lett.* **2009**, *11*, 1523.
- (5) For a Cu-catalyzed intramolecular hydroamination of unactivated alkenes from his groups, see: (a) Ohmiya, H.; Moriya, T.; Sawamura, M. *Org. Lett.* **2009**, *11*, 2145. (b) Ohmiya, H.; Yoshida, M.; Sawamura, M. *Synlett* **2010**, 2136.
- (6) For Cu(II)-catalyzed intramolecular carboalkoxylation of alkenes, see: (a) Miller, Y.; Miao, L.; Hosseini, A. S.; Chemler, S. R. *J. Am. Chem. Soc.* **2012**, *134*, 12149. (b) Bovino, M. T.; Liwosz, T. W.; Kendel, N. E.; Miler, Y.; Tyminska, N.; Zurek, E.; Chemler, S. R. *Angew. Chem., Int. Ed.* **2014**, *53*, 6383. For asymmetric Cu(I) catalysis involving intramolecular oxycupration of allenes, see: (c) Kawai, J.; Chikkade, P. K.; Shimizu, Y.; Kanai, M. *Angew. Chem., Int. Ed.* **2013**, *52*, 7177.
- (7) Ito, H.; Watanabe, A.; Sawamura, M. *Org. Lett.* **2005**, *7*, 1869.
- (8) Stollenz, M.; Meyer, F. *Organometallics* **2012**, *31*, 7708.
- (9) Sawamura, M.; Hamashima, H.; Sugawara, M.; Kuwano, R.; Ito, Y. *Organometallics* **1995**, *14*, 4549.
- (10) For discussion on the effect of the DTBM groups in the enantioselective Cu-catalyzed hydrosilylation of aryl ketones, see: Lipshutz, B. H.; Noson, K.; Chrisman, W.; Lower, A. *J. Am. Chem. Soc.* **2003**, *125*, 8779.
- (11) Saito, T.; Yokozawa, T.; Ishizaki, T.; Moroi, T.; Sayo, N.; Miura, T.; Kumobayashi, H. *Adv. Synth. Catal.* **2001**, *343*, 264.
- (12) The absolute configuration of **2a**^{*} was not determined.

- (13) Crich, D.; Shirai, M.; Brebion, F.; Rumthao, S. *Tetrahedron* **2006**, *62*, 6501.
- (14) Aburel, P. S.; Romming, C.; Ma, K.; Undheim, K. *J. Chem. Soc., Perkin Trans. 1* **2001**, 1458.
- (15) Jeong, Y.; Kim, D.-Y.; Choi, Y.; Ryu, J.-S. *Org. Biomol. Chem.* **2011**, *9*, 374.
- (16) Kim, K. M.; Jeon, D. J.; Ryu, E. K. *Synthesis* **1998**, *30*, 835.

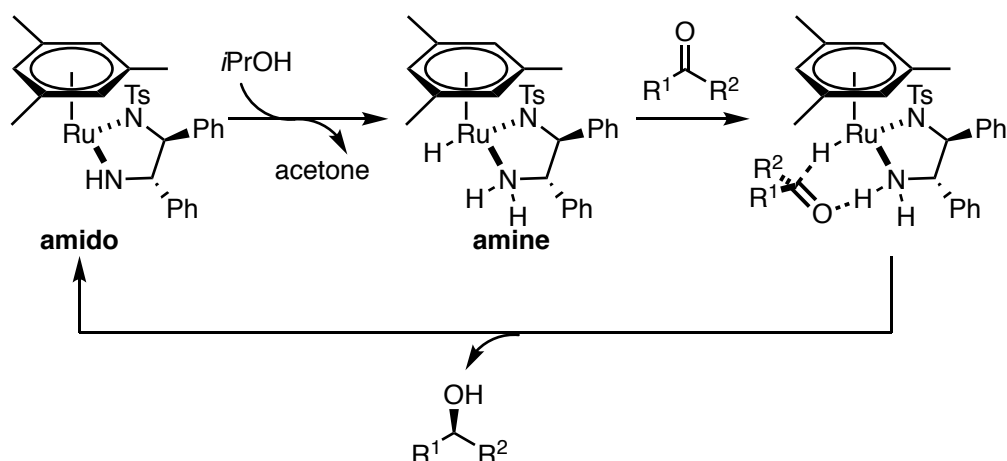
Chapter 2

Iridium-Catalyzed Asymmetric Transfer Hydrogenation of Ketones with a Prolinol-Phosphine Chiral Ligand

Introduction

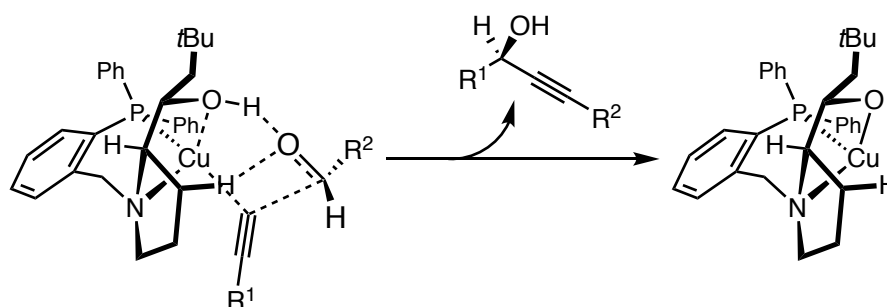
Asymmetric transfer hydrogenation of ketones has been widely studied as a method for the synthesis of chiral secondary alcohols. Mechanistically, many of successful examples involved cooperative action of transition metals and ligands.¹ Ikariya-Noyori asymmetric transfer hydrogenation has been known as the representative reaction.² In the catalytic system, the ruthenium amido complex abstracts hydrogens from alcohols to generate amine-coordinated ruthenium hydride species. The resulting Ru-bound amine acts as a hydrogen bond donor site to assist nucleophilic attack of the hydride to the carbonyl carbon and fixes the orientation of the carbonyl group. Thus, the key of Ikariya-Noyori asymmetric transfer hydrogenation is amine–amide interconversion in the ligands (Scheme 1),^{2d-f} while a few catalytic systems based on interconversion of other functional groups in the ligands have also been reported.³⁻⁵

Scheme 1 Asymmetric Transfer Hydrogenation via Amine-Amido Interconversion



Previously, the author's laboratory showed that chiral prolinol-phosphine ligands promoted copper-catalyzed asymmetric reactions such as alkynylation of aldehydes, alkynylation of α -ketoesters, and Kinugasa reaction producing β -lactams from nitrones and terminal alkynes.⁶ For example, the proposed mechanism of asymmetric alkynylation of aldehydes is shown in Scheme 2.^{6a} In these works, alcohol–alkoxide interconversion at the ligands has been proposed. Based on this knowledge, the author conceived that this ligand may promote transfer hydrogenation of ketones via alcohol-alkoxide interconversion. As a related research, Zhang achieved enantioselective hydrogenation of ketones using a ferrocene-skeleton-contained P/NH/OH ligand.⁷⁻⁹ DFT calculations suggested that the hydrogenation occurs via alcohol-alkoxide interconversion.¹⁰

Scheme 2 Asymmetric Alkynylation of Aldehydes via alcohol-alkoxide interconversion



This chapter describes that a prolinol-phosphine chiral ligand promotes iridium-catalyzed asymmetric transfer hydrogenation of ketones using formic acid as a hydrogen source to give chiral secondary alcohols.¹¹ This catalytic system enabled reduction of various ketones with high enantioselectivity.

Results and Discussion

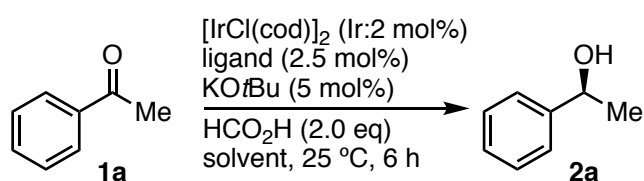
Using acetophenone (**1a**) as a model substrate, applicability of the chiral prolinol-phosphine ligands to asymmetric transfer hydrogenation was examined. At first, the effect of substituents of α -position of hydroxy group in a ligand was examined. Thus, transfer hydrogenation of **1a** (0.2 mmol) was conducted with formic acid (2.0 eq) as a hydrogen source in the presence of $[\text{IrCl}(\text{cod})]_2$ (Ir: 2 mol%), chiral ligand (2.5 mol%), and $\text{KO}t\text{Bu}$ (5 mol%) in THF (1 mL) at 25 °C for 6 h (Table 1, entries 1–6). Ligands bearing primary or tertiary alcohol moieties did not promote the reaction (entries 1, 3). In contrast, the reaction proceeded with the ligand having a secondary alcohol moiety (**L2**) in 11% yield at a good enantioselectivity to give the corresponding secondary alcohol **2a** with 85% ee, suggesting secondary alcohols to be candidates for further screening (entry 2). Next, α -substituents of secondary alcohol moiety were investigated. Employing *tert*-Butyl-substituted ligand **L4**, both the product yield and enantioselectivity were slightly improved (19%, 89% ee, entry 4). Even better yield and enantioselectivity (46%, 92% ee) were provided with **L5** with a neopentyl group (entry 5). Change of the hydroxy group of **L5** into a methoxy group (**L5-OMe**) completely inhibited the reaction, thus indicating a critical role of the alcoholic site (entry 6).

Subsequently, the effect of solvents was examined (entries 7–15). Etheral solvents specifically enabled the reaction to proceed, and no reaction occurred with other-type solvents, such as toluene, dichloromethane, 2-propanol, *N,N*-dimethylformamide and acetonitrile, not suitable (entries 7–11). While the use of 1,4-dioxane resulted in significant decreases in the yield and enantioselectivity (16%, 61% ee, entry 12), diethyl ether and *tert*-butyl methyl ether (TBME) slightly improved the yield with the enantioselectivity almost retained as compared with THF (entries 13, 14). The best solvent among the screened was cyclopentyl methyl ether

(CPME), affording the product in 87% yield with 94% ee (entry 15).

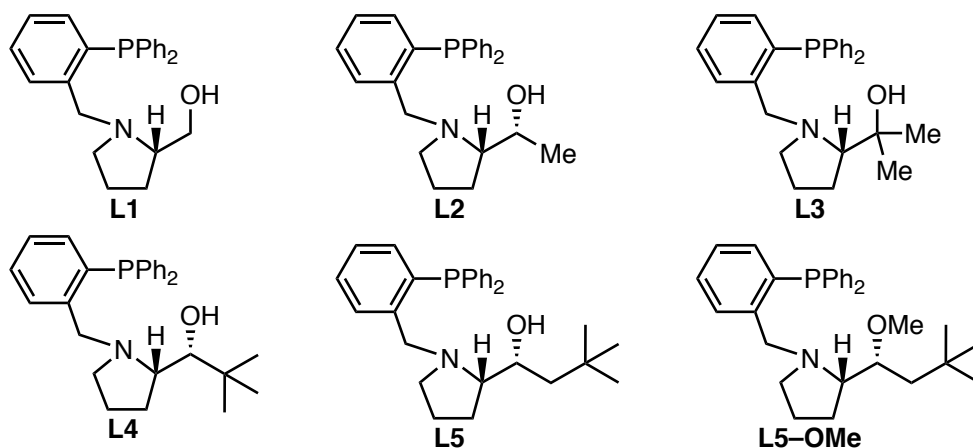
Our assumption for the importance of iridium alkoxide species was supported by following two experiments. First, the reaction did not proceed at all in the absence of external base additive (entry 16). Second, the reactivity of $[\text{IrOMe}(\text{cod})]_2$ instead of $[\text{IrCl}(\text{cod})]_2$ in the absence of base additive was comparable with that of the $[\text{IrCl}(\text{cod})]_2/\text{KO}t\text{Bu}$ system (entry 17). It is important to prepare an iridium alkoxide species in advance. In fact, when formic acid was added before the addition of the base, no reaction occurred.

Table 1 The effect of chiral ligands and solvents in asymmetric transfer hydrogenation of **1a**^a



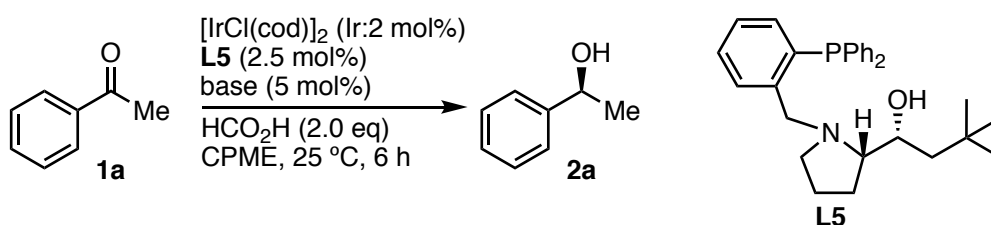
entry	ligand	solvent	yield (%) ^b	ee (%) ^c
1	L1	THF	0	
2	L2	THF	11	85
3	L3	THF	0	
4	L4	THF	19	89
5	L5	THF	46	92
6	L5-OMe	THF	0	
7	L5	toluene	0	
8	L5	CH_2Cl_2	0	
9	L5	<i>i</i> PrOH	0	
10	L5	DMF	0	
11	L5	MeCN	0	
12	L5	1,4-dioxane	16	61
13	L5	Et_2O	60	92
14	L5	TBME	54	91
15	L5	CPME	87	94
16 ^d	L5	CPME	0	
17 ^{d,e}	L5	CPME	83	95

^aCondition: $[\text{IrCl}(\text{cod})]_2$ (Ir:2 mol%), ligand (2.5 mol%), $\text{KO}t\text{Bu}$ (5 mol%), **1a** (0.20 mmol), HCO_2H (0.40 mmol), solvent (1 mL), 25 °C, 6 h. ^bYield of the isolated product. ^cThe enantiomeric excess was determined by HPLC analysis. ^dWithout $\text{KO}t\text{Bu}$. ^e $[\text{IrOMe}(\text{cod})]_2$ was used instead of $[\text{IrCl}(\text{cod})]_2$.



The effect of bases was also examined (Table 2). Potassium *tert*-butoxide promoted the reaction, but no reaction occurred when lithium or sodium *tert*-butoxides were used instead of potassium *tert*-butoxide (entries 1–3). Potassium carbonate was the best base, giving the desired chiral alcohol in 82% yield with 96% ee (entry 4). Inorganic bases such as potassium phosphate and potassium fluoride were not suitable (entries 5 and 6). While a strong amine base such as DBU promoted the asymmetric transfer hydrogenation (85%, 94% ee, entry 7), the product yield was low with diethylamine (16%, 94% ee, entry 8). Hunig's base (*i*Pr₂NEt) promoted no reaction (entries 9).

Table 2 Screening of Bases



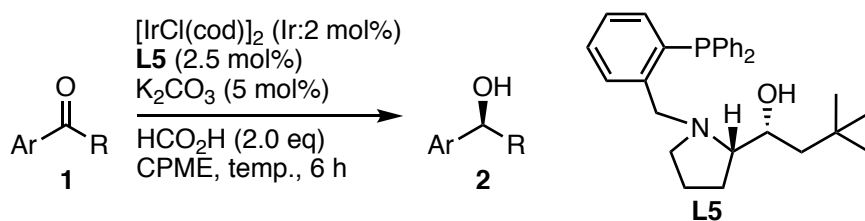
entry	base	yield (%) ^b	ee (%) ^c
1	LiO <i>t</i> Bu	0	
2	NaO <i>t</i> Bu	0	
3	KO <i>t</i> Bu	87	94
4	K ₂ CO ₃	82	96
5	K ₃ PO ₄	0	
6	KF	0	
7	DBU	85	94
8	Et ₂ NH	16	95

^aCondition: [IrCl(cod)]₂ (Ir:2 mol%), **L5** (2.5 mol%), base (5 mol%), **1a** (0.20 mmol), HCO₂H (0.40 mmol), CPME (1 mL), 6 h. ^bYield of the isolated product. ^cThe enantiomeric excess was determined by HPLC analysis.

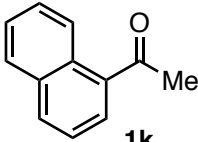
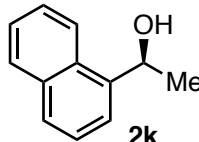
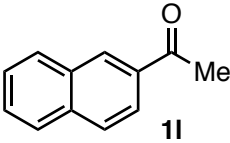
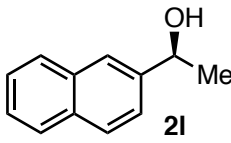
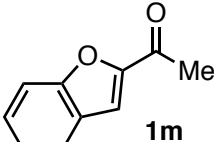
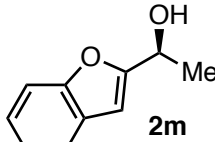
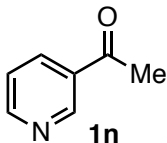
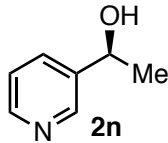
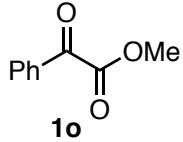
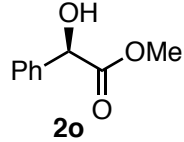
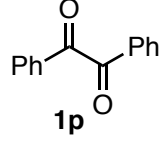
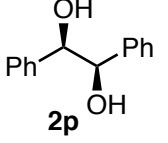
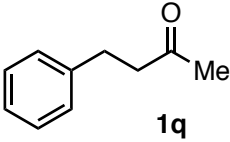
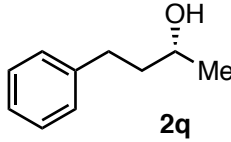
The scope of ketones was examined. The reaction was carried out in the presence of [IrCl(cod)]₂ (Ir:2 mol%), **L5** (2.5 mol%), K₂CO₃ (5 mol%) in CPME. The methyl, methoxy, fluoro, and bromo group as *para*-substituents of the aromatic rings in the ketones were compatible (entries 1–4). The ketone bearing *ortho*-methyl group on the phenyl ring also underwent the transfer hydrogenation (entry 5). A tolerance of this transfer hydrogenation toward sterically demanding substrates is significant. For instance, the reaction of *tert*-butyl phenyl ketone occurred smoothly at 40 °C, giving (*S*)-2,2-dimethyl-1-phenylpropanol in >99% ee (entry 6). Interestingly, hydrogenation of acetophenone and *tert*-butyl phenyl ketone proceeded preferentially from the same prochiral face, regardless of reversal of the relative steric bulkiness between the phenyl and the alkyl substituents of the carbonyl group. This result suggests that the enantioselection is due to attractive forces between the catalyst and the aromatic ring of the substrate, and not a mere steric repulsion model.^{2e,12} Similarly, cyclohexyl phenyl ketone also underwent hydrogenation with the same sense of enantioselection (entry 7). Another attractive feature of this asymmetric transfer hydrogenation is applicability toward aryl heteroaryl ketones. For example, the hydrogenation of 2-benzoylpyridine occurred with 85% ee to give (*R*)-phenyl-(2-pyridyl)methanol (entry 8).¹³ Because the steric bulkiness of phenyl and pyridyl groups is almost same, the chiral iridium complex should differentiate the electronic difference between them. A cyclic ketone such as 1-indanone also reacted (entry 9). Acetonaphthones and heteroaryl ketones reacted with high enantioselectivity (entry 10–13). Moreover, α -carbonyl ketones were also applicable. In the case of α -ketoester, only-reduction of keto moiety afforded α -hydroxyester in over 99% yield with 95% ee (entry 14). Reduction of benzil resulted in producing (*R,R*)-1,2-diphenyl-1,2-diol with 96:4 diastereo ratio and over 99% enantiomeric excess (entry 15).

In sharp contrast to the above mentioned results of aryl ketones, a dialkyl ketone, phenethyl methyl ketone, exhibited both low reactivity and enantioselectivity (25% yield, 42% ee) (entry 16). This result also suggests the importance of attractive interaction between the chiral iridium catalyst and the aryl group of ketones.

Table 3 Substrate Scope^a



entry	temp. (°C)	substrate	product	yield (%) ^b	ee (%) ^c
1	25			81	96
2	40			93	93
3	25			70	95
4	25			77	94
5	40			>99	97
6	40			97	>99
7	40			99	98
8	40			64	85
9	40			>99	87

10	40			97	93
11	25			79	95
12 ^d	25			>99	86
13	40			>99	89
14	40			>99	95
15	40			94 ^e	>99
16	25			25	42

^aCondition: [IrCl(cod)]₂ (Ir:2 mol%), **L5** (2.5 mol%), K₂CO₃ (5 mol%), **1** (0.20 mmol), HCO₂H (0.40 mmol), CPME (1 mL), 6 h. ^bYield of the isolated product. ^cThe enantiomeric excess was determined by HPLC analysis. ^dThe reaction time was 12 h. ^e*dl/meso* = 96:4

Based on the experimental results, the author proposes a catalytic reaction pathway involving a hydrogen-bonding between the chiral ligand (**L5**) and the substrate (**1**), and alcohol-alkoxide interconversion as shown in Figure 1. An iridium-**L5** complex enters to a catalytic cycle in a form of alkoxo(dihydrido)iridium(III) complex **A** upon reaction with the base (K₂CO₃) and formic acid. Etheral solvent specifically enables the reaction to proceed because the solvent seems to weakly coordinate to iridium center to inhibit the formation of inactive hydride-bridged dinuclear iridium complex **A-dimer**.¹⁴ On the other hand, the strong coordination of a solvent prevents the following formation of complex **B**. The complex **A** reacts with formic acid to form dihydridoiridium formate **B** through deprotonation of acidic

proton of formic acid by iridium alkoxide with elimination of solvent from iridium center. The tentative complex **B** undergoes decarboxylation to form trihydrido-iridium (III) complex **C**, in which prolinol-phosphine ligand **L5** presents an alcoholic hydrogen bond donor site. Next, the complex **C** captures ketone **1** by two-point hydrogen bonds involving $\text{OH}_{\text{ligand}} \cdots \text{O}_{\text{carbonyl}}$ and $\text{C}(\text{sp}^3)\text{-H}_{\text{ligand}} \cdots \text{O}_{\text{carbonyl}}$ to form a complex **D**. Then, nucleophilic attack of one of the three hydrides on Ir to the carbonyl carbon and protonation of developing oxyanion with the ligand O-H group occurs in a concerted manner through transition state **E-TS** to form a complex **F**. After elimination of the hydrogenation product **2** from a complex **F**, recoordination of the solvent to the Ir center regenerates the alkoxo(dihydrido)iridium(III) complex **A**.

Based on the characteristic enantioselectivity profile in the reaction of aryl alkyl ketones that the same prochiral face was favored regardless of the relative steric demand between the aryl and alkyl substituents (Table 2), the author postulates a $\text{C}(\text{sp}^3)\text{-H} \cdots \pi$ interaction between one of the $\text{C}(\text{sp}^3)\text{-H}$ bonds located at the 4-position of the pyrrolidine moiety of the chiral ligand **L5** and the aromatic ring of the ketone. The attractive $\text{C}(\text{sp}^3)\text{-H} \cdots \pi$ interaction crucially controls the facial selectivity of the ketones, thereby making the influence of steric factor minor.

Based on this proposed catalytic reaction pathway, the ineffectiveness of the primary (**L1**) or tertiary (**L3**) alcohol type chiral ligands can be explained as follows. The catalyst with the primary alcohol ligand **L1** stays in a form of inactive hydride-bridged dimer because of less steric hindrance around iridium center. On the other hand, a large steric hindrance around the hydroxy group of **L3** may inhibit the coordination of the OH group to Ir or the $\text{OH} \cdots \text{O}/\text{C}(\text{sp}^3)\text{-H} \cdots \text{O}$ two-point hydrogen-bonding.

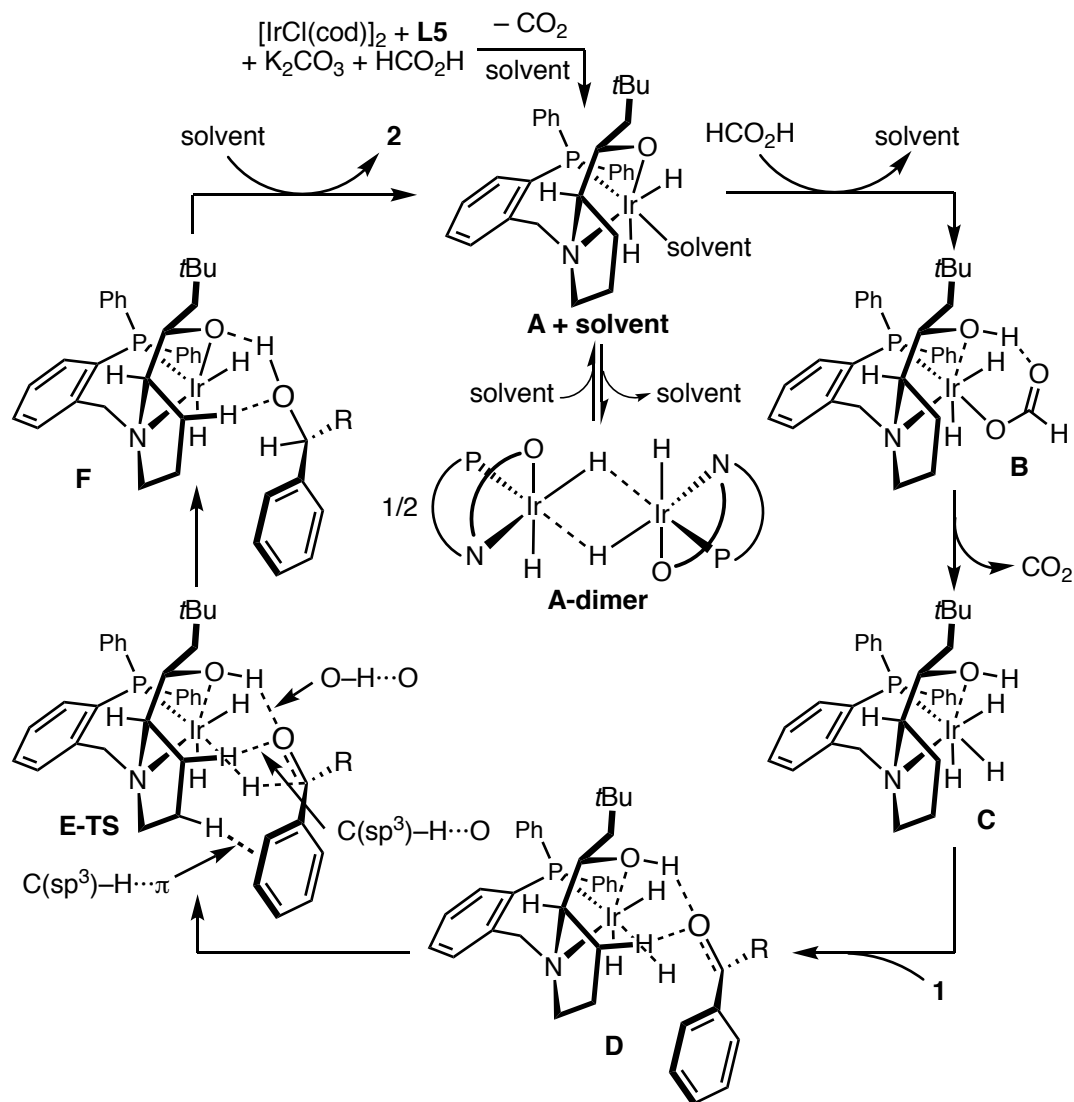
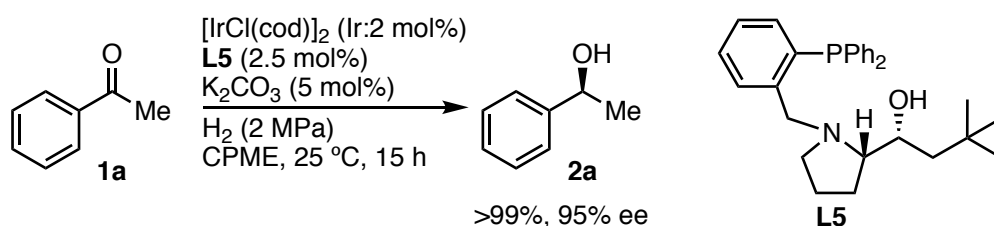


Figure 1 A proposed catalytic reaction pathway.

Prolinol-phosphine iridium catalytic system promotes not only transfer hydrogenation but also hydrogenation with hydrogen gas. In the presence of hydrogen gas (2 MPa), the iridium-L5 catalyst produced (*S*)-1-phenylethanol (**2a**) from acetophenone. In this hydrogenation, the enantioselectivity was almost the same as the transfer hydrogenation (Scheme 3). The hydrogenation seems to proceed via intermediate **D** and transition state **E-TS** in Figure 2.

Scheme 3 Asymmetric Hydrogenation of Acetophenone



Quantum Chemical Calculations

To understand interactions between a ligand and a substrate, DFT calculations were carried out for the transition state of the enantiodiscriminating step (**E-TS** in Figure 1). Non-covalent interactions, like dispersive interaction, can be shown with a method introduced by Erin R. Johnson *et al.*¹⁵ The author used the program MultiWFN and VMD to visualize these areas, displayed in green. The analysis is based on the wave function obtained by the B3LYP+D3(BJ)/def2SVP/W06 level of theory.

Figure 2 shows that the plot of non-covalent interaction of the transition states structures leading to the *S* (Figure 2a: left, **TS_major**) or *R* (Figure 2b: right, **TS_minor**) product complexes using **L5** as the ligand and **1a** as the ketone. Figure 3a, which represents a transition state leading to the major enantiomer, shows not only an OH \cdots O hydrogen bond but also a non-classical hydrogen bond between a non-polar C(sp³)-H of the ligand and the carbonyl oxygen of the ketone.

In addition, there is a C(sp³)-H \cdots π interaction between one of the C(sp³)-H bonds of the 4-position of pyrrolidine ring of the ligand and the phenyl group of the ketone found by bond critical point analyses of the quantum theory of atoms in molecule (QTAIM). On the other hand, a C(sp³)-H \cdots π interaction between the ligand and the substrate is not found in the transition state leading to the minor enantiomer (Figure 3b), while a two-point hydrogen-bonding involving a C(sp³)-H \cdots O interaction is retained as in the TS leading to the major enantiomer. The TS leading to the minor enantiomer without C(sp³)-H \cdots π interaction, **TS_minor**, is 15.6 kJ mol⁻¹ and 10.1 kJ mol⁻¹ higher in Gibbs free energy at the B3LYP+D3BJ/def2SVP and the M06-2X/def2SVP level, respectively. Since no steric repulsion between the catalyst and the substrate and resulting strain is indicated in the both TSs and these catalyst structures are almost superimposable, this energy difference should mostly be ascribed to the C(sp³)-H \cdots π interaction found only in the **TS_major**. Overall, it is inferred that the OH \cdots O/C(sp³)-H \cdots O two-point hydrogen-bonding fixes the orientation of the carbonyl group of the ketone, and the catalyst recognizes the enantiotopic faces of the aryl alkyl ketone through the C(sp³)-H \cdots π interaction.

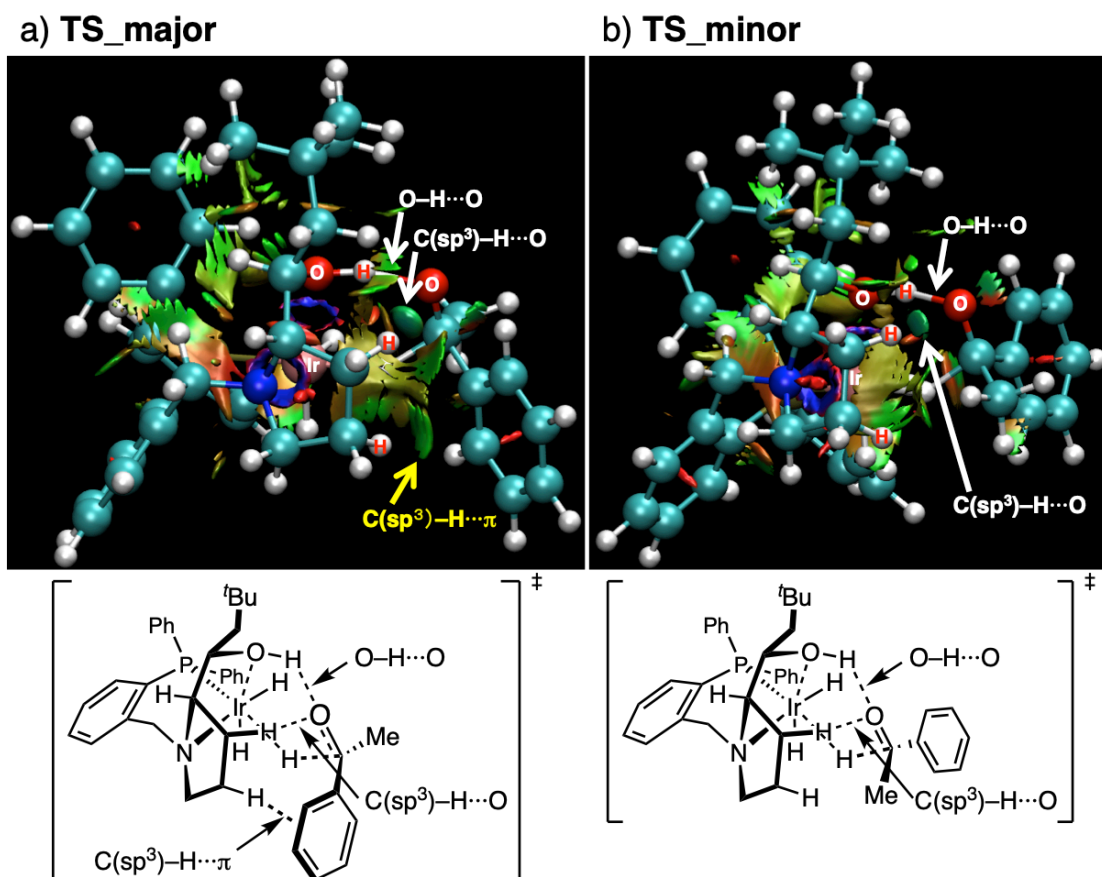


Figure 2 Plot of non-covalent interaction of the transition states structures

Note that the activation Gibbs energy of the enantiodiscriminating step for the major pathway is 24.1 kJ/mol (Figure 3). A hydride transfer from Ir to the carbonyl carbon is accompanied by a proton transfer from a OH group of the ligand to the carbonyl oxygen of the ketone.

Remarkably, the catalyst also discriminates a phenyl group and 2-pyridyl group in the reaction of phenyl 2-pyridyl ketone (**1i**) (Table 2, entry 8). This fact suggests that $C-H \cdots \pi$ interaction is more efficient with the phenyl group than with the 2-pyridyl group.

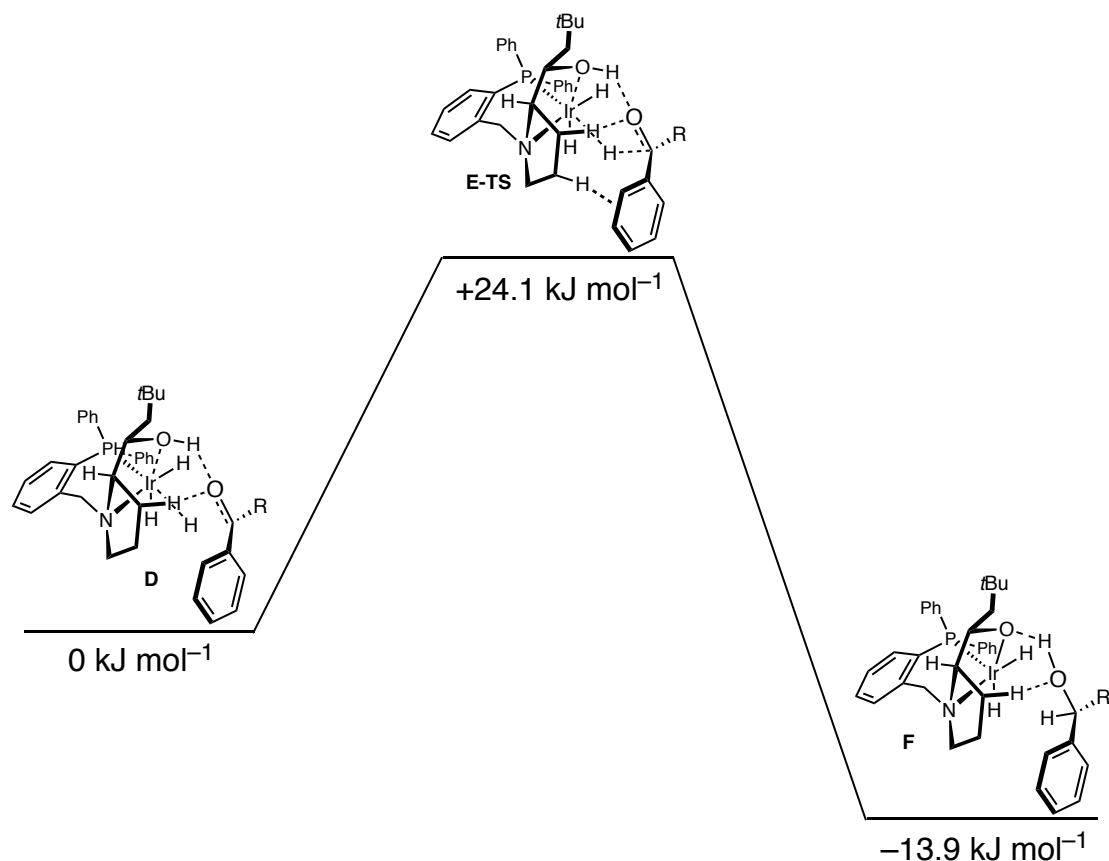


Figure 3 DFT Calculations for the Reaction Pathway

Conclusion

Prolinol-phosphine-iridium catalyzed the asymmetric transfer hydrogenation and asymmetric hydrogenation of ketones, giving chiral secondary alcohols. This system is also applicable to bulky ketones and diaryl ketones. The ketones reacted preferentially with the same prochiral face, regardless of reversal of the order of steric demands of the carbonyl substituents. A catalytic reaction pathway involving the two-point hydrogen bonding between the ligand and the carbonyl oxygen of the ketone and a $C(sp^3)\text{-H}\cdots\pi$ interaction between the ligand and the aryl group of the ketone is proposed. The proposed hydrogen-bonding and non-covalent interactions have been supported by DFT calculations including dispersion corrections.

Experimental Section

Instrumentation and Chemicals

NMR spectra were recorded on a JEOL ECX-400, operating at 400 MHz for ^1H NMR and 100.5 MHz for ^{13}C NMR. Chemical shift values for ^1H and ^{13}C are referenced to Me_4Si . Chemical shifts are reported in δ ppm. Mass spectra were obtained with Thermo Fisher Scientific Exactive, JEOL JMS-T100LP or JEOL JMS-700TZ at the Instrumental Analysis Division, Equipment Management Center, Creative Research Institution, Hokkaido University. Elemental analysis was performed at the Instrumental Analysis Division, Equipment Management Center, Creative Research Institution, Hokkaido University. HPLC analyses were conducted on a HITACHI ELITE LaChrom system with a HITACHI L-2455 diode array detector. TLC analyses were performed on commercial glass plates bearing 0.25-mm layer of Merck Silica gel 60F₂₅₄. Silica gel (Kanto Chemical Co., Silica gel 60 N, spherical, neutral) was used for column chromatography.

All reactions were carried out under nitrogen or argon atmosphere. Materials were obtained from commercial suppliers or prepared according to standard procedures unless otherwise noted. $[\text{IrCl}(\text{cod})]_2$ was prepared according to the reported procedure.¹⁶ $[\text{IrOMe}(\text{cod})]_2$ was prepared according to the reported procedure.¹⁷ K_2CO_3 was purchased from Junsei Chemical Co.. THF, 1,4-dioxane, Et_2O , and TBME were purchased from Kanto Chemical Co., stored over molecular sieves under nitrogen. CPME was purchased from FUJIFILM Wako Pure Chemical Co., stored over molecular sieves under nitrogen. Formic acid was purchased from Kanto Chemical Co.. Ketones 1a-f, 1h-k, 1n-1q were purchased from TCI Chemical Co.. Ketone 1l was purchased from Kanto Chemical Co.. Ketone 1m was purchased from FUJIFILM Wako Pure Chemical Co.. Ketone 1g is a known compound.¹⁸

Preparation of Chiral Ligands

L1-L5 and **L5-OMe** were prepared through reductive amination with the corresponding aminoalcohols and 2-(diphenylphosphino)benzaldehyde according to the literature procedures.⁶

Procedures for Iridium(I)-Catalyzed Transfer Hydrogenation of Ketones

The reaction in Table 2, entry 4 is representative. In a glove box, **L5** (2.2 mg, 0.0050 mmol) and was placed in a screw vial containing a magnetic stirring bar. CPME (1 mL), $[\text{IrCl}(\text{cod})]_2$ (1.3 mg, 0.0020 mmol) and K_2CO_3 (1.4 mg, 0.010 mmol) were added to the vial and the mixture was stirred at room temperature for 5 min to give a pale yellow solution. Next, formic acid (18.4 mg, 0.40 mmol) and ketone **1a** (24.0 mg, 0.20 mmol) were added. The vial

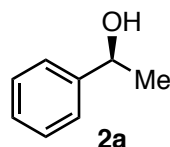
was sealed with a screw cap, and was removed from the glove box. After 6 h stirring at 25 °C, the mixture was quenched with saturated K₂CO₃ aq and diluted with Et₂O. The organic layer was dried over anhydrous MgSO₄, filtered, and evaporated under reduced pressure. Flash chromatography on silica gel (0–10% EtOAc/hexane) gave **2a** (19.7 mg, 0.16 mmol) in 82% yield. The ee value (96% ee) was determined by chiral HPLC analysis: CHIRALCEL[®] OD-H column 4.6 mm × 250 mm, Daicel Chemical Industries, *i*-PrOH/hexane = 05:95, 1.0 mL/min 40 °C, 220 nm UV detector, retention time = 7.6 min for (*R*) isomer and 8.4 min for (*S*) isomer.

Typical Procedure for Asymmetric Hydrogenation of **1a**.

The reaction in Scheme 3 is representative. In a glove box, **L5** (2.2 mg, 0.0050 mmol) and was placed in a 30 mL glass tube containing a magnetic stirring bar. CPME (1 mL), [IrCl(cod)]₂ (1.3 mg, 0.0020 mmol) and K₂CO₃ (1.4 mg, 0.010 mmol) were added to the vial and the mixture was stirred at room temperature for 5 min to give a pale yellow solution. Next, ketone **1a** (24.0 mg, 0.15 mmol) were added. After being capped with a septum, the tube was removed from the glove box. The septum was removed, and the tube was placed in a autoclave. Hydrogen was initially introduced into the autoclave at a pressure of 2.5 MPa, before being reduced to 2 MPa by carefully releasing the stop valve. This procedure was repeated five times, and the vessel was pressurized to 2 MPa. After the reaction mixture was stirred at 25 °C for 15 h, the hydrogen gas was carefully ventilated. The mixture was filtered through a short plug of silica gel. The solvent was removed under reduced pressure. Flash chromatography on silica gel (0–10% EtOAc/hexane) gave **1a** (24.0 mg, 0.20 mmol) in >99% yield. The ee value (95% ee) was determined by chiral HPLC analysis.

Characterization Data for Secondary Alcohols

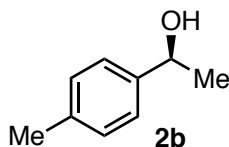
(*S*)-1-Phenylethanol (**2a**)



The product **2a** was purified by flash chromatography on silica gel (0–10% EtOAc/hexane) (19.7 mg, 82% isolated yield from **1a**). **2a** was consistent with the the literature data.¹⁹ [α]_D²⁴ –39.7 (*c* 0.90, CHCl₃). The ee value (96% ee) was determined by chiral HPLC analysis of **2a**^{*}, [CHIRALCEL[®] OD-H column, 4.6 mm × 250 mm, Daicel Chemical Industries,

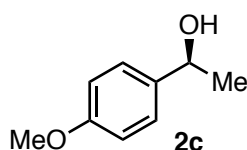
i-PrOH/hexane = 05/95, 1.0 mL/min, 40 °C, 220 nm UV detector, retention time = 7.6 min for (*R*) isomer and 8.4 min for (*S*) isomer].

(*S*)-1-(4-Methylphenyl)ethanol (**2b**)



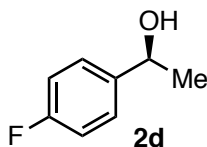
The product **2b** was purified by flash chromatography on silica gel (0–10% EtOAc/hexane) (22.1 mg, 81% isolated yield from **1b**). **2b** was consistent with the the literature data.¹⁹ $[\alpha]_D^{23} -49.9$ (*c* 0.63, CHCl₃). The ee value (96% ee) was determined by chiral HPLC analysis of **2b**, [CHIRALCEL[®] OJ-H+OJ-3 column, 4.6 mm × 250 mm, Daicel Chemical Industries, *i*-PrOH/hexane = 05/95, 0.5 mL/min, 40 °C, 220 nm UV detector, retention time = 26.1 min for (*S*) isomer and 28.9 min for (*R*) isomer].

(*S*)-1-(4-Methoxyphenyl)ethanol (**2c**)



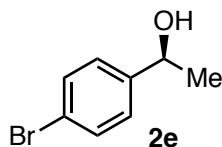
The product **2c** was purified by flash chromatography on silica gel (5–15% EtOAc/hexane) (28.3 mg, 93% isolated yield from **1c**). **2c** was consistent with the the literature data.¹⁹ $[\alpha]_D^{24} -28.7$ (*c* 0.21, CHCl₃). The ee value (93% ee) was determined by chiral HPLC analysis of **2c**, [CHIRALCEL[®] OD-H column, 4.6 mm × 250 mm, Daicel Chemical Industries, *i*-PrOH/hexane = 02/98, 1.0 mL/min, 40 °C, 220 nm UV detector, retention time = 19.3 min for (*R*) isomer and 22.0 min for (*S*) isomer].

(*S*)-1-(4-Fluorophenyl)ethanol (**2d**)



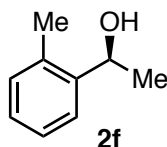
The product **2d** was purified by flash chromatography on silica gel (0–10% EtOAc/hexane) (19.6 mg, 70% isolated yield from **1d**). **2d** was consistent with the the literature data.¹⁹ $[\alpha]_D^{24} -38.7$ (*c* 0.52, CHCl₃). The ee value (95% ee) was determined by chiral HPLC analysis of **2d**, [CHIRALCEL[®] OD-H+OD-3×2 column, 4.6 mm × 250 mm, Daicel Chemical Industries, *i*-PrOH/hexane = 05/95, 0.5 mL/min, 40 °C, 220 nm UV detector, retention time = 33.8 min for (*S*) isomer and 35.9 min for (*R*) isomer].

(S)-1-(4-Bromophenyl)ethanol (**2e**)



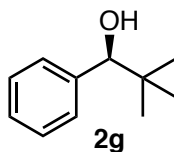
The product **2e** was purified by flash chromatography on silica gel (0–10% EtOAc/hexane) (30.6 mg, 77% isolated yield from **1e**). **2e** was consistent with the literature data.¹⁹ $[\alpha]_{\text{D}}^{24} -33.4$ (*c* 0.60, CHCl₃). The ee value (94% ee) was determined by chiral HPLC analysis of **2e**, [CHIRALCEL[®] OD-H column, 4.6 mm × 250 mm, Daicel Chemical Industries, *i*-PrOH/hexane = 03/97, 1.0 mL/min, 40 °C, 220 nm UV detector, retention time = 11.0 min for (*S*) isomer and 12.0 min for (*R*) isomer].

(S)-1-(2-Methylphenyl)ethanol (**2f**)



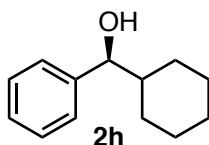
The product **2f** was purified by flash chromatography on silica gel (0–10% EtOAc/hexane) (27.2 mg, >99% isolated yield from **1f**). **2f** was consistent with the literature data.¹⁹ $[\alpha]_{\text{D}}^{24} -68.8$ (*c* 0.58, CHCl₃). The ee value (97% ee) was determined by chiral HPLC analysis of **2f**, [CHIRALCEL[®] AD-H column, 4.6 mm × 250 mm, Daicel Chemical Industries, *i*-PrOH/hexane = 02/98, 1.0 mL/min, 40 °C, 220 nm UV detector, retention time = 12.2 min for (*R*) isomer and 13.8 min for (*S*) isomer].

(S)-2,2-Dimethyl-1-phenylpropanol (**2g**)



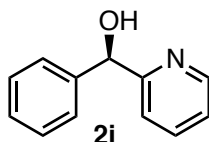
The product **2g** was purified by flash chromatography on silica gel (0–10% EtOAc/hexane) (31.9 mg, 97% isolated yield from **1g**). **2g** was consistent with the literature data.²⁰ $[\alpha]_{\text{D}}^{24} -31.7$ (*c* 1.05, CHCl₃). The ee value (>99% ee) was determined by chiral HPLC analysis of **2g**, [CHIRALCEL[®] OD-H column, 4.6 mm × 250 mm, Daicel Chemical Industries, *i*-PrOH/hexane = 02/98, 1.0 mL/min, 40 °C, 220 nm UV detector, retention time = 8.9 min for (*S*) isomer and 12.8 min for (*R*) isomer].

(S)-Cyclohexyl(phenyl)methanol (**2h**)



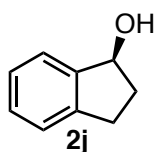
The product **2h** was purified by flash chromatography on silica gel (0–10% EtOAc/hexane) (37.7 mg, 99% isolated yield from **1h**). **2h** was consistent with the the literature data.¹⁹ $[\alpha]_D^{24} -35.8$ (*c* 0.43, CHCl₃). The ee value (98% ee) was determined by chiral HPLC analysis of **2h**, [CHIRALCEL[®] OD-H column, 4.6 mm × 250 mm, Daicel Chemical Industries, *i*-PrOH/hexane = 01/99, 0.5 mL/min, 40 °C, 220 nm UV detector, retention time = 31.1 min for (*S*) isomer and 40.8 min for (*R*) isomer].

(*R*)-Phenyl(2-pyridyl)methanol (2i)



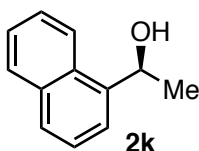
The product **2i** was purified by flash chromatography on silica gel (10–20% MeOH/CHCl₃) (23.7 mg, 64% isolated yield from **1i**). **2i** was consistent with the the literature data.²¹ $[\alpha]_D^{24} -101.2$ (*c* 0.98, CHCl₃). The ee value (85% ee) was determined by chiral HPLC analysis of **2i**, [CHIRALCEL[®] AD-H column, 4.6 mm × 250 mm, Daicel Chemical Industries, *i*-PrOH/hexane = 05/95, 1.0 mL/min, 40 °C, 220 nm UV detector, retention time = 14.9 min for (*R*) isomer and 18.2 min for (*S*) isomer].

(*S*)-2,3-Dihydro-1*H*-indenol (2j)



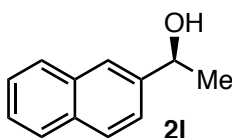
The product **2j** was purified by flash chromatography on silica gel (0–10% EtOAc/hexane) (26.8 mg, >99% isolated yield from **1j**). **2j** was consistent with the the literature data.²² $[\alpha]_D^{24} 26.7$ (*c* 0.52, CHCl₃). The ee value (87% ee) was determined by chiral HPLC analysis of **2j**, [CHIRALCEL[®] OD-H column, 4.6 mm × 250 mm, Daicel Chemical Industries, *i*-PrOH/hexane = 03/99, 1.0 mL/min, 40 °C, 220 nm UV detector, retention time = 11.5 min for (*S*) isomer and 12.7 min for (*R*) isomer].

(*S*)-1-(1-Naphthyl)ethanol(2k)



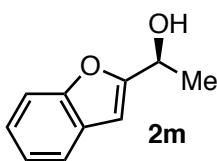
The product **2k** was purified by flash chromatography on silica gel (0–10% EtOAc/hexane) (33.4 mg, 97% isolated yield from **1k**). **2k** was consistent with the literature data.¹⁹ $[\alpha]_D^{24} -55.1$ (*c* 0.58, CHCl₃). The ee value (93% ee) was determined by chiral HPLC analysis of **2k**, [CHIRALCEL[®] OD-H column, 4.6 mm × 250 mm, Daicel Chemical Industries, *i*-PrOH/hexane = 05/95, 1.0 mL/min, 40 °C, 220 nm UV detector, retention time = 13.3 min for (*S*) isomer and 20.0 min for (*R*) isomer].

(*S*)-1-(2-Naphthyl)ethanol (**2l**)



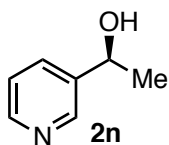
The product **2l** was purified by flash chromatography on silica gel (0–10% EtOAc/hexane) (27.2 mg, 79% isolated yield from **1l**). **2l** was consistent with the literature data.¹⁹ $[\alpha]_D^{24} -55.8$ (*c* 0.34, CHCl₃). The ee value (95% ee) was determined by chiral HPLC analysis of **2l**, [CHIRALCEL[®] OJ-H column, 4.6 mm × 250 mm, Daicel Chemical Industries, *i*-PrOH/hexane = 05/95, 1.0 mL/min, 40 °C, 220 nm UV detector, retention time = 20.3 min for (*S*) isomer and 26.0 min for (*R*) isomer].

(*S*)-1-(2-Benzofuryl)ethanol (**2m**)



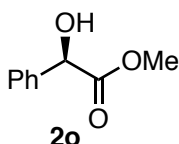
The product **2m** was purified by flash chromatography on silica gel (5–15% EtOAc/hexane) (32.0 mg, >99% isolated yield from **1m**). **2m** was consistent with the literature data.²³ $[\alpha]_D^{24} -24.8$ (*c* 0.10, CHCl₃). The ee value (86% ee) was determined by chiral HPLC analysis of **2m**, [CHIRALCEL[®] OJ-H column, 4.6 mm × 250 mm, Daicel Chemical Industries, *i*-PrOH/hexane = 05/95, 1.0 mL/min, 40 °C, 220 nm UV detector, retention time = 15.6 min for (*R*) isomer and 17.4 min for (*S*) isomer].

(*S*)-1-(3-pyridyl)ethanol (**2n**)



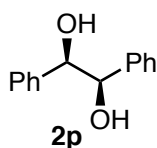
The product **2n** was purified by flash chromatography on silica gel (10–30% EtOAc/hexane) (24.6 mg, >99% isolated yield from **1n**). **2n** was consistent with the the literature data.¹⁹ $[\alpha]_D^{23} -33.8$ (*c* 0.54, CHCl₃). The ee value (89% ee) was determined by chiral HPLC analysis of **2n**, [CHIRALCEL[®] OJ-H column, 4.6 mm × 250 mm, Daicel Chemical Industries, *i*-PrOH/hexane = 10/99, 1.0 mL/min, 40 °C, 220 nm UV detector, retention time = 6.4 min for (*S*) isomer and 7.9 min for (*R*) isomer].

Methyl (*R*)-2-hydroxy-2-phenylacetate (**2o**)



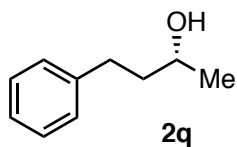
The product **2o** was purified by flash chromatography on silica gel (5–15% EtOAc/hexane) (33.2 mg, >99% isolated yield from **1o**). **2o** was consistent with the the literature data.²⁴ $[\alpha]_D^{23} -169.5$ (*c* 0.58, CHCl₃). The ee value (95% ee) was determined by chiral HP LC analysis of **2o**, [CHIRALCEL[®] AD-H column, 4.6 mm × 250 mm, Daicel Chemical Industries, *i*-PrOH/hexane = 20/80, 1.0 mL/min, 40 °C, 220 nm UV detector, retention time = 5.3 min for (*S*) isomer and 7.1 min for (*R*) isomer].

(1*R*, 2*R*)-1,2-diphenylethane-1,2-diol (**2p**)



The product **2p** (*dl/meso* 96:4) was purified by flash chromatography on silica gel (0–3% MeOH/CHCl₃) (40.3 mg, 94% isolated yield from **1p**). **2p** was consistent with the the literature data.²⁵ $[\alpha]_D^{23} 83.8$ (*c* 0.58, CHCl₃). The ee value (>99% ee) was determined by chiral HPLC analysis of **2p**, [CHIRALCEL[®] OJ-H column, 4.6 mm × 250 mm, Daicel Chemical Industries, *i*-PrOH/hexane = 10/90, 0.5 mL/min, 40 °C, 220 nm UV detector, retention time = 25.2 min for (*S*) isomer, 27.9 min for (*R*) isomer and 33.9 min for *meso* isomer].

(*R*)-4-phenylbutanol (**2q**)



The product **2q** was purified by flash chromatography on silica gel (0–3% EtOAc/hexane) (7.5 mg, 25% isolated yield from **1q**). **2q** was consistent with the the literature data.²⁶ $[\alpha]_{\text{D}}^{23} - 1.1$ (*c* 0.10, CHCl₃). The ee value (42% ee) was determined by chiral HPLC analysis of **2p**, [CHIRALCEL[®] OD-H column, 4.6 mm × 250 mm, Daicel Chemical Industries, *i*-PrOH/hexane = 05/90, 0.7 mL/min, 40 °C, 220 nm UV detector, retention time = 13.0 min for (*R*) isomer, 17.9 min for (*S*) isomer].

Computational Details

All calculations were performed by Gaussian 09 Rev. E.01 program package.²⁷ Based on the investigations of conformations of the pyrrolidine and *P, N*-chelate rings with the copper atom in previous studies on Cu(I)-catalyzed alkynylation of acetaldehyde, we chose three conformations (A-T10, B-E6, and B-T5; these notations were already described in the Chem. Eur. J. 2013 paper). We have initially performed the geometry optimizations including the Grimme's empirical dispersion correction (DFT+D3 with Becke-Johnson damping)²⁸ using the BP86+D3(BJ) functional²⁹ in conjunction with the def2-SVP basis set including the W06 density fitting approximation.³⁰ This level is denoted as DF-BP86+D3(BJ)/def2-SVP. On this level normal coordinate analysis has been performed and the resulting structures have been confirmed as local minima or transition states and to estimate thermal corrections at 298.15 K and 1 atm. The imaginary modes of the transition states have been followed with intrinsic reaction coordinates (IRC)³¹ to describe the reaction pathway. Gibbs energies were computed at 298 K. Then, geometry optimizations for stationary points with higher level followed by normal coordinate analyses were carried out at the DF-B3LYP+D3(BJ)/def2-SVP level with the W06 density fitting approximation.^{32,33} In the major and minor TSs shown in Figure 2, geometry optimizations at the M06-2X/def2SVP level (@M06-2X reference:; Zhao; Y.; Truhlar, D. G. *Theor. Chem. Acc.* **2008**, *120*, 215.) and normal coordinate analyses of the optimized structures were carried out.

The quantum theory of atoms in molecules (QTAIM) and non-covalent interactions are analyzed with the program MultiWFN 3.6^{14,34,35} and visualized with VMD 1.9.3.³⁶

precursor complex in Major conformer 1 at the DF-B3LYP+D3(BJ)/def2-SVP level
SCF Done: E(RB3LYP) = -2088.21838110 A.U. after 1 cycles
NFOck= 1 Conv=0.25D-08 -V/T= 2.0445
Sum of electronic and thermal Enthalpies= -2087.421818 A.U.
Sum of electronic and thermal Free Energies= -2087.538703 A.U.

Center Number	Atomic Number	Atomic Type	Coordinates (Angstroms)		
			X	Y	Z
1	6	0	3.595910	-0.430400	-1.898210
2	6	0	2.857142	-0.900832	-3.119793
3	1	0	2.501203	-0.030029	-3.684482

4	1	0	3.480694	-1.545407	-3.756154
5	1	0	1.977172	-1.472609	-2.780019
6	8	0	3.501413	0.734369	-1.512877
7	1	0	1.894803	1.153937	-0.939154
8	8	0	1.011697	1.239294	-0.519990
9	6	0	1.117992	1.944661	0.717617
10	6	0	1.372026	0.976561	1.884198
11	1	0	1.286170	1.571520	2.816228
12	7	0	0.353726	-0.110728	1.943065
13	15	0	-2.114607	-0.358891	-0.228729
14	6	0	2.726087	0.247566	1.873125
15	1	0	3.107707	0.172822	0.850733
16	1	0	3.465385	0.806594	2.464351
17	6	0	2.445660	-1.161159	2.443766
18	1	0	3.066170	-1.393466	3.321479
19	1	0	2.635341	-1.919729	1.674961
20	6	0	0.960925	-1.140381	2.816808
21	1	0	0.448069	-2.099180	2.674984
22	1	0	0.835358	-0.829515	3.874278
23	6	0	-0.907745	0.412144	2.511072
24	1	0	-1.199695	1.285394	1.914292
25	1	0	-0.707174	0.777713	3.537111
26	6	0	-2.779608	-0.920923	1.400016
27	6	0	-3.867676	-1.795679	1.508290
28	6	0	-2.062099	-0.560351	2.565150
29	6	0	-4.252675	-2.312461	2.749408
30	1	0	-4.418524	-2.082322	0.611427
31	6	0	-2.463804	-1.080957	3.799695
32	6	0	-3.549012	-1.956711	3.899364
33	1	0	-5.104551	-2.993967	2.812739
34	1	0	-1.913810	-0.794184	4.700182
35	1	0	-3.840968	-2.356748	4.873191
36	6	0	-3.256580	-1.147127	-1.436026
37	6	0	-4.491864	-0.580662	-1.786390
38	6	0	-2.877961	-2.374210	-2.001946

39	6	0	-5.338900	-1.235678	-2.683921
40	1	0	-4.793250	0.377209	-1.358247
41	6	0	-3.730124	-3.030207	-2.893129
42	1	0	-1.906446	-2.797265	-1.739988
43	6	0	-4.961095	-2.462989	-3.236520
44	1	0	-6.297217	-0.784564	-2.953480
45	1	0	-3.427466	-3.986099	-3.327934
46	1	0	-5.623982	-2.974280	-3.939148
47	6	0	-2.626100	1.411808	-0.310787
48	6	0	-3.538939	2.010944	0.569724
49	6	0	-2.015639	2.197478	-1.302995
50	6	0	-3.836383	3.373323	0.459745
51	1	0	-4.015891	1.409742	1.347166
52	6	0	-2.325897	3.552772	-1.421718
53	1	0	-1.279512	1.737092	-1.965527
54	6	0	-3.234516	4.145241	-0.537660
55	1	0	-4.544843	3.832035	1.154223
56	1	0	-1.843120	4.154142	-2.195551
57	1	0	-3.467235	5.209451	-0.622621
58	6	0	4.440510	-1.392732	-1.135442
59	6	0	4.289465	-2.781477	-1.277150
60	6	0	5.373104	-0.891668	-0.212235
61	6	0	5.049329	-3.652845	-0.496970
62	1	0	3.548844	-3.182668	-1.969381
63	6	0	6.141882	-1.763022	0.556315
64	1	0	5.477292	0.189660	-0.112612
65	6	0	5.977206	-3.145806	0.418198
66	1	0	4.912295	-4.731788	-0.597347
67	1	0	6.869488	-1.366993	1.268596
68	1	0	6.573133	-3.830415	1.026763
69	77	0	0.137047	-0.893352	-0.265221
70	1	0	-0.280389	-2.379466	0.021551
71	1	0	1.665344	-1.479014	-0.271126
72	1	0	0.078747	-1.344644	-1.782037
73	1	0	0.127090	2.399697	0.866139

74	6	0	2.180375	3.042766	0.663539
75	1	0	2.375526	3.368245	1.699727
76	1	0	3.118548	2.591743	0.300542
77	6	0	1.869719	4.305300	-0.177255
78	6	0	1.645178	3.959881	-1.660051
79	1	0	2.499454	3.398367	-2.070102
80	1	0	0.747466	3.343603	-1.797358
81	1	0	1.526615	4.882648	-2.251479
82	6	0	0.632285	5.028951	0.378516
83	1	0	-0.278526	4.420095	0.282938
84	1	0	0.764980	5.284798	1.443060
85	1	0	0.453677	5.967308	-0.170946
86	6	0	3.088965	5.236681	-0.064250
87	1	0	3.996126	4.749353	-0.456908
88	1	0	2.929545	6.164164	-0.637346
89	1	0	3.282988	5.517450	0.984150

Major TS conformer 1 at the DF-B3LYP+D3(BJ)/def2-SVP level

SCF Done: E(RB3LYP) = -2088.20887871 A.U. after 1 cycles

NFock= 1 Conv=0.29D-08 -V/T= 2.0445

Imaginary frequency: 167.0180i cm⁻¹

Sum of electronic and thermal Enthalpies= -2087.414188 A.U.

Sum of electronic and thermal Free Energies= -2087.529512 A.U.

Center Number	Atomic Number	Atomic Type	Coordinates (Angstroms)		
			X	Y	Z
1	6	0	2.984502	-0.718740	-1.610684
2	6	0	2.511152	-1.160749	-2.993400
3	1	0	1.746767	-0.463373	-3.357485
4	1	0	3.385697	-1.115002	-3.664826
5	1	0	2.105332	-2.180173	-3.005074
6	8	0	3.204899	0.533637	-1.447342

7	1	0	1.956239	1.160283	-1.005605
8	8	0	1.037218	1.359972	-0.568731
9	6	0	1.205302	2.036874	0.671990
10	6	0	1.492728	1.048365	1.817265
11	1	0	1.411455	1.622146	2.761934
12	7	0	0.480840	-0.048552	1.865400
13	15	0	-2.058939	-0.360355	-0.166622
14	6	0	2.854313	0.327257	1.777773
15	1	0	3.277988	0.357788	0.768861
16	1	0	3.565101	0.833726	2.445828
17	6	0	2.571727	-1.127121	2.217784
18	1	0	3.237889	-1.466570	3.023461
19	1	0	2.701209	-1.813822	1.373613
20	6	0	1.115270	-1.114092	2.672414
21	1	0	0.585820	-2.063424	2.523579
22	1	0	1.044875	-0.841502	3.745386
23	6	0	-0.760077	0.442850	2.501501
24	1	0	-1.103055	1.315584	1.930580
25	1	0	-0.513758	0.802680	3.518779
26	6	0	-2.621037	-0.966591	1.475010
27	6	0	-3.671197	-1.880998	1.619615
28	6	0	-1.880234	-0.564231	2.609279
29	6	0	-3.997970	-2.397203	2.877280
30	1	0	-4.237282	-2.195941	0.741847
31	6	0	-2.223610	-1.087067	3.860382
32	6	0	-3.272649	-2.000550	4.000511
33	1	0	-4.820544	-3.109608	2.974923
34	1	0	-1.656519	-0.772736	4.740556
35	1	0	-3.519689	-2.400170	4.986764
36	6	0	-3.182385	-1.196515	-1.352548
37	6	0	-4.430929	-0.652241	-1.690438
38	6	0	-2.795840	-2.427980	-1.903510
39	6	0	-5.283717	-1.334791	-2.561672
40	1	0	-4.738473	0.309378	-1.276415
41	6	0	-3.653321	-3.109560	-2.769106

42	1	0	-1.815873	-2.836987	-1.654087
43	6	0	-4.897962	-2.565257	-3.100251
44	1	0	-6.251933	-0.900634	-2.822595
45	1	0	-3.343751	-4.067501	-3.193840
46	1	0	-5.564752	-3.097136	-3.783358
47	6	0	-2.618961	1.391664	-0.209415
48	6	0	-3.594674	1.906512	0.657386
49	6	0	-2.009040	2.241723	-1.146118
50	6	0	-3.955568	3.255312	0.587213
51	1	0	-4.067613	1.252851	1.393673
52	6	0	-2.379468	3.585406	-1.220166
53	1	0	-1.223054	1.847739	-1.793054
54	6	0	-3.351179	4.095248	-0.352584
55	1	0	-4.711928	3.651106	1.269445
56	1	0	-1.895371	4.240204	-1.948079
57	1	0	-3.632099	5.149856	-0.404445
58	6	0	3.945103	-1.682713	-0.933331
59	6	0	3.654134	-3.047460	-0.787561
60	6	0	5.163625	-1.190692	-0.450721
61	6	0	4.563014	-3.902082	-0.164287
62	1	0	2.690419	-3.429779	-1.131618
63	6	0	6.075468	-2.045804	0.174277
64	1	0	5.373485	-0.127306	-0.575444
65	6	0	5.777877	-3.402890	0.320554
66	1	0	4.320738	-4.961242	-0.045930
67	1	0	7.023565	-1.650545	0.548264
68	1	0	6.488282	-4.071943	0.812607
69	77	0	0.150885	-0.690454	-0.399556
70	1	0	-0.183259	-2.220473	-0.205107
71	1	0	1.811754	-1.125613	-0.794905
72	1	0	-0.076044	-0.997186	-1.925818
73	1	0	0.233208	2.512920	0.879978
74	6	0	2.286591	3.114974	0.586309
75	1	0	2.515124	3.442183	1.615566
76	1	0	3.203802	2.643467	0.198306

77	6	0	1.976762	4.377320	-0.254858
78	6	0	1.722595	4.028713	-1.732350
79	1	0	2.550069	3.432783	-2.148425
80	1	0	0.805042	3.438890	-1.853976
81	1	0	1.627813	4.950858	-2.329341
82	6	0	0.759228	5.122019	0.317142
83	1	0	-0.160892	4.523585	0.242319
84	1	0	0.912540	5.382818	1.377797
85	1	0	0.583957	6.059407	-0.235275
86	6	0	3.210069	5.293165	-0.167772
87	1	0	4.103045	4.791298	-0.573937
88	1	0	3.053225	6.220069	-0.742674
89	1	0	3.426702	5.575862	0.875719

product complex in Major conformer 1 at the DF-B3LYP+D3(BJ)/def2-SVP level

SCF Done: E(RB3LYP) = -2088.22157180 A.U. after 1 cycles

NFock= 1 Conv=0.35D-08 -V/T= 2.0445

Sum of electronic and thermal Enthalpies= -2087.422361 A.U.

Sum of electronic and thermal Free Energies= -2087.543982 A.U.

Center Number	Atomic Number	Atomic Type	Coordinates (Angstroms)		
			X	Y	Z
1	6	0	3.042033	-0.967170	-1.569903
2	6	0	2.853028	-1.375302	-3.033320
3	1	0	2.068172	-0.752113	-3.486593
4	1	0	3.794450	-1.216595	-3.581850
5	1	0	2.562020	-2.432567	-3.128164
6	8	0	3.380504	0.382801	-1.466562
7	1	0	2.553443	0.871250	-1.188323
8	8	0	1.154457	1.300057	-0.495168
9	6	0	1.279527	2.031709	0.692484
10	6	0	1.448588	1.080902	1.893420
11	1	0	1.378779	1.668111	2.829215

12	7	0	0.346918	0.062446	1.910994
13	15	0	-2.113483	-0.371390	-0.209630
14	6	0	2.746120	0.242158	1.895325
15	1	0	3.234397	0.273306	0.914479
16	1	0	3.456795	0.653027	2.625818
17	6	0	2.318415	-1.198672	2.251575
18	1	0	2.954209	-1.660688	3.019677
19	1	0	2.365173	-1.844278	1.364104
20	6	0	0.874913	-1.057999	2.719459
21	1	0	0.260710	-1.954753	2.569286
22	1	0	0.832910	-0.781491	3.792564
23	6	0	-0.896104	0.621571	2.481041
24	1	0	-1.193753	1.478351	1.860252
25	1	0	-0.678130	1.014661	3.491856
26	6	0	-2.702391	-0.882917	1.452871
27	6	0	-3.748185	-1.800134	1.611783
28	6	0	-2.034883	-0.369424	2.589161
29	6	0	-4.150369	-2.208952	2.886614
30	1	0	-4.253681	-2.199462	0.731261
31	6	0	-2.454529	-0.789129	3.856426
32	6	0	-3.502959	-1.700408	4.012037
33	1	0	-4.969000	-2.924073	2.995397
34	1	0	-1.944714	-0.395264	4.739459
35	1	0	-3.808033	-2.013666	5.013101
36	6	0	-3.129244	-1.334211	-1.392828
37	6	0	-4.373803	-0.864578	-1.840049
38	6	0	-2.660996	-2.579755	-1.837989
39	6	0	-5.145161	-1.639287	-2.710066
40	1	0	-4.741636	0.109823	-1.516228
41	6	0	-3.436833	-3.351980	-2.703849
42	1	0	-1.680134	-2.926441	-1.509586
43	6	0	-4.680194	-2.884599	-3.140580
44	1	0	-6.110934	-1.263868	-3.056568
45	1	0	-3.063626	-4.319775	-3.046916
46	1	0	-5.283013	-3.487520	-3.823988

47	6	0	-2.721958	1.358701	-0.359067
48	6	0	-3.868028	1.800979	0.320799
49	6	0	-1.991605	2.260515	-1.149108
50	6	0	-4.287282	3.128137	0.198468
51	1	0	-4.427906	1.110329	0.955149
52	6	0	-2.418140	3.584728	-1.271108
53	1	0	-1.070133	1.928419	-1.632454
54	6	0	-3.565020	4.020087	-0.600122
55	1	0	-5.177760	3.467685	0.732986
56	1	0	-1.842773	4.281577	-1.884363
57	1	0	-3.891242	5.058901	-0.691334
58	6	0	4.040686	-1.849905	-0.843576
59	6	0	3.736773	-3.193998	-0.579634
60	6	0	5.270393	-1.337392	-0.415041
61	6	0	4.643373	-4.009924	0.099077
62	1	0	2.770432	-3.598306	-0.894526
63	6	0	6.180522	-2.153405	0.263664
64	1	0	5.490030	-0.288054	-0.614432
65	6	0	5.871258	-3.490916	0.523820
66	1	0	4.389386	-5.053184	0.304048
67	1	0	7.137478	-1.740402	0.593781
68	1	0	6.581524	-4.127126	1.057846
69	77	0	0.046392	-0.455642	-0.326578
70	1	0	-0.301003	-2.002808	-0.125569
71	1	0	2.049230	-1.156441	-1.064415
72	1	0	-0.094424	-0.675758	-1.890357
73	1	0	0.338985	2.596455	0.865600
74	6	0	2.429049	3.043756	0.629761
75	1	0	2.582854	3.448612	1.646559
76	1	0	3.351409	2.501733	0.365058
77	6	0	2.269725	4.243823	-0.336313
78	6	0	2.199043	3.786308	-1.803860
79	1	0	3.076433	3.177351	-2.072758
80	1	0	1.311931	3.166082	-1.984465
81	1	0	2.170444	4.661460	-2.474663

82	6	0	1.010220	5.055154	0.009362
83	1	0	0.091763	4.472171	-0.154015
84	1	0	1.020455	5.382825	1.062673
85	1	0	0.945495	5.957229	-0.620770
86	6	0	3.505747	5.142889	-0.157446
87	1	0	4.430845	4.590409	-0.388670
88	1	0	3.458730	6.016143	-0.828345
89	1	0	3.584970	5.515846	0.877316

Minor TS conformer 1 at the DF-B3LYP+D3(BJ)/def2-SVP level

SCF Done: E(RB3LYP) = -2088.20515843 A.U. after 1 cycles

NFock= 1 Conv=0.39D-08 -V/T= 2.0445

Imaginary frequency: 358.7357i cm-1

Sum of electronic and thermal Enthalpies= -2087.411079 A.U.

Sum of electronic and thermal Free Energies= -2087.527532 A.U.

Center Number	Atomic Number	Atomic Type	Coordinates (Angstroms)		
			X	Y	Z
1	6	0	2.781483	1.905060	-1.161916
2	8	0	3.468581	0.966620	-0.610118
3	1	0	2.547317	0.096253	0.057669
4	8	0	1.716759	-0.483954	0.328205
5	6	0	1.905248	-1.839353	-0.054465
6	6	0	1.548534	-2.058850	-1.536310
7	1	0	1.539298	-3.154241	-1.705378
8	7	0	0.187311	-1.538192	-1.855385
9	15	0	-1.804482	-0.085193	0.293081
10	6	0	2.477224	-1.394607	-2.575009
11	1	0	3.073324	-0.600197	-2.109486
12	1	0	3.178136	-2.140293	-2.975987
13	6	0	1.540074	-0.832178	-3.669837
14	1	0	1.848074	-1.116645	-4.686252

15	1	0	1.507076	0.263357	-3.621931
16	6	0	0.167102	-1.401157	-3.325552
17	1	0	-0.675045	-0.769066	-3.634302
18	1	0	0.036256	-2.403850	-3.782486
19	6	0	-0.841317	-2.487309	-1.382529
20	1	0	-0.676689	-2.648681	-0.309325
21	1	0	-0.676037	-3.461982	-1.880947
22	6	0	-2.874355	-1.034739	-0.860888
23	6	0	-4.211896	-0.692936	-1.094159
24	6	0	-2.273027	-2.067009	-1.617000
25	6	0	-4.961946	-1.367516	-2.062257
26	1	0	-4.671786	0.110816	-0.517612
27	6	0	-3.039645	-2.734281	-2.578128
28	6	0	-4.375343	-2.390544	-2.806588
29	1	0	-6.004791	-1.089533	-2.232090
30	1	0	-2.579100	-3.537547	-3.159347
31	1	0	-4.953032	-2.921959	-3.566385
32	6	0	-2.909967	1.212707	0.971867
33	6	0	-3.804530	0.928551	2.015980
34	6	0	-2.880926	2.502219	0.420592
35	6	0	-4.665141	1.918907	2.494425
36	1	0	-3.826185	-0.067707	2.461287
37	6	0	-3.744632	3.489073	0.900744
38	1	0	-2.167912	2.724686	-0.373969
39	6	0	-4.637876	3.200394	1.936287
40	1	0	-5.355434	1.689668	3.309868
41	1	0	-3.712197	4.491961	0.468407
42	1	0	-5.308349	3.976119	2.314323
43	6	0	-1.557100	-1.212495	1.725059
44	6	0	-2.334759	-2.358013	1.948899
45	6	0	-0.514398	-0.899427	2.612675
46	6	0	-2.072737	-3.180912	3.048753
47	1	0	-3.142444	-2.611091	1.258350
48	6	0	-0.263687	-1.716978	3.715223
49	1	0	0.112379	-0.027448	2.415772

50	6	0	-1.040150	-2.860150	3.934178
51	1	0	-2.678550	-4.075223	3.214186
52	1	0	0.552614	-1.469183	4.397310
53	1	0	-0.834627	-3.505215	4.791739
54	77	0	0.064660	0.574844	-0.740346
55	1	0	-0.900061	1.359468	-1.714236
56	1	0	1.452875	1.389873	-1.512771
57	1	0	0.027493	1.893139	0.104592
58	6	0	2.372441	3.070901	-0.272534
59	6	0	1.571567	4.127140	-0.729991
60	6	0	2.821104	3.085224	1.052529
61	6	0	1.217361	5.169956	0.124652
62	1	0	1.186382	4.113478	-1.751364
63	6	0	2.465568	4.128012	1.912024
64	1	0	3.446561	2.259364	1.393246
65	6	0	1.661663	5.173275	1.452103
66	1	0	0.583387	5.981478	-0.241886
67	1	0	2.818988	4.124123	2.946516
68	1	0	1.379726	5.988330	2.123467
69	6	0	3.198864	2.296555	-2.579004
70	1	0	2.454787	2.920238	-3.091437
71	1	0	4.141120	2.864581	-2.502984
72	1	0	3.391247	1.396210	-3.176156
73	1	0	1.187313	-2.419938	0.547623
74	6	0	3.323138	-2.325826	0.251244
75	1	0	3.457995	-3.298343	-0.253650
76	1	0	4.032802	-1.627955	-0.221808
77	6	0	3.714691	-2.506698	1.738355
78	6	0	3.662118	-1.173427	2.505583
79	1	0	4.279000	-0.408483	2.008139
80	1	0	2.638597	-0.781659	2.562332
81	1	0	4.044551	-1.309169	3.530802
82	6	0	2.793460	-3.532086	2.419338
83	1	0	1.752939	-3.179467	2.470470
84	1	0	2.802794	-4.495664	1.882632

85	1	0	3.123895	-3.722676	3.453287
86	6	0	5.159259	-3.035825	1.765846
87	1	0	5.503168	-3.186913	2.801802
88	1	0	5.243032	-4.000511	1.238507
89	1	0	5.848790	-2.325529	1.281754

Major TS conformer 1 at the M06-2X/def2-SVP level

SCF Done: E(RM062X) = -2087.03232661 A.U. after 1 cycles

NFock= 1 Conv=0.30D-08 -V/T= 2.0440

Imaginary frequency: 484.3376i cm⁻¹

Sum of electronic and thermal Enthalpies= -2086.232484 A.U.

Sum of electronic and thermal Free Energies= -2086.346560 A.U.

Center Number	Atomic Number	Atomic Type	Coordinates (Angstroms)		
			X	Y	Z
1	6	0	2.995296	-0.801952	-1.642569
2	6	0	2.460684	-1.284937	-2.980102
3	1	0	1.717010	-0.569054	-3.348178
4	1	0	3.317514	-1.303348	-3.673160
5	1	0	2.013927	-2.284017	-2.929978
6	8	0	3.224589	0.431863	-1.511070
7	1	0	1.963975	1.137017	-1.022059
8	8	0	1.072837	1.352302	-0.582301
9	6	0	1.261144	2.034966	0.642755
10	6	0	1.505478	1.051343	1.800717
11	1	0	1.463745	1.639101	2.741036
12	7	0	0.465289	-0.002808	1.874662
13	15	0	-2.061629	-0.328153	-0.178821
14	6	0	2.834051	0.278044	1.737516
15	1	0	3.210454	0.254334	0.708288
16	1	0	3.594473	0.778662	2.351957
17	6	0	2.512301	-1.145501	2.239489
18	1	0	3.174584	-1.471453	3.051781

19	1	0	2.606725	-1.869633	1.419958
20	6	0	1.062016	-1.061715	2.706831
21	1	0	0.496730	-1.996204	2.594068
22	1	0	1.014230	-0.750494	3.771127
23	6	0	-0.761207	0.531854	2.482918
24	1	0	-1.086319	1.398234	1.889053
25	1	0	-0.519706	0.907676	3.496415
26	6	0	-2.636258	-0.883797	1.478382
27	6	0	-3.698761	-1.775586	1.644024
28	6	0	-1.902313	-0.454036	2.603948
29	6	0	-4.045084	-2.241773	2.913714
30	1	0	-4.262824	-2.115339	0.773583
31	6	0	-2.265739	-0.926817	3.866133
32	6	0	-3.327634	-1.817547	4.026989
33	1	0	-4.877386	-2.937918	3.026672
34	1	0	-1.703004	-0.589763	4.739925
35	1	0	-3.590420	-2.177616	5.022637
36	6	0	-3.223238	-1.151288	-1.335098
37	6	0	-4.468357	-0.593085	-1.649260
38	6	0	-2.868838	-2.390979	-1.880676
39	6	0	-5.350592	-1.271568	-2.489339
40	1	0	-4.752475	0.379249	-1.242794
41	6	0	-3.756021	-3.068740	-2.715338
42	1	0	-1.888770	-2.812981	-1.653052
43	6	0	-4.997476	-2.511321	-3.020431
44	1	0	-6.316382	-0.825918	-2.732176
45	1	0	-3.471118	-4.034170	-3.136091
46	1	0	-5.687955	-3.040393	-3.679226
47	6	0	-2.579464	1.437105	-0.236898
48	6	0	-3.580286	1.970114	0.585101
49	6	0	-1.903663	2.274883	-1.133909
50	6	0	-3.903470	3.324907	0.507178
51	1	0	-4.103529	1.325185	1.295793
52	6	0	-2.235946	3.627085	-1.214667
53	1	0	-1.095739	1.864250	-1.745400

54	6	0	-3.233610	4.153434	-0.393321
55	1	0	-4.680681	3.734984	1.153996
56	1	0	-1.703130	4.274251	-1.913740
57	1	0	-3.486003	5.213449	-0.451036
58	6	0	3.913558	-1.767410	-0.915490
59	6	0	3.608021	-3.126023	-0.772956
60	6	0	5.111137	-1.276482	-0.392006
61	6	0	4.485977	-3.977900	-0.109997
62	1	0	2.654167	-3.503836	-1.148209
63	6	0	5.991039	-2.129875	0.275015
64	1	0	5.331226	-0.215424	-0.519025
65	6	0	5.680646	-3.480740	0.417605
66	1	0	4.235193	-5.033500	0.006316
67	1	0	6.924537	-1.737965	0.682609
68	1	0	6.366823	-4.148890	0.940670
69	77	0	0.118712	-0.724213	-0.414579
70	1	0	-0.248699	-2.213543	-0.209689
71	1	0	1.758335	-1.194740	-0.743346
72	1	0	-0.113663	-1.062517	-1.903562
73	1	0	0.312348	2.566441	0.838064
74	6	0	2.401204	3.047762	0.547754
75	1	0	2.671732	3.359407	1.571780
76	1	0	3.278461	2.518292	0.136014
77	6	0	2.148478	4.319423	-0.287235
78	6	0	1.794252	3.977718	-1.739914
79	1	0	2.543006	3.301646	-2.181638
80	1	0	0.819382	3.475774	-1.803447
81	1	0	1.756541	4.897570	-2.344627
82	6	0	1.023529	5.157603	0.330171
83	1	0	0.057941	4.629829	0.302874
84	1	0	1.248340	5.414104	1.377772
85	1	0	0.898809	6.098802	-0.227462
86	6	0	3.444990	5.137910	-0.271663
87	1	0	4.271416	4.569213	-0.724380
88	1	0	3.322916	6.072246	-0.840466

89 1 0 3.735380 5.401572 0.757360

Minor TS conformer 1 at the M06-2X/def2-SVP level

SCF Done: E(RM062X) = -2087.02778299 A.U. after 1 cycles

 NFock= 1 Conv=0.66D-08 -V/T= 2.0440

Imaginary frequency: 534.5936i cm-1

Sum of electronic and thermal Enthalpies= -2086.228172 A.U.

Sum of electronic and thermal Free Energies= -2086.343305 A.U.

Center Number	Atomic Number	Atomic Type	Coordinates (Angstroms)		
			X	Y	Z
1	6	0	2.838556	1.967553	-1.078031
2	8	0	3.490765	1.046885	-0.510508
3	1	0	2.536801	0.077898	0.141735
4	8	0	1.729334	-0.505886	0.361723
5	6	0	1.939472	-1.840878	-0.052792
6	6	0	1.573111	-2.032298	-1.534939
7	1	0	1.595940	-3.123252	-1.737336
8	7	0	0.211984	-1.537507	-1.846635
9	15	0	-1.804753	-0.093007	0.289573
10	6	0	2.486646	-1.307678	-2.541476
11	1	0	3.024623	-0.489290	-2.045633
12	1	0	3.239350	-2.003960	-2.934779
13	6	0	1.545286	-0.777776	-3.645368
14	1	0	1.870638	-1.055329	-4.656281
15	1	0	1.475249	0.316657	-3.595845
16	6	0	0.189674	-1.391175	-3.309533
17	1	0	-0.669649	-0.781168	-3.618201
18	1	0	0.092126	-2.395036	-3.773384
19	6	0	-0.801257	-2.493353	-1.380777
20	1	0	-0.644950	-2.657415	-0.305062
21	1	0	-0.630200	-3.465792	-1.883320
22	6	0	-2.850888	-1.047550	-0.885828

23	6	0	-4.185063	-0.718043	-1.137745
24	6	0	-2.235893	-2.080253	-1.625279
25	6	0	-4.918447	-1.406014	-2.106497
26	1	0	-4.659976	0.088195	-0.576121
27	6	0	-2.985987	-2.760641	-2.586206
28	6	0	-4.318943	-2.429629	-2.832039
29	1	0	-5.959315	-1.136128	-2.290478
30	1	0	-2.513240	-3.565644	-3.153938
31	1	0	-4.883918	-2.972059	-3.591399
32	6	0	-2.952370	1.161024	0.978603
33	6	0	-3.865950	0.833432	1.988789
34	6	0	-2.938877	2.460140	0.458543
35	6	0	-4.762430	1.789684	2.462419
36	1	0	-3.875873	-0.172201	2.414043
37	6	0	-3.839336	3.413191	0.933520
38	1	0	-2.209314	2.720502	-0.309714
39	6	0	-4.752133	3.080205	1.933081
40	1	0	-5.467762	1.526222	3.251995
41	1	0	-3.819786	4.424397	0.524520
42	1	0	-5.451930	3.829403	2.306907
43	6	0	-1.558747	-1.254580	1.695856
44	6	0	-2.365071	-2.376776	1.921393
45	6	0	-0.480376	-0.994933	2.552701
46	6	0	-2.097356	-3.228006	2.994155
47	1	0	-3.200556	-2.592358	1.250138
48	6	0	-0.222738	-1.842727	3.629238
49	1	0	0.169989	-0.139343	2.351691
50	6	0	-1.028503	-2.960788	3.849409
51	1	0	-2.726172	-4.103949	3.161280
52	1	0	0.620458	-1.635893	4.290778
53	1	0	-0.819250	-3.628807	4.686454
54	77	0	0.045813	0.616771	-0.710679
55	1	0	-0.901826	1.401352	-1.650462
56	1	0	1.410390	1.399487	-1.484175
57	1	0	-0.016449	1.906961	0.128285

58	6	0	2.360307	3.125189	-0.222377
59	6	0	1.570110	4.163170	-0.728002
60	6	0	2.751544	3.155463	1.116735
61	6	0	1.169901	5.208546	0.097656
62	1	0	1.228428	4.131841	-1.764111
63	6	0	2.349269	4.202546	1.946120
64	1	0	3.372705	2.341924	1.492849
65	6	0	1.557511	5.230616	1.439696
66	1	0	0.544932	6.008274	-0.303371
67	1	0	2.657393	4.215484	2.992990
68	1	0	1.240050	6.049334	2.087586
69	6	0	3.226359	2.314344	-2.507168
70	1	0	2.464189	2.901500	-3.031603
71	1	0	4.156413	2.902793	-2.454743
72	1	0	3.433401	1.393969	-3.066706
73	1	0	1.248337	-2.455693	0.551463
74	6	0	3.376508	-2.291257	0.206253
75	1	0	3.543558	-3.235156	-0.341702
76	1	0	4.047042	-1.539382	-0.245950
77	6	0	3.795369	-2.512108	1.674030
78	6	0	3.655804	-1.225690	2.497752
79	1	0	4.185721	-0.390754	2.012531
80	1	0	2.602576	-0.932924	2.604216
81	1	0	4.084900	-1.372425	3.501543
82	6	0	2.959411	-3.625089	2.315452
83	1	0	1.897617	-3.346114	2.393588
84	1	0	3.030511	-4.559350	1.735720
85	1	0	3.319939	-3.833471	3.334757
86	6	0	5.268578	-2.937565	1.665913
87	1	0	5.627350	-3.119294	2.690445
88	1	0	5.411027	-3.863104	1.086431
89	1	0	5.899197	-2.154418	1.218252

References and Notes

- (1) (a) Wang, D.; Astruc, D. *Chem. Rev.* **2015**, *115*, 6621. (b) Foubelo, F.; Nájera, C.; Yus, M. *Tetrahedron: Asymmetry* **2015**, *26*, 769.
- (2) (a) Hashiguchi, S.; Fujii, A.; Takehara, J.; Ikariya, T.; Noyori, R. *J. Am. Chem. Soc.* **1995**, *117*, 7562. (b) Fujii, A.; Hashiguchi, S.; Uematsu, N.; Ikariya, T.; Noyori, R. *J. Am. Chem. Soc.* **1996**, *118*, 2521. (c) Haack, K.-J.; Hashiguchi, S.; Fujii, A.; Ikariya, T.; Noyori, R. *Angew. Chem. Int. Ed. Engl.* **1997**, *36*, 285. For mechanistic studies, see: (d) Yamakawa, M.; Ito, H.; Noyori, R. *J. Am. Chem. Soc.* **2000**, *122*, 1466. (e) Yamakawa, M.; Yamada, I.; Noyori, R. *Angew. Chem., Int. Ed.* **2001**, *40*, 2818. (f) Noyori, R.; Yamakawa, M.; Hashiguchi, S. *J. Org. Chem.* **2001**, *66*, 7931.
- (3) For hydrogenation through alcohol–ketone interconversion, see: (a) Blum, Y.; Czarkie, D.; Rahamim, Y.; Shvo, Y. *Organometallics* **1985**, *4*, 1459. (b) Shvo, Y.; Czarkie, D.; Rahamim, Y. *J. Am. Chem. Soc.* **1986**, *108*, 7400.
- (4) For hydrogenation through aromatization–dearomatization interconversion, see: (a) Zhang, J.; Leitus, G.; Ben-David, Y.; Milstein, D. *Angew. Chem., Int. Ed.* **2006**, *45*, 1113. (b) Langer, R.; Leitus, G.; Ben-David, Y.; Milstein, D. *Angew. Chem., Int. Ed.* **2011**, *50*, 2120.
- (5) For asymmetric hydrogenation through carboxylic acid–carboxylate interconversion, see: Yu, J.; Long, J.; Yang, Y.; Wu, W.; Xue, P.; Chung, L. W.; Dong, X.-Q.; Zhang, X. *Org. Lett.* **2017**, *19*, 690.
- (6) a) Ishii, T.; Watanabe, R.; Moriya, T.; Ohmiya, H.; Mori, S.; Sawamura, M. *Chem. –Eur. J.* **2013**, *19*, 13547. (b) Schwarzer, M. C.; Fujioka, A.; Ishii, T.; Ohmiya, H.; Mori, S.; Sawamura, M. *Chem. Sci.* **2018**, *9*, 3484. (c) Takayama, Y.; Ishii, T.; Ohmiya, H.; Iwai, T.; Schwarzer, M. C.; Mori, S.; Taniguchi, T.; Monde, K.; Sawamura, M. *Chem. –Eur. J.* **2017**, *23*, 8400.
- (7) Yu, J.; Duan, M.; Wu, W.; Qi, X.; Xue, P.; Lan, Y.; Dong, X.-Q.; Zhang, X. *Chem. –Eur. J.* **2017**, *23*, 970.
- (8) Other P/NH/OH chiral ligands were reported by Clarke *et al.*. For detail, see: (a) Díaz-Valenzuela, M. B.; Phillips, S. D.; France, M. B.; Gunn, M. E.; Clarke, M. L. *Chem. –Eur. J.* **2009**, *15*, 1227. (b) Phillips, S. D.; Fuentes, J. A.; Clarke, M. L. *Chem. –Eur. J.* **2010**, *16*, 8002. (c) Fuentes, J. A.; Phillips, S. D.; Clarke, M. L. *Chem. Cent. J.* **2012**, *6*, 151.
- (9) Other tridentate ligands such as P/N/OH Schiff base-unit-contained ligands promoted asymmetric transfer hydrogenation. For detail, see: (a) Kwong, H.-L.; Lee, W.-S.; Lai,

- T.-S.; Wong, W.-T. *Inorg. Chem. Commun.* **1999**, 266. (b) Dai, H.; Hu, X.; Chen, H.; Bai, C.; Zheng, Z. *Tetrahedron: Asymmetry* **2003**, *14*, 1467.
- (10) Because excess amount of NaOH was used in Zhang's catalytic system, it is likely that the alcohol group of the ligand might take alkoxide form during the reaction. Thus suggested alcohol–alkoxide interconversion may not occur in this system.
- (11) For achiral ruthenium complex-catalyzed transfer hydrogenation using formic acid as a hydrogen source, see: (a) Watanabe, Y.; Ota, T.; Tsuji, Y. *Chem. Lett.* **1980**, 1980. (b) Watanabe, Y.; Ohta, T.; Tsuji, Y. *Bull. Chem. Soc. Jpn.* **1982**, *55*, 2441. For an asymmetric reaction at formic acid–triethylamine system, see ref. 2b.
- (12) (a) Dub, P. A.; Ikariya, T. *J. Am. Chem. Soc.* **2013**, *135*, 2604. (b) Matsuoka, A.; Sandoval, C. A.; Uchiyama, M.; Noyori, R.; Naka, H. *Chem. –Asian J.* **2015**, *10*, 112.
- (13) For asymmetric transfer hydrogenation of aryl *N*-heteroaryl ketones, see: (a) Hems, W. P.; Jackson, W. P.; Nightingale, P.; Bryant, R. *Org. Process Res. Dev.* **2012**, *16*, 461. (b) Wang, B.; Zhou, H.; Lu, G.; Liu, Q.; Jiang, X. *Org. Lett.* **2017**, *19*, 2094. (c) Liu, Q.; Wang, C.; Zhou, H.; Wang, B.; Lv, J.; Cao, L.; Fu, Y. *Org. Lett.* **2018**, *20*, 971.
- (14) For dinuclear iridium hydride complexes, see: Schnabel, R. C.; Roddick, D. M. *Organometallics* **1993**, *12*, 704.
- (15) Johnson, E. R.; Keinan, S.; Mori-Sanchez, P.; Contreras-Garcia, J.; Cohen, A. J.; Yang, W. *J. Am. Chem. Soc.* **2010**, *132*, 6498.
- (16) Herde, J. L.; Lambert, J. C.; Senoff, C. V. *Inorg. Synth.* **1974**, *15*, 18.
- (17) Uson, R.; Oro, L. A.; Cabeza, J. A. *Inorg. Synth.* **1983**, *23*, 128.
- (18) Weiberth, F. J.; Hall, S. S. *J. Org. Chem.* **1987**, *52*, 3901.
- (19) Li, Y.; Yu, S.; Wu, X.; Xiao, J.; Shen, W.; Dong, Z.; Gao, J. *J. Am. Chem. Soc.* **2014**, *136*, 4031.
- (20) Widegren, M. B.; Harkness, G. J.; Slaxwin, A. M. Z.; Cordes, D. B.; Clarke, M. L. *Angew. Chem., Int. Ed.* **2017**, *56*, 5825.
- (21) Heller, B.; Redkin, D.; Gutnov, A.; Fischer, C.; Bonrath, W.; Karge, R.; Hapke, M. *Synthesis* **2008**, 69.
- (22) Yadav, J. S.; Reddy, B. V. S.; Sreelakshmi, C.; Rao, A. B. *Synthesis* **2009**, 1881.
- (23) Bosiak, M. J.; Krzemiński, M. P.; Jaisankar, P.; Zaidlewicz, M. *Tetrahedron: Asymmetry* **2008**, *19*, 956.
- (24) Alamsetti, S. K.; Sekar, G. *Chem. Commun.* **2010**, 46, 7235.
- (25) Neyyappadath, R. M.; Chisholm, R.; Greenhalgh, M. D.; Rodríguez-Escrich, C.; Pericaàs, M. A.; Hähner, G.; Smith, A. D. *ACS Catal.* **2018**, *8*, 1067.
- (26) Inagaki, T.; Ito, A.; Ito, J.; Nishiyama, H. *Angew. Chem., Int. Ed.* **2010**, *49*, 9384.

- (27) Frisch, M. J.; Trucks, G. W.; Schlegel, H. B.; Scuseria, G. E.; Robb, M. A.; Cheeseman, J. R.; Scalmani, G.; Barone, V.; Mennucci, B.; Petersson, G. A.; Nakatsuji, H.; Caricato, M.; Li, X.; Hratchian, H. P.; Izmaylov, A. F.; JBloino, J.; Zheng, G.; Sonnenberg, J. L.; Hada, M.; Ehara, M.; Toyota, K.; Fukuda, R.; Hasegawa, J.; Ishida, M.; Nakajima, T.; Honda, Y.; Kitao, O.; Nakai, H.; Vreven, T.; Montgomery, J. A. Jr; Peralta, J. E.; Ogliaro, F.; Bearpark, M.; Heyd, J. J.; Brothers, E.; Kudin, K. N.; Staroverov, V. N.; Kobayashi, R.; Normand, J.; Raghavachari, K.; Rendell, A.; Burant, J. C.; Iyengar, S. S.; Tomasi, J.; Cossi, M.; Rega, N.; Millam, N. J.; Klene, M.; Knox, J. E.; Cross, J. B.; Bakken, V.; C. Adamo; Jaramillo, J.; Gomperts, R.; Stratmann, R. E.; Yazyev, O.; Austin, A. J.; Cammi, R.; Pomelli, C.; Ochterski, J. W.; Martin, R. L.; Morokuma, K.; Zakrzewski, V. G.; Voth, G. A.; Salvador, P.; Dannenberg, J. J.; Dapprich, S.; Daniels, A. D.; Farkas, Ö.; Foresman, J. B.; Ortiz, J. V.; Cioslowski, J.; Fox, D. J. *Gaussian 09*, Revision E.01, Gaussian, Inc., Wallingford CT **2013**.
- (28) Grimme, S.; Ehrlich, S.; Goerigk, L. *J. Compt. Chem.* **2011**, *32*, 1456.
- (29) (a) Becke, A. D. *Phys. Rev. A* **1988**, *38*, 3098. (b) Perdew, J. P. *Phys. Rev. B* **1986**, *33*, 8822.
- (30) (a) Schafer, A.; Huber, C.; Ahlrichs, R. *J. Chem. Phys.* **1994**, *100*, 5829. (b) Weigend, F.; Ahlrichs, R. *Phys. Chem. Chem. Phys.* **2005**, *7*, 3297. (c) Weigend, F. *Phys. Chem. Chem. Phys.* **2006**, *8*, 1057.
- (31) (a) Fukui, K. *J. Phys. Chem.* **1970**, *74*, 4161. (b) Fukui, K. *Acc. Chem. Res.* **1981**, *14*, 363. (c) Gonzales, C. and Schlegel, H. B. *J. Chem. Phys.* **1989**, *90*, 2154. (d) Gonzalez, C.; Schlegel, H. B. *J. Phys. Chem.* **1990**, *94*, 5523. (e) Hratchian, H. P.; Schlegel, H. B. *J. Chem. Phys.* **2004**, *120*, 9918. (f) Hratchian, H. P.; Schlegel, H. B. *J. Chem. Theor. Comput.* **2005**, *1*, 61.
- (32) Becke, A. D. *J. Chem. Phys.* **1993**, *98*, 5648.
- (33) Lee, C.; Yang, W.; Parr, R. G. *Phys. Rev. B* **1988**, *37*, 785.
- (34) Bader, R. W. *Atoms in Molecules: A Quantum Theory*; Oxford University Press: New York, 1994.
- (35) Contreras-Garcia, J.; Johnson, E. R.; Keinan, S.; Chaudret, R.; Piquemal, J.-P.; Beratan, D. N.; Yang, W. *J. Chem. Theory Comput.* **2011**, *7*, 625.
- (36) Humphrey, W.; Dalke, A.; Schulten, K. *J. Molec. Graphics* **1996**, *14*, 33. See also: <http://www.ks.uiuc.edu/Research/vmd/>

Publication List

I Parts of the present thesis have been published in the following journal

- 1) Copper(I)-Catalyzed Intramolecular Hydroalkoxylation of Unactivated Alkenes
Murayama, H.; Nagao, K.; Ohmiya, H.; Sawamura, M. *Org. Lett.* **2015**, *17*, 2039.

II Other publication not included in this thesis

- 1) Phosphine-Catalyzed Vicinal Acylcyanation of Alkynoates
Murayama, H.; Nagao, K.; Ohmiya, H.; Sawamura, M. *Org. Lett.* **2016**, *18*, 1706.
- 2) Asymmetric Synthesis of α -Alkylidene- β -Lactams through Copper Catalysis with a Prolinol-Phosphine Chiral Ligand
Imai, K.; Takayama, Y.; Murayama, H.; Ohmiya, H.; Shimizu, Y.; Sawamura, M. *Org. Lett.* **2019**, *in press*.

Acknowledgement

The studies described in this thesis have been carried out under the direction of Professor Masaya Sawamura at Graduate School of Chemical Sciences and Engineering, Hokkaido University from April 2013 to March 2019.

The author wishes to express his grateful acknowledgement to Professor Masaya Sawamura for giving opportunities to study in his laboratory, and for his kind guidance, constant encouragement and valuable discussion. He is deeply grateful to Professor Hirohisa Ohmiya for his practical guidance, helpful discussions and considerable suggestions. He would also like to express his appreciation to Lecturer Yohei Shimizu, Assistant Professor Tomohiro Iwai and Assistant Professor Fernand Arteaga Arteaga for their kind discussions, advices and supports.

The author is much grateful to Professor Keiji Tanino, Professor Hideaki Oikawa, Professor Tamaki Nakano and Associate Professor Hisanori Senboku for their accurate advices and considerable suggestions on this thesis. He is thankful to Professor Seiji Mori at Institute of Quantum Beam Science, Ibaraki University for significant assistance with computer calculations in Chapter 2. He is also thankful to Mr. Yutthana Wongnongwa and Associate Professor Siriporn Jungsuttiwong at Faculty of Science, Ubon Ratchathani University for computer calculations in Chapter 2.

The author expresses his thanks to all the members of Sawamura's group for their kind discussions. Especially, he would like to express his appreciation to Dr. Kazunori Nagao for excellent collaborations. He is also thankful to Mr. Koji Imai for the excellent collaborations and the works not included on this thesis.

Finally, he would like to express his gratitude for his family, Mr. Masaru Murayama and Ms. Kayoko Murayama for warm encouragement and continuous assistance.

Hiroaki Murayama
Graduate School of Chemical Sciences and Engineering
Hokkaido University
March 2019